Characterization of a Novel Protein Kinase Involved in Flowering

by

Le Wang

A thesis submitted in partial fulfillment of the requirements for the degree of

Master of Science

in

Plant Biology

Department of Biological Sciences

University of Alberta

Abstract

Reversible protein phosphorylation is one of the most dynamic post-translational modifications (PTMs) regulating eukaryotic cell functions. It is catalyzed by two opposing protein families, protein kinases (PKs) and phosphatases (PPs). PKs represent enzymes with high substrate specificity that catalyze reversible protein phosphorylation events through the transfer of the γ-phosphoryl group from adenosine triphosphate (ATP) to the target substrate. Such enzymes play an important role in the regulation of a wide range of plant cellular and developmental processes such as plant metabolism, stress tolerance, and plant flowering. Despite the transcriptional and genetic networks of flowering being well-established, the impact of post-translational modifications such as reversible protein phosphorylation remains largely unknown. Here, PROTEIN KINASE 4 (PXK4), a novel flowering-related protein in *Arabidopsis thaliana* (Arabidopsis) is described. Initial phosphoproteomic screening of *pxk4* T-DNA insertional mutant line 2 (*pxk4-2*) found significant decreases in the phosphorylation of multiple key flowering transition proteins. Further, phenotypic characterization of multiple *pxk4* mutant alleles (*pxk4-2, -4, -5*) revealed an early flowering phenotype across all alleles, which was supported by qPCR analysis of known flowering genes in *pxk4-2* plants that found significantly reduced *FLC* and elevated *FT* expression. Subsequent protein-protein interactome analysis of the putative PXK4 substrate and flowering transition regulator HISTONE MONO-UBIQUITINATION 2 (HUB2), using tandem affinity purification fusion proteins expressed in WT (Col-0) and *pxk4-2* found that loss of PXK4 impacted various flowering regulatory complexes, indicating a potential mechanism by which PXK4 regulates flowering transition. Taken together, these findings suggest that PXK4 plays a key role in flowering through the likely regulation of multiple proteins involved flowering transition. In particular, results suggest PXK4 functions to regulate HUB2 complex formation in response to photoperiod, ultimately resulting in the modulation of *FLC* and *FT* levels.

Acknowledgements

I can never accomplish my thesis work without the great support of many people. First of all, I would like to thank my supervisor, Dr. R. Glen Uhrig, for providing me with the chance of doing research and learning. I also thank you for your scientific training in multiple aspects. Every piece of your advice and care really encouraged me to take the challenges and move forward. I would also like to thank the post-docs in our lab who provided tremendous help throughout my master's thesis. I thank Dr. Devang Mehta, for the long-term mentoring, and Dr. Sabine Scandola, for the support in qPCR, plant imaging, and plant breeding. I thank all my colleagues, Maria Rodriguez Gallo, Meagan Hussey, Maryalle Tan, Rachael McCullough, Rachael Protzman, Kallum McDonald, Ibrahim Khodabocus, who have been working really hard to create an excellent lab environment and provided various support. I would like to thank my supervisory committee member, Dr. Enrico Scarpella, for giving me such great advice at annual committee meetings, and microscopy training. I would also like to thank Dr. Janice Cooke for the research advice, and Cooke Lab member, Colleen Fortier, Marion Mayerhofer, for technical support and Dr. Landon Zarony from Dr. Robert Campbell Lab for helping with florescence screening.

I would like to acknowledge Department of Biological Sciences, University of Alberta, Natural Sciences and Engineering Research Council of Canada (NSERC), for financial support throughout my entire thesis. I would like to acknowledge Arabidopsis Biological Resource Center (ABRC), the European Arabidopsis Stock Centre, Dr. Robin Cameron from McMaster University, Mieke Van Lijsebettens (VIB Center for Plant Systems Biology, Ghent University, Belgium), for providing the seeds and plasmid constructs.

Lastly, I would like to thank my dear friends, Yicong Luo, Xin Zhou, Zitong Xu, Jinyu Zhao, Yingyi Liu, Mengmeng Liu, and Jin Ren, for the encouragement and support all the way through, and my parents, Mr. Weijun Wang and Mrs. Yazhen Zhou, for the great love and additional financial support.

Table of Contents

List of Tables

List of Figures

List of Abbreviations

Abbreviations	Descriptions
ABA	Abscisic acid
ABRC	Arabidopsis Biological Resources Center
Arabidopsis	*Arabidopsis thaliana*
ARF	Auxin Response Factors
Asp (D)	Aspartate
AtBRM	Arabidopsis BRAMA
ATHENA	Arabidopsis THaliana ExpressioN Atlas
ATP	Adenosine TriphosPhate
AtSF1	Arabidopsis Splicing Factor 1
BASTA	Glufosinate-ammonium
bp	Base-pair
BSA	Bovine Serum Albumin
C'	C-terminus
CCA1	Circadian Clock Associated 1
CDS	Coding Sequence
CL	Continuous-Light
CO	CONSTANS
Col-0	Columbia-0
COOLAIR	Cold-induced FLC antisense lncRNA transcripts.
DK	Dual-specificity Kinase
DMSO	DiMethyl SulfOxide
DNA	DeoxyriboNucleic Acid
DNase	DeoxyriboNuclease
DSLP	Dentin Sialophosphoprotein-Like Protein
DTB	Days to Bolting
DTT	Dithiothreitol
EDTA	Ethylenediamine tetraacetic acid
ELF	Early Flowering
EtOH	Ethanol
FD	Flowering Locus D

FLC	Flower Locus C
FLM	FLOWERING LOCUS M
FT	Flower Locus T
FVE	FLOWERING LOCUS VE
GA	Gibberellic Acid
GI	GIGANTEA
H3K27me3	The tri-methylation at the 27th lysine residue of the histone H3 protein
H3K4me3	The tri-methylation at the 4th lysine residue of the histone H3 protein
His	Histidine
HOS1	High Expression of Osmotically Responsive Gene 1
HUB1	Histone Monoubiquitination 1
HUB2	Histone Monoubiquitination 2
kDa	Kilo Dalton
KHD1	RNA-Binding KH Domain-Containing Protein
LB	Lysogeny Broth
LCB	Leaf Counts at Bolting
LD	Long-Day
LHY	Late Elongated Hypocotyl
MBSU	Molecular Biology Service Unit, University of Alberta
MD	Mid-Day
min	Minute
mol	Mole
MS	Murashige and Skoog
N'	N-Terminus
O/N	Overnight
OPCA	OPR/PC/AID Motif
Paf1 Complex (Paf1C)	Paf1 Complex
PAGE	Polyacrylamide Gel Electrophoresis
PB1	Octicosapeptide/Phox/Bem1p Domain
PCR	Polymerase Chain Reaction
pH	Negative logarithm of hydrogen ion concentration
PK	Protein Kinase
PP	Protein Phosphatase

PRR	Pseudo-Response Regulator
PTM	Post-Translational Modification
RNA	Ribonucleic Acid
RNase	Ribonuclease
RRM	RNA Recognition Motif
SAM	Shoot Apical Meristem
SD	Short-Day
SDS	Sodium Dodecyl Sulfate
Ser (S)	Serine
SnRK1/2	Sucrose Non-Fermenting Kinase 1/2
SOC1	Suppressor of Overexpression of CO 1
SPEN3	Nucleic Acid Binding Protein
STK	Serine/Threonine Kinase
SUMO	Small Ubiquitin-Like Modifier
SVP	Short Vegetative Phase
TK	Tyrosine Kinase
Tm	Midpoint of Temperature Induced Transition
TOC1	Timing of Cab Expression 1
Tyr (Y)	Tyrosine
UBC1	E2 Ubiquitin-Conjugating Enzyme 1
UBC2	E2 Ubiquitin-Conjugating Enzyme 2
UV	Ultraviolet
V	Volt
VIP4	Vernalization Independent 4
YFP	Yellow Florescent Protein
ZT	Zeitgeber Time

*Other important flowering genes are listed in **S.1**.

Chapter 1: General Introduction

1.1 Post-translational modifications

Post-translational modification (PTM) of proteins is a regulatory process that occurs after mRNA translation, whereby the synthesized proteins are modified through a series of chemical changes (covalent addition or proteolytic cleavage) to drive protein functionalization (Singh et al, 2017; Mann & Jensen, 2003; Bürkle, 2001). These chemical changes require the assistance of various enzyme classes to recognize the unique side chains of the target substrates (Bürkle, 2001), and to catalyze the chemical modification, which in many cases is reversible (Swaney & Villén, 2016; Humphrey et al., 2015; Walsh, 2006; Mann & Jensen, 2003). For example, reversible protein ubiquitylation (Ebner et al., 2017; Hu & Sun, 2016; Uhrig et al., 2008) is catalyzed by ubiquitinating enzymes and deubiquitinating enzymes (DUBs) that work in opposition for regulating biological functions (eg. immune response in human or enzyme activities in plants). Similarly, reversible phosphorylation is catalyzed by the opposing activities of protein kinases and protein phosphatases to affect protein functions such as enzyme activities (Kanno et al., 2018; Humphrey et al.,2015; Jin & Pawson, 2012; Michniewicz et al., 2007), protein localization (Humphrey et al.,2015; Vincent et al., 2001) and protein-protein interactions (Yang et al., 2019; Humphrey et al.,2015) amongst others. Other PTMs include, but are not limited to, protein acetylation, protein methylation, and SUMOylation, which have also been shown to possess dynamic regulatory roles across eukaryotes (Han et al., 2018; Zhang et al., 2018; Terman & Kashina 2013; Hannoun et al., 2010; Bürkle, 2001) and to

also be catalyzed by opposing sets of enzymes. The prevalence of PTMs enables the diversification of the proteome into proteoforms, thus becoming a powerful tool that the organisms deploy to regulate their cellular environments.

1.2 Protein Phosphorylation

Although over 200 types of PTMs have been identified to date (Humphrey et al., 2015; Walsh, 2006), protein phosphorylation represents the most influential PTM due to its reversible nature as well as the overwhelming involvement in key cellular processes such as signal transduction, transcription, metabolism, cell division, immunity amongst others (Humphrey et al., 2015; Cohen, 2002; Manning et al., 2002a; Manning et al., 2002b). In eukaryotic cells, it is estimated that approximately 1.5%-2.5% of the genome encodes PKs (Manning et al., 2002b), with recent human phosphoprotome studies finding that 75% of the human proteome can be phosphorylated, and more than 90% of the annotated proteome being predicted to possess phosphorylation sites (Sharma et al., 2014).

When the term “protein kinases” was initially annotated in the 1970s, it was also believed by Walsh and Krebs (1973) that PKs were substrate specific. The specific residues recognized by the active sites of PKs was later found to be serine (Ser)/ threonine (Thr)/ tyrosine (Tyr) side chains of substrate proteins (**Figure 1.2.1**; Ubersax et al., 2007). The specificity of PKs for each type of target residue depends on PK catalytic domains. PKs with a consensus DLRAAN or DLAARN motif in sub-domain VI, PI/VK/RWT/MAPE motif in sub-domain VIII or a CW(X_6)RPXF motif in the sub-domain XI, are more likely to confer tyrosine specificity. Alternatively, serine/threonine-specific PKs

are likely to possess a DLKPEN motif in sub-domain VI or a GT/SXXY/FXAPE motif in sub-domain VIII (Rudrabhatla et al., 2006). With the onset of phosphorylation at the PK activation loop, a PK then catalyzes the transfer of a γ-phosphoryl from ATP to the hydroxyl oxygen (OH) of the Ser/Thr/Tyr residue of a substrate protein with the aid of a cation (eg. Mg^{2+}) (**Figure 1.2.1**.; Humphrey et al., 2015; Ubersax et al., 2007; Cohen, 2002).

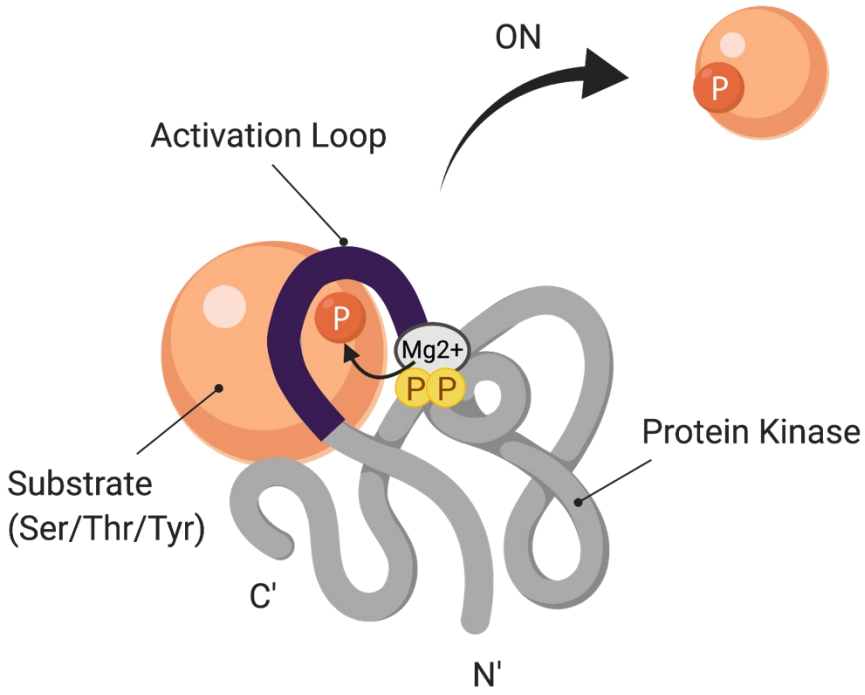

Figure 1.2.1. Schematic diagram of a PK. The cartoon PK is represented by the elongated grey polypeptide. The PK activation loop is highlighted in purple, with phosphoryl groups denoted by "P" molecules in either orange (γ-phosphoryl) or yellow (α, β-phosphoryl). The specific side chain (Serine; Ser /Threonine; Thr / Tyrosine; Tyr) of the protein substrate is positioned at the activation loop of the PK. To turn "ON" the molecular switch for the downstream biological processes, the protein substrate is phosphorylated by receiving a γ-phosphoryl of ATP with the assistance of Mg^{2+} catalyzed by the PK.

Unlike PKs, which form one large superfamily with a largely conserved catalytic mechanism, PPs are more diverse, encoding four distinct families (Kerk et al., 2008). Derived from different ancestors, Ser/Thr-specific phosphatases have been divided into phosphoprotein phosphatase (PPP) and Mg^{2+}-dependent phosphoprotein metallophosphatase (PPM), whereas Tyr phosphatases (PTP) and Asp-based phosphatases, are classified by an unique catalytic $C(X)_5R$ and DXDXT/V motif, respectively (Jin & Pawson, 2012; Kerk et al., 2008).

Like other eukaryotes, plant PKs consist of a large group of proteins that also play an essential role in biological regulation. For example, pre-mRNA PROCESSING 4 KINASES (PPR4K), initially known to modulate pre-mRNA splicing in fungi and mammals (Eckert et al., 2016; Lehti-Shiu et al., 2012; Huang et al., 2000), have recently been revealed to alter alternative splicing as a dual-specificity kinase in Arabidopsis by phosphorylating a group of splicing factors and RNA-binding proteins (Kanno et al., 2018). Approximately 1000 PKs are encoded by 4% of the genes in Arabidopsis (Zulawski, et al. 2014; Lehti-Shiu et al., 2012). Research to date has found plant PKs important for the multifaceted regulation of cell signaling (Yang et al., 2019), metabolism (Robaglia et al., 2012), mRNA processing (Kanno et al., 2018), amongst others.

1.3 PXK4 Kinase

Great efforts have been made by the molecular plant community to uncover the underlying regulatory networks associated with plant PKs, of which the functions of many remain unresolved. PROTEIN KINASE 4 (PXK4; At2g35050) is one such case. Phylogenetic analysis of PXK4 in Arabidopsis has grouped it to PB1

domain/octicosapeptide repeat-containing GmPK6-like kinases (Joshi et al., 2011; Swarbreck, 2008; Lin et al.,1999), along with At1g16270, At1g79570, At1g04700, At3g24720, At5g57610, At3g46920 (Rudrabhatla et al., 2006), some of which seem to function similarly. For example, together with its relatives, RAF18 and RAF20, PXK4 (RAF24), was recently found to involved in the regulation of ABA-independent subclass I SNF1-related protein kinase 2 (SnRK2s) in response to osmotic stress (Soma et al., 2020; Lin et al., 2020; Stecker et al., 2014). Using PFAM, an online tool for searching protein sequences for protein domains (https://pfam.xfam.org/), PXK4 was found to possess an octicosapeptide/Phox/Bem1 (PB1) domain (190-276) with a conserved lysine residue (K) at the N-terminus (**Figure 1.3.1**; Finn et al., 2015). PB1 domains act as protein scaffolds that mediate protein-protein interactions through dimerization or oligomerization among all the kingdoms (Suminoto et al., 2007; Ito et al., 2001). There are three types of PB1 domains: Type I (A), Type II (B), or Type I/II(A/B). They comprise either acidic residues (OPR/PC/AID motif or OPCA motif), or an invariant lysine residue (K), or both (**Figure 1.3.1**; Suminoto et al. 2007; Moscat et al., 2006; Noda et al., 2003). Specifically, the Type I domain harbors an acidic OPCA motif, whereas the Type II domain conserves an invariant Lys residue on β strand at N-terminus. Type I/II domain is characterized by having both OPCA motif and Lys residue (**Figure 1.3.1**).

For example, in yeast cells, Bem1p, a PB1-domain-containing protein, recruits another PB1-domain-conserved protein Cdc24p to form a PB1-K-PC-PB1 heterodimeric complex facilitating the polarity establishment, thus is exclusively important for the budding and mating of *Saccharomyces cerevisiae* (Noda et al., 2003). In plants, it was also reported by Korasick et al. (2015) and Nanao et al. (2014) that the auxin response

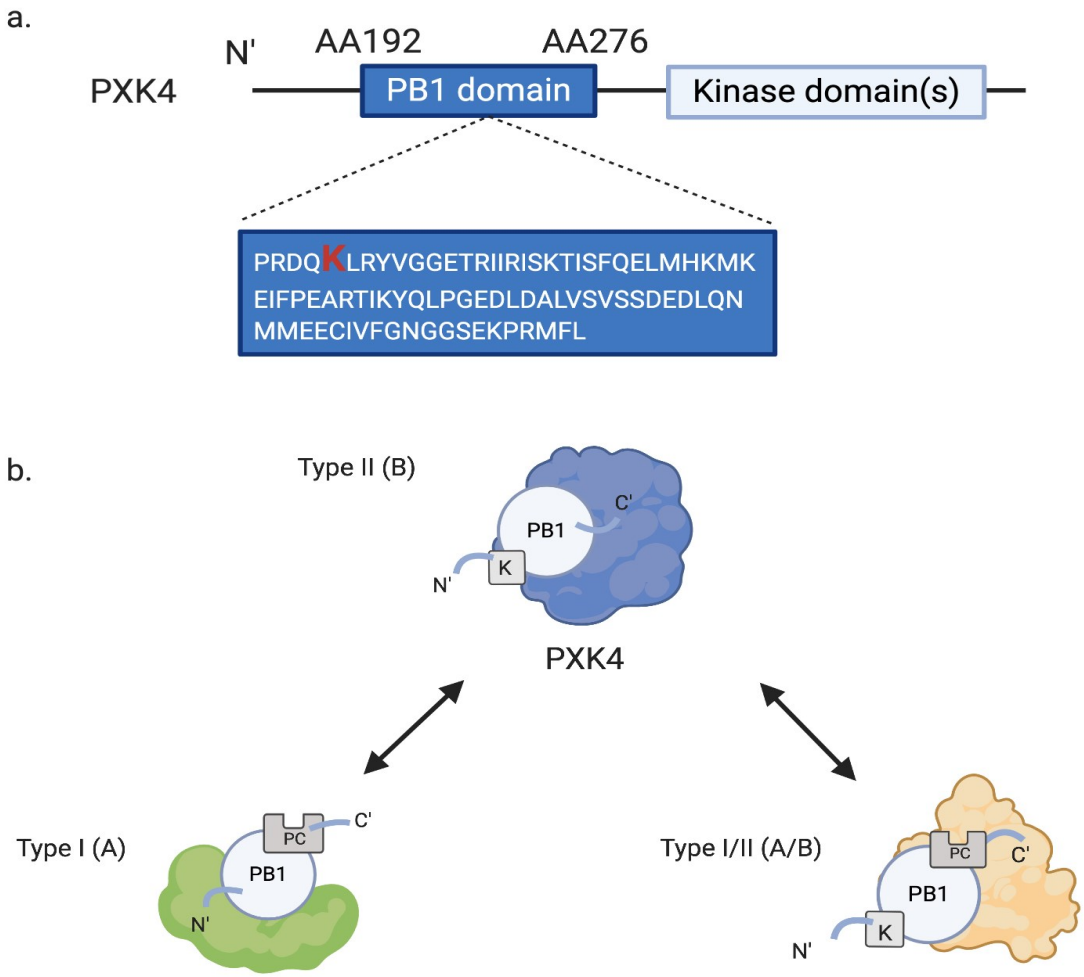

Figure 1.3.1 Characteristics of PXK4 kinase. a. PXK4 kinase possesses an unique PB1 domain from amino acid 192 to 276, and a putative kinase domain at C' (Swarbreck, 2008). The invariant lysine residue is highlighted in red near N'. **b.** PXK4 conserves a Type II (B) PB1 domain, which may interact with either Type (A) or Type I/II PB1 domain through PC motif at C' to mediate the downstream reactions.

factors (ARF7 and ARF5) possess type I/II PB1domains, and thus can interact with auxin/indole 3-acetic acid-inducible repressor proteins (Aux/IAA) or other PB1-containing proteins, including ARF7 and ARF5 themselves, for auxin signaling. Likewise, since the

type II PB1 domain of PXK4 kinase maintains an invariant Lys residue at N-terminus (**Figure 1.3.1**), it is possible that the PB1 domain of PXK4 is also involved in protein-protein interactions through the formation of PB1-K-PC-PB1 heterodimers.

1.4 Flowering in Plants

Flowering is an unique physiological process that angiosperms have evolved for reproduction (Ó'Maoiléidigh et al., 2014). From an agricultural perspective, crop and fruit yields are highly dependent on the corresponding timing of flowering (Blümel et al., 2015). Therefore, understanding the underlying molecular mechanisms governing flowering transitions is not only essential to developing deeper fundamental insights, but also to the development of enhanced crop varieties.

1.4.1 Known flowering pathways

Flowering transition is a change that plants undergo to develop from vegetative growth to reproduction. The entire developmental process is regulated by the intersection of multiple signaling pathways that emanate from a combination of light, temperature, hormones, autonomous or age (Park et al., 2016; Boss et al., 2004). Of the pathways known to impact flowering transition, photoperiod, vernalization, ambient temperature, hormones (e.g. Gibberellic acid), autonomous and aging pathways represent the main pathways identified to date (**Figure 1.4.1**; Srikanth & Schmid, 2011).

Over the years, the regulatory mechanisms of flowering have been extensively studied (Srikanth & Schmid, 2011; Kobayashi & Weigel, 2007). To date, the photoperiodic flowering mechanism has been well resolved at the molecular levels in the model plant Arabidopsis. Generally, a photoperiodic transcriptional factor named CONSTANS (CO) is

regulated to output light-driven flowering signals to induce FLOWERING LOCUS T (FT) (Song et al., 2015; Song et al., 2013; Valverde, 2011). This results in an increased prevalence of flowering transition signals being integrated by leaf-mediated florigens to promote flowering (Matsoukas, 2015; Turck et al., 2008).

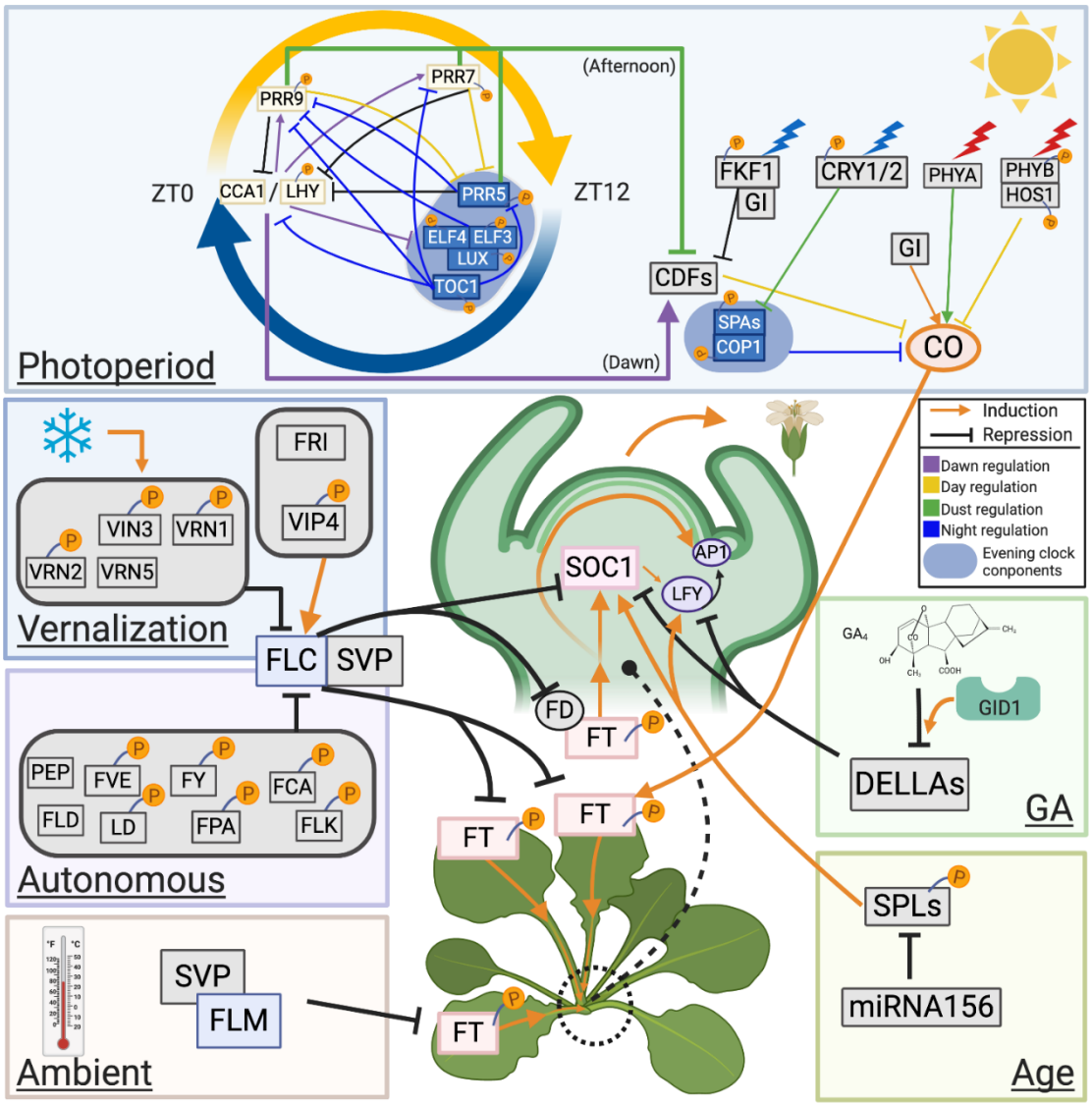

Figure 1.4.1 Schematic of the regulatory signaling networks governing flowering. The corresponding transcription factors are depicted in bricks or ovals. The proteins with at least one phosphorylation site are depicted with "P" tails (Details are available in **S.1**). Arrows indicate induction; the T-junctions represent repression. Within the photoperiod pathway, the colors of inducers and repressors correspond to the timing of regulation occurring within a 24-h cycle (purple = dawn; yellow = daytime; green = dust; blue = evening/night). The evening clock components were highlighted and shaded in blue.

Circadian oscillators are the group of proteins that are responsible for regulating the biological clock of plants in response to photoperiodic changes. In anticipation of light induction, CIRCADIAN CLOCK ASSOCIATED 1 (CCA1) and LATE ELONGATED HYPOCOTYL (LHY) accumulate, stimulating PSEUDO-RESPONSE REGULATOR 9 (PRR9) and PRR7 within a negative feedback loop to reduce the transcript levels of evening clock genes such as *PRR5*, *TOC1*, *LUX ARRHYTHMO* (*LUX*), *EARLY FLOWERING 3* (*ELF3*), and *ELF4* (**Figure 1.4.1**; Park et al., 2016; Shim & Imaizumi, 2015; Chow et al., 2012; Nagel & Kay, 2012; Nakamichi et al., 2010). In turn, PRR9, PRR7, or PRR5 also directly target the promoters of *CCA1* and *LHY*, leading to CCA1 and LHY repression from morning to midnight (ZT2 to ZT16) (**Figure 1.4.1**; Nakamichi et al., 2010). Conversely, in the transition to evening, the morning clock genes are repressed by various evening clock proteins. For example, the evening complex ELF3-ELF-LUX is recruited to repress *PPR9* expression (**Figure 1.4.1**; Park et al., 2016; Chow et al., 2012). The protein TOC1 acts in a similar manner in the evening, whereby it inhibits *CCA1*/*LHY*, *PRR9*, *PRR7*, *ELF4*, *LUX*, *GIGANTEA* (*GI*), in addition to itself at the corresponding promoter regions (**Figure 1.4.1;** Shim & Imaizumi, 2015; Nagel & Kay, 2012; Huang et al., 2012)

CCA1/LHY and PRR proteins also regulate transcript levels of *CYCLING OF FACTORs* (*CDFs*), a family of genes that has been recognized to stabilize *CO* expression throughout the day (**Figure 1.4.1**; Blümel et al., 2015; Shim & Imaizumi, 2015; Nakamichi et al., 2010). Under long-day, *CO* abundance is inhibited by the activation of *CDF1* by CCA1 and LHY at dawn (Song et al., 2012; Nakamichi et al., 2010). Meanwhile during the day, the blue-light-dependent photoreceptor, FLAVIN-BINDING, KELCH REPEAT, F-

BOX1 (FKF1) interacts with GIGANTEA (GI) (**Figure 1.4.1**) to inhibit *CDF1* and *CDF2* and to de-repress *CO* expression (Fornara et al., 2009; Sawa et al., 2007). In the afternoon, *CDFs*, particularly *CDF1*, *CDF2*, *CDF3*, *CDF5*, are continuously repressed by PRR proteins, thus, giving rise to peak *CO* expression (Song et al., 2015; Song et al., 2012; Fornara et al., 2009; Nakamichi et al., 2007). Conversely, under short-day, when FKF1 peaks in the evening, light-sensitive FKF1-GI complex no longer accumulates due to the mismatch of protein expression (**Figure 1.4.1**; Shim & Imaizumi, 2015; Sawa et al., 2007).

Post-translational modification of CO also plays an essential role in regulating FT levels (**Figure 1.4.1**; Song et al., 2013). In the daytime, HIGH EXPRESSION OF OSMOTICALLY RESPONSIVE GENE 1 (HOS1), a RING finger containing E3 ubiquitin ligase, physically interacts with a red-light photoreceptor PHYTOCHROME B (PHYB) to degrade CO (Song et al., 2013; Valverde, 2004). Alternatively, in the afternoon, far-red light PHYTOCHROME A (PHYA) antagonizes PHYB to stabilize CO levels (Shim & Imaizumi, 2015; Valverde, 2004). Meanwhile, two blue-light-sensitive photoreceptors, Cryptochrome (CRY) 1 and 2 function similarly to PHYA, but alternatively interact with SUPPRESSOR OF PHYA 1 (SPA1), to induce CO by interrupting CONSTITUTIVE PHOTOMORPHOGENIC 1 (COP1) activities (Liu et al., 2011; Zuo et al., 2011). At night, COP1 interacts with SUPPRESSOR OF PHYA-105s (SPAs/SPA1,2,3,4) in the place of PHYB and HOS1 to inhibit CO through ubiquitylation (Lazaro et al., 2015; Piñeiro & Jarillo, 2013; Song et al., 2013; Liu et al., 2008; Laubinger et al., 2004). Altogether, with CO accumulated at dust, longer photoperiods promote flowering early by inducing *FT* and

other flower integrators such as SUPPRESSOR OF OVEREXPRESSION OF CO 1 (SOC1) (Yoo et al., 2005).

Flowering transition is not only impacted by a single factor, but it is determined by the crosstalk of multiple signaling pathways, which can intersect with the photoperiod pathway (Blümel et al., 2015). For example, flowering transition can be regulated by independent upstream autonomous and vernalization signals (Whittaker & Dean, 2017; Alexandre & Hennig, 2008) such as MADS-box proteins FLOWER LOCUS C (FLC) and SHORT VEGETATIVE PHASE (SVP), which heterodimerize and antagonize the functions of CO to repress flowering (Park et al., 2016). This is because FLC binds to the first intron of *FT* or the promoter of *SOC1* and FLOWER LOCUS D (FD) in leaves or the apical meristem (**Figure 1.4.1**; Li et al., 2008; Searle et al., 2006).

As summarized by Cheng et al. (2017), the main transcription factors involved in the autonomous pathway are FLOWERING LOCUS CA (FCA) (Macknight et al., 1997), FLOWERING LOCUS KH DOMAIN (FLK) (Mockler et al., 2004), PEPPER (PEP) (José Ripoll et al., 2006), FLOWERING LOCUS PA (FPA) (Schomburg et al., 2001), FLOWERING LOCUS Y (FY) (Simpson et al., 2003) for RNA processing, or through chromatin modification by FLOWERING LOCUS D (FLD) (He et al., 2003), LUMINIDEPENDENS (LD) (Lee et al., 1994), and FLOWERING LOCUS VE (FVE) (Ausín et al., 2004).

Another key factor that affects flowering is prolonged or ambient temperature. Once exposed to seasonal cold temperatures, *FLC* expression is largely reduced due to VIVIPAROUS1/ABI3-LIKE1 (VAL1) transcriptional repression and transient accumulation of its antisense transcripts, *COLD INDUCED LONG ANTISENSE INTRAGENIC RNA*

(*COOLAIR*) (Whittaker & Dean, 2017; Swiezewski et al., 2009). With continuous prolonged exposure to cold, VERNALIZATION INSENSITIVE 3 (VIN3) and VERNALIZATION 5 (VRN5) are involved through association with PLANT HOMEDOMAIN-POLYCOMB REPRESSIVE COMPLEX 2 (PRC2/VRN2), which forms a VIN3-VIN5-PRC2 complex that binds the first intron of *FLC* gene (Whittaker & Dean, 2017). As a result, *FLC* transcription is halted because FLC transcriptional activation marks, histone H3 Lys 36 trimethylation (H3K36me3) and H3K4me3, which were overtaken by Polycomb-repressive H3K27me3 to maintain epigenetic silencing despite a decrease of *COOLAIR* abundance (Whittaker & Dean, 2017; Swiezewski et al., 2009; De Lucia et al., 2008; Sung et a., 2004). Eventually, as H3K27me3 extends over the FLC locus with the assistance of chromodomain protein LIKE HETEROCHROMATIN PROTEIN (LHP1), plants can inherit the epigenetic maintenance of silencing during cell divisions (Whittaker & Dean, 2017; Swiezewski et al., 2009; Alexandre & Hennig, 2008).

Unlike vernalization maintaining a genetic record for seasonal changes, the way that Arabidopsis can respond to changes in ambient temperature is temporal. Instead of impacting *FLC* transcription, the exogenous regulation occurs between SVP and FLOWERING LOCUS M (FLM), a clade member of FLC subject to alternative splicing (**Figure 3.1.2** ; Capovilla et al., 2015; Posé et al., 2013). It was reported by Posé et al. (2013) that two FLM variants, FLM-β and FLM-δ compete for SVP binding to alternate flowering time. In the circumstances where the temperature is low (~16℃), FLM-β actively interacts with SVP to inhibit precocious flowering by targeting downstream *FT*, *TWINSISTER OF FT* (*TSF*), or *SOC1* (Lee et al., 2014; Lee et al., 2013; Posé et al. 2013). When the temperature increases, degradation of the FLM-β-SVP complex occurs, while

FLM-δ proteins take over the position from FLM-β to alleviate the repression power (Lee et al., 2013; Posé et al. 2013)

In most scenarios, the flowering signals generated from these aforementioned pathways are integrated into companion cells to promote *FT* abundance (**Figure 1.4.1**; Srikanth & Schmid, 2011; Lee & Lee, 2010; Giakountis & Coupland, 2008; Turck et al., 2008). Subsequently, FT proteins travel through sieve elements to the shoot apex meristem to first activate *SOC1* at the inflorescence meristem and then *APETALA 1* (*AP1*), at floral meristem, where the floral primordia initiate, with assistance from a bZIP transcription factor; FD (**Figure 1.4.1**; Srikanth & Schmid, 2011; Lee & Lee, 2010; Turck et al., 2008). Floral organs are not established until floral meristem identity is established. Prior to floral organ development, maintenance of floral meristem identity is required to prevent abnormal floral reversions caused by AP1 and LEAFY (LFY) deficit (Lee & Lee, 2010; Giakountis & Coupland, 2008). *AP1* is directly induced by FT, whereas *LFY* is under the control of a feedback loop created by SOC1 and AGAMOUS-LIKE 24 (AGL24) complex (Giakountis & Coupland, 2008; Lee et al., 2008). *LFY* and *SOC1* levels can also be affected by gibberellic acid or SQUAMOSA PROMOTER BINDING PROTEIN-LIKE (SPLs) from the aging pathway localized to the shoot apical meristem (**Figure 1.4.1**; Srikanth & Schmid, 2011; Mutasa-Göttgens & Hedden, 2009).

1.4.2 The importance of PTMs in regulating flowering

Taking advantage of its rapid and reversible nature in response to stimuli, PTMs also play an essential role in regulating flowering signaling (Kwak et al., 2016a; Humphrey et al., 2015; Mulekar & Huq, 2015). Many PTMs have been found in Arabidopsis to affect the stability and functions of floral proteins (eg. FLC and CO). Some PTMs that have been

implicated in the regulation of flowering transition include protein: ubiquitylation (Jung et al., 2014; Piñeiro & Jarillo, 2013), sumoylation (Kwak et al., 2016a; Kwak et al., 2016b), acetylation (He et al., 2003), methylation (He et al., 2004), and phosphorylation (Heidari et al., 2013; Mulekar et al., 2012; Ogiso et al., 2010). Some more well characterized examples include the E3 ubiquitin ligases HOS1, COP1, and FKF1, which modulate flowering by impeding clock components CO, GI, CDF1 expression (Jung et al; 2014; Piñeiro & Jarillo, 2013; Song et al., 2012; Jang et al., 2010; Sawa et al., 2007; Imaizumi et al., 2005).

To date however, the role of protein phosphorylation in regulating flowering is still poorly understood. Even so, great progress is now being made. For example, SHAGGY-like kinase 12 was found to be involved in flowering through its site-specific phosphorylation of photoperiodic output CO (Chen et al., 2020). SUCROSE NON-FERMENTING KINASE 1 (SnRK1), a known regulator of sugar metabolism and ABA signaling (Jossier et al., 2009), has also been shown to impact flowering through its phosphorylation (Jeong, et al., 2015). Lastly, casein kinase II (CK2), is also known to have a role in regulating flowering by phosphorylating the key clock components CCA1 and LHY, or through autonomous pathway (Mulekar & Huq, 2015; Mulekar & Huq, 2014; Mulekar & Huq, 2012; Lu et al., 2011; Ogiso et al., 2010).

Specific examination of the known flowering-related genes using the ATHENA (Arabidopsis THaliana ExpressioN Atlas) phosphoproteome database, has suggested that 61 out of 98 known flowering proteins (~62%) possess phosphorylation sites (**Figure 1.4.1**; **S.1**). For example, multiple circadian clock proteins implicated in flowering were found to be phosphorylated. PRR9 was annotated to have three phosphorylation sites at

Ser-365, Ser-193, and Ser-197 (**S.2**), while PRR5 and PRR7 maintain three and seven serine phosphorylation sites, respectively (**S.2**). This suggests that these PRRs could work as a substrate of multiple or individual Ser/Thr or dual-specificity PKs that could potentially regulate flowering by affecting downstream clock regulated genes. Overall, how protein phosphorylation regulates flowering remains poorly resolved and the identification of flowering related PKs remain to be revealed.

Chapter 2: Discovery of A Novel Protein Kinase Involved in Flowering

2.1 Introduction

As a PK, PXK4 encodes a putative kinase domain that likely functions to provide PXK4 its ability to phosphorylate its substrates (Waese et al., 2017; Humphrey et al., 2015; Rudrabhatla et al., 2006). When examining PXK4 in the ATHENA phosphorylation database (Mergner et al., 2020), we found PXK4 itself possesses 27 annotated phosphorylation sites (**Figure 2.1.1**). Further analysis of diurnal phosphoproteome datasets found PXK4 to undergo changes in phosphorylation (Uhrig et al., 2019). Given the number of sites falling outside of the PK activation site, coupled with the fact that some sites are diurnally fluctuating, it is likely that PXK4 could function as an intermediate that responds to, and also delivers, signaling information within a signaling cascade.

Previous phosphoproteomic analysis of the *pxk4-2* mutant by Dr. R. Glen Uhrig as part of a larger, multi-mutant screen, revealed a number of proteins to be differentially phosphorylated (**S.3**). With *pxk4-2* known to possess early flowering at this point, my mining of this data was for proteins involved in flowering. This identified a number of putative PXK4 substrates. Accordingly, analysis of the phosphoproteomics data revealed five potential PXK4 substrate candidates (**Table 2.2**), including: 1) HISTONE MONOUBIQUITINATION 2 (HUB2; AT1G55250); 2) BRAMA (AtBRM/BRM; AT2G46020); 3) ARABIDOPSIS THALIANA SPLICING FACTOR 1 (AtSF1/SF1; AT5G51300); 4) VERNALIZATION

Peptide NO.	Peptide sequence
1-52	MDQAKGYEHVRYTAPDPRDEGLG**p(S$_{24}$)**INQRFSHDSSTNVNTYVRPPDYGVSTPA
53-108	RPVLNYSIQTGEEFAFEFMRDRVIMKPQFIPNVYGEHSGMPVSVNLSALGMVHPMS
109-158	ESGPNATVLNIEEKRQ**p(S$_{125}$)**FEHERKPPSRIEDKTYHELVQ**p(S$_{147}$)**APVISSKNDTG
159-216	QRRHSLVSSRASDSSLNRAKFLCSFGGKVIPRPRDQKLRYVGGETRIIRISKTISFQE
217-272	LMH**K**MKEIFPEARTIKYQLPGEDLDALVSVSSDEDLQNMMEECIVFGNGGSEKPRM
273-324	FLFSSSDIEEAQFVMEHAEGDSEVQYVVAVNGMDLSSRRS**p(S$_{313}$)**LGLSPPGNNLD
325-381	ELLHGNFDRKIDRAATEPAVASLTPLAGNESLPASQTSQPVTGFSTGNEPFSQPYL
382-438	GQQLQFPGLGNHQIYTSGHMASIGYIDEKRSAPLHVQPQPHYIPYSVNPETPLESLV
439-489	PHYPQKPEQGFLREEQIFHVQDPETSSKEAKMRRDD**p(S$_{474}$)**FQKVNDHPISTVESN
490-539	L**p(S$_{491}$)**AKEPKMRRESSTPRVNEYPVSSMPSDLIVPDDLPKEEAPIVTQT**p(S$_{536}$)**SST
540-581	PDPSSSTL**p(S$_{548}$)**EK**p(S$_{551}$)**LRK**p(S$_{555}$)**EDHVENNL**p(S$_{564}$)**AKEPKMRKEHSTTRVNE
582-616	YSVS**p(S$_{586}$)**V**p(S$_{588}$)p(S$_{589}$)**DSMVPDQALKEEAPI**p(S$_{605}$)**MKI**p(S$_{609}$)**N**p(S$_{611}$)**TPDPK
617-667	SLVYPEK**p(S$_{624}$)**LRTSQEKTGAFDTTNEGMKKNQDNQFCLLGGFSVSGHGTSNNS
668-719	SSNVSNFDQPVTQQRVFHSERTVRDPTETNRL**p(S$_{700}$)**KSDDSLASQFVMAQTTSDA
720-772	FLPISESSETSHEANMESQNVHPTAPVIPAPDSIWTAEGSMSQSEKKNVETN**p(T$_{772}$)**
773-822	PEHV**p(S$_{777}$)**QTETSAKAVPQGHNEKGDIVVDINDRFPREFLADILKTKE**p(S$_{818}$)**LNFP
823-877	GLGPLHADGAGVSLNIQNNDPKTWSYFRNLAQDEFERKDLSLMDQDHPGFPTSMT
878-936	NTNGVPIDYSYPPLQSEKVASSQIHPQIHFDGNIKPDVSTITIPDLNTVDTQEDYSQS
937-992	QIKGAESTDATLNAGVPLIDFMAADSGMRSLQVIKNDDLEELKELGSGTFGTVYHGK
993-1041	WRGTDVAIKRIKRSCFIGR**p(S$_{1012}$)p(S$_{1013}$)**EQERLTSEFWHEAEILSKLHHPNVMAFY
1042-1098	GVVKDGPGGTLATVTEYMVNGSLRHVLLSNRHLDRRKRLIIAMDAAFGMEYLHSKSI
1099-1147	VHFDLKCDNLLVNLKDPARPICKVGDFGLSKIKRN**p(T$_{1134}$)**LV**p(T$_{1137}$)**GGVRGTLPW
1148-1205	MAPELLSGSSSKVSEKVDVFSFGIVLWEILTGEEPYANMHYGAIIGGIVNNTLRPTVP
1206-1256	NYCDPEWRMLMEQCWAPDPFVRPAFPEIARRLRTMSSAVHTKPHAVNHQIHK

Activation loop

Figure 2.1.1. Illustration of PXK4 protein sequence. The PXK4 protein sequence consists of 1256 amino acids with 27 identified phosphorylatable serine (**pS**)/ tyrosine (**pT**) sites (ATHENA). Lysine-conserved (K) Type II PB1 domain of PXK4 is underlined.

INDEPENDENT 4 (VIP4; AT5G61150), and 5) DENTIN SIALOPHOSPHOPROTEIN-LIKE PROTEIN (DSLP; At3G54760).

Histone H2B monoubiquitylation (H2Bub1) is essential for regulating transcriptional elongation in eukaryotes mediated by RNA polymerase II (Bourbousse et al., 2012; Himanen et al., 2012). In Arabidopsis, two E3 ligases, HUB2 and its homolog HUB1, interact to transcriptionally modulate plant development such as flowering transition (Woloszynska et al., 2019; Himanen et al., 2012; Gu et al., 2009). E2 ubiquitin-conjugating enzymes, UBC1 and UBC2 are recruited by HUB1 and HUB2, forming a hetero-tetrameric complex that functions to repress flowering by H2B monoubiquitylation of flower repressor genes such as *FLC* (Xu et al., 2009). Recently, another study found that HUB2 coordinates HUB1, SPEN3 and KHD1 to influence pre-mRNA processing of the essential clock gene, CCA1(Woloszynska et al., 2019). Genetic studies of HUB2 have shown that both single mutant accessions, *hub2-1* and *hub2-2*, give an early flowering phenotype compared with Col-0 under both long-day (LD; 16:8) and short-day (SD; 8:16) photoperiods (Woloszynska et al., 2019; Cao et al., 2008). Yet, the phenotype of *hub1*/*hub2* double mutants do not change relative to single mutants, indicating the essential roles of both HUB1 and HUB2 in flowering (Cao et al., 2008). Moreover, mutation of *HUB1* and *HUB2* had differential effects on *FLC* expression in response to CL, with *hub1* and *2* mutants exhibiting a decrease and no effect; respectively (Cao et al., 2008); however, in MD condition when a photoperiod is considered, *FLC* levels were found to decrease in *hub2-2* (Xu et al., 2009). Null alleles of *ubc1* and *ubc2* also show an early flowering phenotype in Arabidopsis (Cao et al., 2008). By contrast, SPEN3 seems to have multiple roles, as *hub1-4*/*spen3-1* double mutants flower like *hub1-4*, whereas a delayed flowering phenotype was observed in *spen3* plants due to an increase of *FLC* regulation by noncoding *FLC* antisense *COOLAIR* (Woloszynska et al., 2019).

Interestingly, while *hub2-2* was successfully rescued by native promoter-driven *HUB2* (Cao et al., 2008), Woloszynska and colleagues found that constitutive over-expression of HUB2 also resulted in an early flowering phenotype but did not elaborate a mechanism. The early flowering phenotype of *hub2* mutants as well as constitutive HUB2 over-expression indicates that HUB2 may form additional, yet unresolved protein complexes involved in flowering transition regulation.

In *Drosophila* and mammals, BRM was known as Trithorax Group (TrxG) SWI/SNF-type chromatin-remodeling ATPase that interplays against repressive Polycomb group (PcG) to regulate gene expression (Li et al., 2015; Farrona et al., 2004). Similarly, in Arabidopsis, BRM (AtBRM) is suggested to have a role in inhibiting PcG activities during plant development (Li et al., 2015). It was demonstrated by Li et al. (2015) that AtBRM can replace PcG proteins that binds to *SVP*, resulting in a decrease of H3K27me3, which is known as a histone marker for transcriptional inactivation. As a PcG member, POLYCOMB REPRESSIVE COMPLEX 2 (PRC2) functions to suppress gene transcription by catalyzing H3K27me3 (Schmitges et al., 2011). AtBRM is also recruited by SOC1 to intersect with the histone demethylase RELATIVE OF EARLY FLOWERING 6 (REF6), and age-regulated transcription factor SQUAMOSA PROMOTER BINDING PROTEIN-LIKE 9 (SPL9) to reduce H3K27me3 levels (Richter et al., 2019; Li et al., 2016). Furthermore, phenotypic analysis of *brm* mutants with observed early flowering under both LD and SD conditions (Farrona et al., 2004) revealed a role of BRM in regulating flowering in response to photoperiod. Molecular analysis of AtBRM found it represses the photoperiod pathway as loss-of-function *brm* gives rise to increased *CO* expression levels, as well as increases in the downstream floral integrator, *FT*, in respect to Col-0 (Farrona

et al., 2011). Consistent with these findings, when *ft-10/brm-2* and *co*/*brm-2* double mutants were compared with their corresponding single mutants, the delayed flowering phenotype of *ft-10* and *co* is partially rescued, which provides genetic evidences on BRM involvements in response to photoperiod (Farrona et al., 2011).

VERNALIZATION INDEPENDENT PROTEIN 4 (VIP4) is a member of Arabidopsis RNA polymerase II-associated factor 1 (Paf1) Complex (Paf1C) which is homologous to the budding yeast protein, Leo1 (Oh et al., 2004; Zhang & Van Nocker, 2002). In yeast, Paf1 Complex (Paf1C) is known to activate transcriptional regulation through histone H3 methylation (Krogan et al., 2003). Likewise, Arabidopsis Paf1C complex (VIP2,3,4,5,6, CDC73) is involved in transcriptional regulation of FLC before vernalization (Yun et al., 2011; Yu & Michaels, 2010; Park et al., 2010; He et al., 2004). Genetic evidence indicates that multiple *VIP* genes are involved in flowering, as mutations of *vip-2*/*elf7*, *vip-3*, *vip-4*, *vip-5*, *vip-6/elf8* and *cdc73* all displayed early flowering phenotypes. Correspondingly, loss-of-function *paf1c* mutants giving rise to significant decreases in *FLC* transcript levels in vegetative tissues (Yu & Michaels, 2010; He et al., 2004; He et al., 2004; Oh et al., 2004; Henderson et al., 2003).

Alternative splicing of precursor messenger RNA (pre-mRNA) plays an important role in diversifying the proteome for the biological activities across all eukaryotes (Nilsen & Graveley, 2010). In plants, Arabidopsis Splicing Factor 1 (AtSF1) has been characterized to participate in alternative splicing of Arabidopsis pre-mRNA (Jang et al., 2014). In a similar manner to its homolog, mammalian SF1, AtSF1 interacts with two spliceosomal U2 small nuclear ribonucleoproteins (snRNPs) auxiliary factor 65 isoforms, AtU2AF65a and AtU2AF65b, to affect plant development (eg. flowering transition) by

recognizing the 3'-splice sites (Park et al., 2019). Genetic analysis of single *sf* mutants has demonstrated early flowering phenotypes (Jang et al., 2014), whereas *atu2af65a* and *atu2af65b* mutants exhibited delayed flowering and slight early flowering, respectively (Park et al., 2019; Xiong et al., 2019). Maintaining a conserved functional RNA recognition motif (RRM) domain, AtSF1 has also recently been described to alter the pre-mRNA splicing of *FLM* genes following a change in temperature (**Figure 3.1.2**; Lee et al., 2017). Although the RRM domain of AtSF1 is not the main factor determining its temperature dependent binding to AtU2AF65 proteins, it does affect the alternative splicing of *FLM*, resulting in a decrease in *FLM-β* expression in *atsf1* mutants (Lee et al., 2017). At a low ambient temperature, flowering integrators like FT and SOC1 are highly suppressed due to the accumulation and binding of *FLM-β*-SVP inhibitive complexes (Wang et al., 2020). Meanwhile, AtU2AF65a is sensitive to ambient temperature for pre-mRNA splicing of *FLM* (Verhage et al., 2017) and AtU2AF65b is suggested to be involved in the alternative splicing of *FLC* and *ABSCISIC ACID- INSENSITIVE 5* (*ABI5*) in response to ABA signals (Xiong et al., 2019).

Unlike the other putative PXK4 substrates, there is only preliminary evidence that DSLP (Dentin Sialophosphoprotein-Like Protein; AT3G54760) is involved in flowering. The role of DSLP in flowering transition has been suggested to occur through FVE/MSI4, which is a known promoter of flowering that functions by suppressing FLC through histone de-acetylation (Kenzior & Folk, 2015; Ausín et al., 2004). Evolved from gene duplication event and further specialization, DSLP possesses a unique RNA recognition motif (RRM) domain near C-termini, which is homologous to other plant-specific RRM proteins, thus allowing it to interact with FVE (Kenzior & Folk, 2015). Although the biological functions

of DSLP have not yet been fully understood (Zhou et al., 2018), the connections between its RRM proteins and FVE have suggested a role in the regulation of flowering.

The onset of flowering is determined by intersection of different flowering networks (Blümel et al., 2015). With five PXK4 substrate candidates related to flowering being resolved by the phosphoproteomic analysis of *pxk4-2*, it is likely that PXK4 regulates flowering transition through one or more flowering related substrates, potentially in relation to the time-of-day / photoperiod. In this chapter, I provide genetic evidence that implicates *PXK4* in the regulation of these flowering regulators. In particular, I focus on HUB2, which maintained the largest fold-change in its phosphorylation status in the *pxk4-2* mutant.

2.2. Materials and Methods

2.2.1 Plant Growth Conditions

Arabidopsis seeds were imbibed in a 0.5x Murashige and Skoog medium (MS), pre-sterilized with a solution of 0.05% (v/v) Triton X-100 and 70% ethanol for 10 minutes, followed by 95% ethanol for 5 minutes. Sterile seeds were subsequently stratified for 48 h at 4℃. Seeds were then grown under either continuous (CL; 24:0), long-day (LD; 16:8), mid-day (MD; 12:12), or short-day (SD; 8:16) growth conditions for either 7 or 14 days before transplanting. Individual seedlings of interest were introduced to into 2 ½ ″ pots containing pre-moist soil (Sungro Horticulture Professional Growing Mix; http://www.sungro.com/), and then brought to the corresponding chambers for growth subject to change (22 °C, 60% RH, level 1, Conviron).

2.2.2 Generation of Single Mutant Lines

Single mutant line seeds, *pxk4-2* (*SALK_107170*; **Figure 2.3.1**), *brm-3* (*SALK_088462*), *brm-5* (Tang et al., 2008), *vip4-1* (*CS68978*), *hub2-1* (*GABI_634H04*), *hub2-2* (*SALK_071289*), *sf1-1* (*SALK_009238*), *fve* (*SALK_062232C*), *ft-10* (Yoo et al., 2005), *flc-1* (*SALK_041126*), were obtained from the Arabidopsis Biological Resource Center (ABRC). Two other *pxk4* mutant lines, *pxk4-4* (*GABI_776D02*), *pxk4-5* (*GABI_702G09*) were obtained from the University of Bielefeld (https://www.gabi-kat.de/). Transgenic *soc1-2* seeds (Lee et al., 2000) were obtained from Cameron Lab (Department of Biology, McMaster University, ON, Canada). The primers used for verifying homozygosity are listed in **Table 2.2.1**. Given the mutation type associated with the *vip4-1* mutant plant line, *vip4-1* plants were selected from 30 µg/µl BASTA 0.5x MS plates (Zhang & Van Nocker, 2002). All the control groups used the same primers for PCR screening, except for *soc1-2* was screened by soc1-2_Col-0 and soc1-2_RP. For the extraction of genomic DNA, Arabidopsis rosettes were ground in 1xDNA extraction buffer (Tris-HCl, pH=8.0, NaCl, EDTA, 10% (w/v) SDS). The homozygosity of each line was confirmed by PCR (**Figure 2.2.1**).

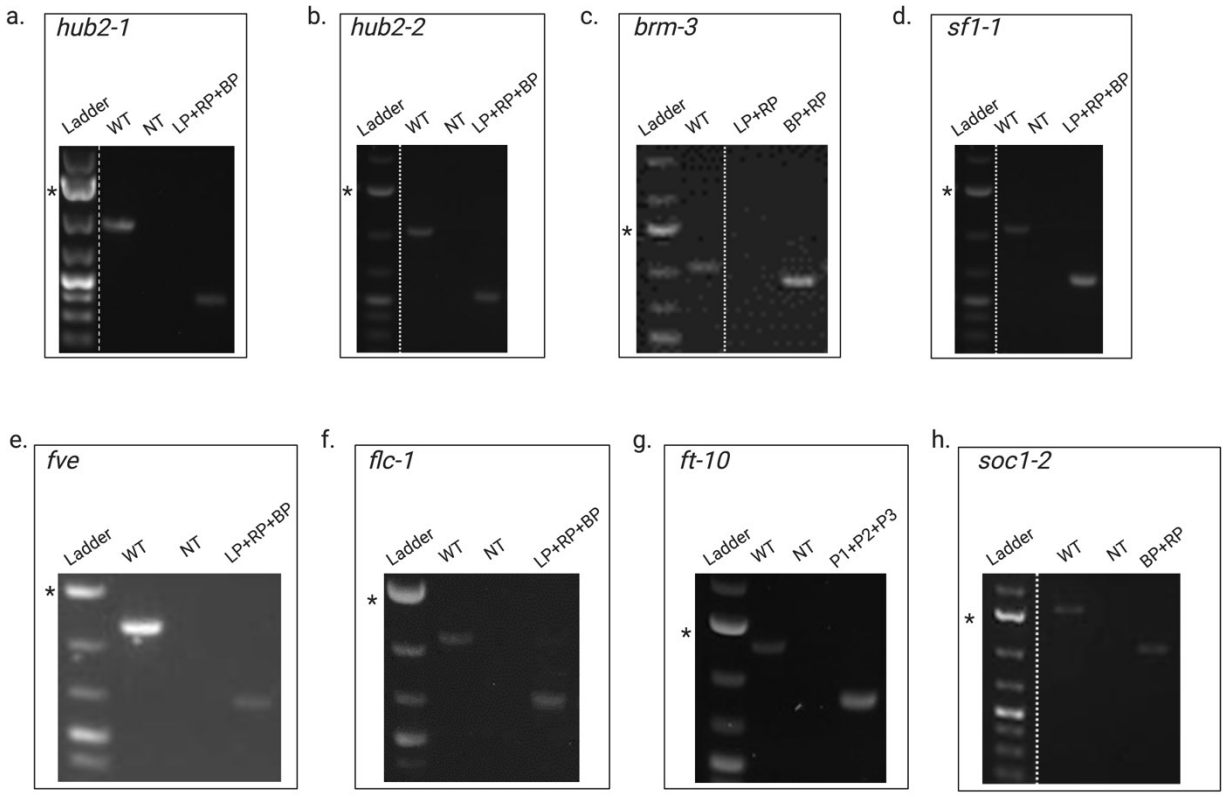

Figure 2.2.1 Homozygous Arabidopsis accessions. a-g. Homozygous *hub2-1*, *hub2-2*, *brm-3*, *sf1-1*, *fve*, *flc-1*, *ft-10*, *soc1-2*. "*" =1500 bp; WT= Col-0; NT = water control; LP = Left primer; BP = Border primers; RP = Right primers.

Table 2.2.1 Primers used for PCR screening.

Primers	(5' → 3')
brm-3_LP	CTGGGAATGAAGAAGAGGGAG
brm-3R_RP	GACCTTCCTTGTCGATTCTCC
hub2-1_LP	CCGTTTTGTGCTTTTCTTGTC
hub2-1_RP	TTGGTTCTGTGTCTGCATGTC
hub2-2_LP	CATGGTACCACATCCAAGGTC
hub2-2_RP	CCTCTTTAGGCCGATCAAAAC
sf1-1_LP	AAGGGAAGTTCGAGAAGGTTG
sf1-1_RP	TCATCCAAAGGCATACCAGAC
fve_LP	GGAGAGCATGTGCTGAGAGTC
fve_RP	ACCTGATCCCTTACCAGCTTC
ft-10_P1	TAAGCTCAATGATATTCCCGTACA
ft-10_P2	CAGGTTCAAAACAAGCCAAGA
ft-10_P3	CCCATTTGACGTGAATGTAGACAC
pxk4-2_LP	CTTGTGGATTTGGTGGTTGAC
pxk4-2_RP	TTATGGCATTTTACGGCGTAG
pxk4-4_LP	GCTTTCAGCACCTTTGATTTG
pxk4-4_RP	ATCAAGCCCTCAAGGAAGAAG
pxk4-5_LP	ATCAAGCCCTCAAGGAAGAAG
pxk4-5_RP	GCTTTCAGCACCTTTGATTTG
flc-1_LP	CAAGGCTGGACCTAACTAGGG
flc-1_RP	TCATTGGATCTCTCGGATTTG
soc1-2_Col-0	TGACTTCATCAGTCTTCTCCCA
soc1-2_BP	GTTCACGTAGTGGGCCATC
soc1-2_RP	ATATCACAAACCGTTTAGAAGCTTC

2.2.3 Generation of Double Mutant Lines

The candidate single mutant lines *hub2-1* and *hub2-2* were manually crossed with *pxk4-2* to generate two double mutant lines (*hub2-1/pxk4-2* and *hub2-2/pxk4-2*). The newly opened flowers or maturing buds were selected for the crosses (**Figure 2.2.2**), with

dissected maternal flowers of the candidate lines keeping only the pistils; we then dipped the candidate pistils with pollen (on the tip of stamens) from *pxk4-2* flowers. Pollinated pistils were then wrapped with plastic seals to prevent pollen contamination. Subsequently, F1 seeds were collected from dried siliques, then germinated as above and screened by PCR for the presence of a T-DNA insert in both genes of interest as heterozygotes. Next, the heterozygous double mutant lines were grown for another generation F2 as above (2.2.1 Plant Growth Conditions). This generation was examined again for the homozygosity by PCR. Homozygous plant seeds were then harvested for phenotyping.

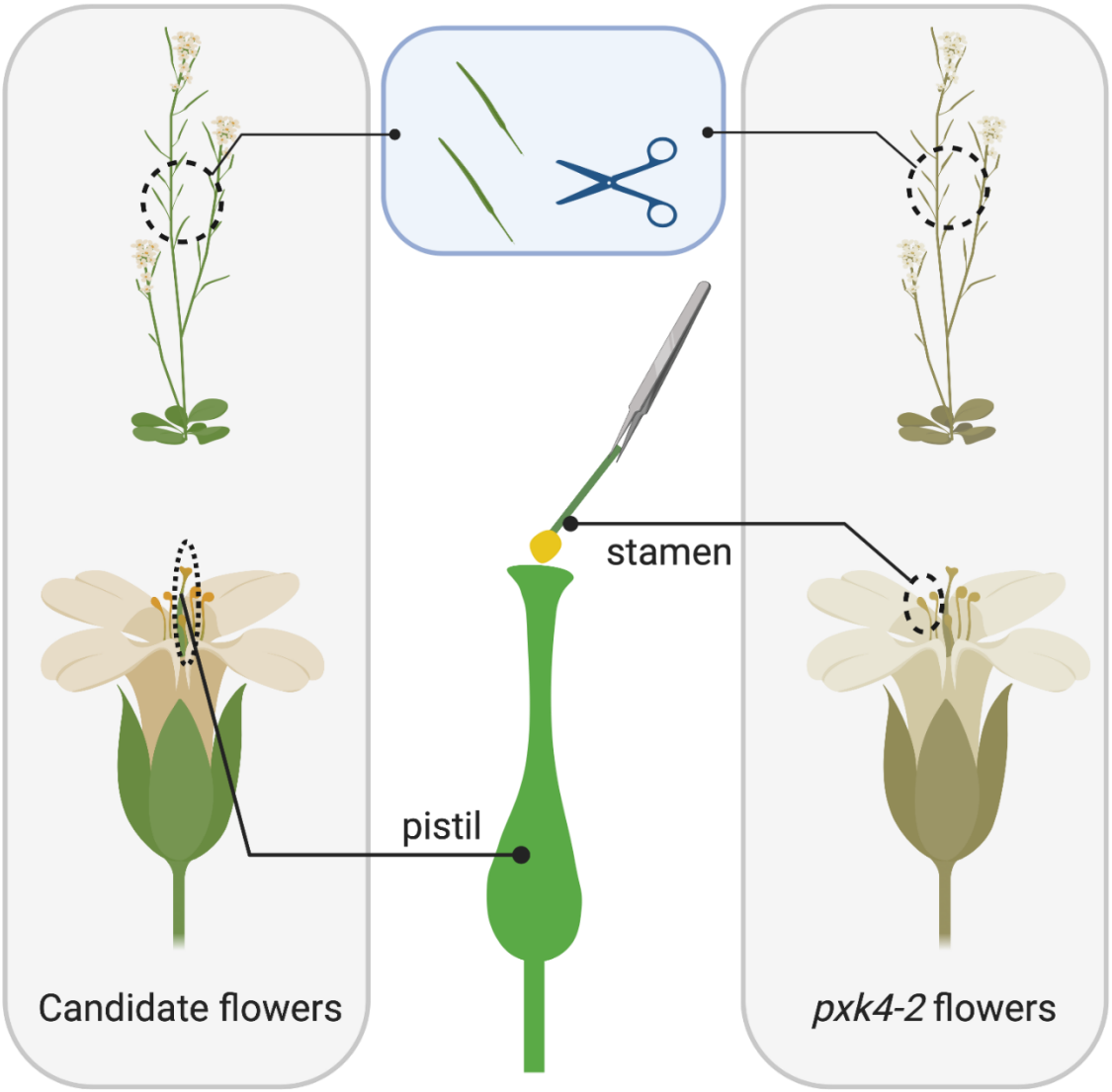

Figure 2.2.1 Illustration of Arabidopsis cross-pollination. Siliques, petals, and stamens of maternal plants (left) were removed prior to cross-pollination. The “naked” pistils of candidate flowers were pollinated manually with *pxk4-2* stamens as indicated.

2.2.4 Phenotyping

Pre-sterilized and pre-stratified (4℃, 24h) homozygous *brm-3*, *brm-5*, *pxk4-2*, *flc-1*, *hub2-1*, *hub2-2*, *sf1-1*, *vip4-1*, *ft-10*, *soc1-2*, *fve* and Col-0 Arabidopsis seeds were imbibed in 0.5x MS plates and placed in custom-built controlled LED light enclosures

(G2V Optics Inc.) with exposure to either CL, LD, MD or SD light for 7 days (d). Subsequently, five of the young seedlings for each line were transplanted to 2 ½″ pots containing pre-moist soil correspondingly. Photos were taken automatically each day using a custom Raspberry Pi camera setup constructed in-house, with all images processed using the PlantCV phenomics suite (Berry et al., 2018; Gehan et al., 2017; Abbasi et al., 2017; Fahlgren et al., 2015; https://plantcv.danforthcenter.org/). Days-to-bolting (DTB) and Leaf Counts at Bolting (LCB) were recorded accordingly.

Homozygous *pxk4-2*, *pxk4-4*, *pxk4-5*, *hub1-2*, *hub2-1, hub2-1/pxk4-2, hub2-2/pxk4-2*, and Col-0 were imbibed as above and placed in custom-built controlled LED light enclosures with exposure to continuous and long-day light for 7 d prior to transplanting. Photos were taken automatically by Raspberry Pi camera as previously described above. All photos were processed using the PlantCV phenomics suite (Berry et al., 2018; Gehan et al., 2017; Abbasi et al., 2017; Fahlgren et al., 2015; https://plantcv.danforthcenter.org/). DTB and LCB were recorded accordingly.

2.3 Results

2.3.1 Discovery of PXK4 substrates related to flowering

Examination of *pxk4-2* found five flowering-related proteins whose phosphorylation status significantly declined (**Table 2.3.1**), among which, HUB2 phosphorylation decreased below detection at $pSer^{314}$ (**Table 2.3.1**). Four other flowering-related proteins also exhibited decreases in phosphorylation. These include: AtSF1, VIP4, DSLP, and AtBRM (**Table 2.3.1**).

Table 2.3.1 Identification of PXK4 substrates. Decreases in the phosphorylation status of Arabidopsis SF1, VIP4, BRM, HUB2, DSLP proteins in *pxk4-2* plants in relation to Col-0. Data were obtained by comparatively assessing quantitative changes in the phosphoproteome between *pxk4-2* and Col-0. (Student's t-test, *p-value ≤ 0.05*)

Leading proteins	Description	SUBA3	Phosphorylation site	Phospho (STY) Probabilities	Log2FC	TTEST	Pathway (s)	References
AT2G46020	BRM transcription regulatory protein SNF2	nucleus	pSer2055	0.889	-1.24531	0.02817202	Autonomous	Li et al., 2015; Farrona et al., 2011; Tang et al., 2008; Hurtado et al., 2006; Farrona et al., 2004
AT3G54760	DSLP,dentin sialophosphoprotein-like protein	nucleus	pSer389	0.946	-0.529786	0.03608485	Autonomous	Kenzior and Folk, 2015
AT5G61150	VIP4, leo1-like family protein	nucleus	pSer600 pSer605	1	-0.522254	0.02572128	Vernalization	Zhang et al., 2002
AT5G51300	SF1,splicing factor-like protein	nucleus	pSer77 pSer 84	1	-0.149607	0.0460342	Ambient	Lee et al., 2017
AT1G55250	HUB2, histone mono-ubiquitination 2	nucleus	pSer314	0.94	Inf	0.01712188	Autonomous Photoperiod	Chen et al., 2019; Gu et al., 2009; Cao et al., 2008; Liu et al., 2007

- SUBA3 = Subcellular localization
- Inf = Infinity
- pSer = phosphorylated Serine

2.3.2 Genetic connections between PXK4 and its substrates for flowering regulation

To understand where PXK4 is positioned within the complex network of flowering transition, the *pxk4-2* mutant allele was examined for its DTB and LCB properties relative to Col-0. Here, *pxk4-2* was found to take significantly fewer DTB with fewer LCB than Col-0 under CL, LD, and MD (**Figure 2.3.3a-c; Figure 2.3.4; Figure 2.3.5a)**, whereas no early flowering phenotype, but significantly fewer LCB, was observed in SD (**Figure 2.3.3d; Figure 2.3.4; Figure 2.3.6**). Likewise, the leaf area of *pxk4-2* was much smaller compared to Col-0 even in SD conditions (**Figure 2.3.7-2.3.8**).

Subsequent analysis of two additional *pxk4* mutant lines, *pxk4-4* and *pxk4-5*, supported earlier findings observed with *pxk4-2*. In particular, that *pxk4-4* and *pxk4-5* also possess early flowering phenotypes under LD (**Figure 2.3.9a, c**). Interestingly, neither *pxk4-4* nor *pxk4-5* flowered early under CL like *pxk4-2* (**Figure 2.3.9a, c**). Consistent with the phenotypic data, *PXK4* transcripts in *pxk4-2* are significantly less abundant when assessed using primers amplifying the 5' terminus (P1) versus 3' terminus (P2), while no difference between P1 and P2 was observed in *pxk4-4* or *pxk4-5* (**Figure 2.3.1c)**. With *pxk4-2* showing the strongest phenotype of the 3 lines, *pxk4-2* was ultimately selected for studying how *PXK4* is regulating flowering.

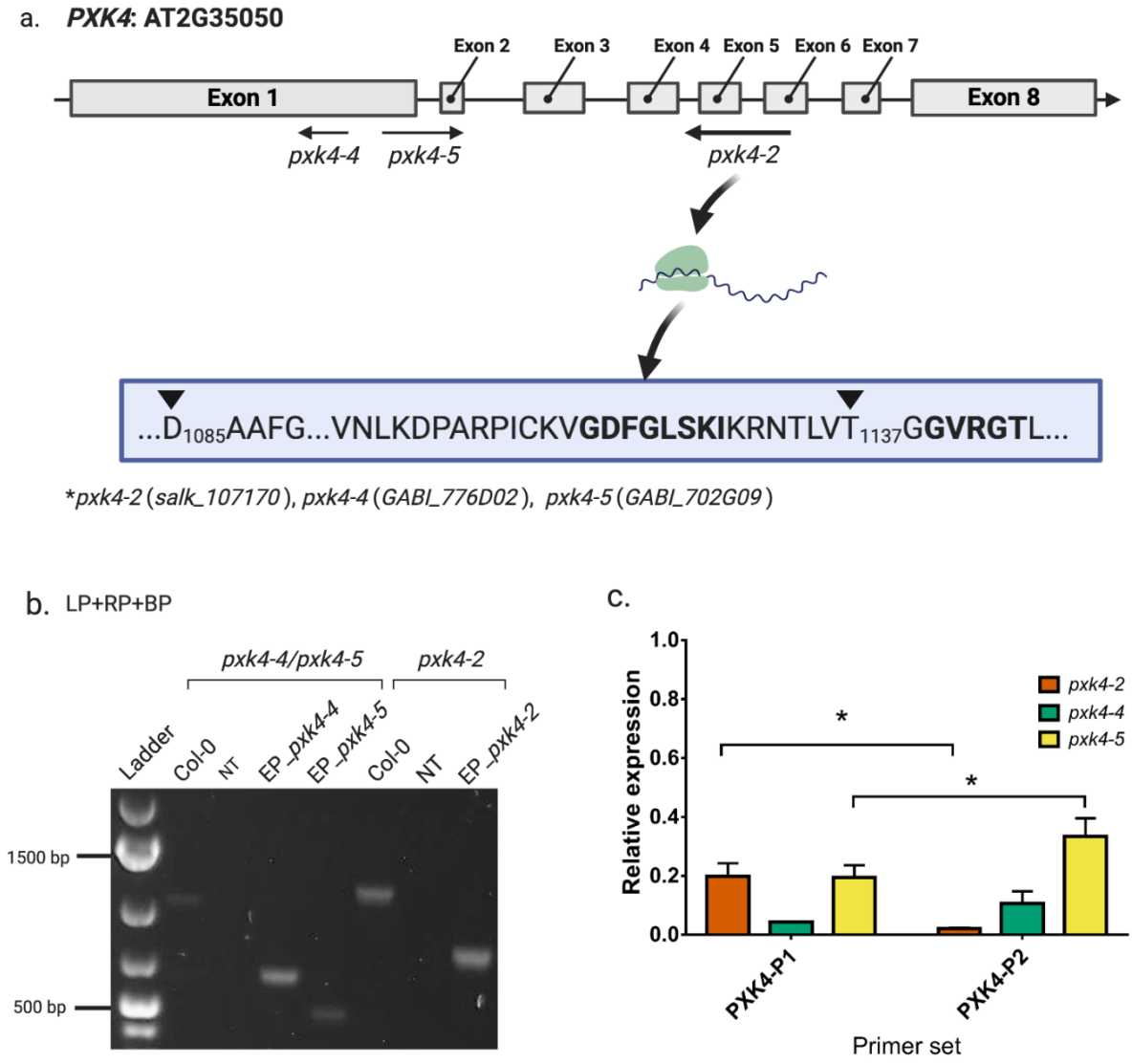

Figure 2.3.1 Arabidopsis *pxk-2*, *pxk4-4*, *pxk4-5* T-DNA insertion lines. a. *PXK4* T-DNA insertion lines, *pxk4-2* (Exon 5 and 6), *pxk4-4* (Exon 1), and *pxk4-5* (Exon 1 and 2) at the *PXK4* loci. T-DNA insertion of *pxk4-2* occurs between D_{1085} and T_{1137} as indicated. Activation loop is in bold. **b.** Arabidopsis *pxk4-2* SALK line and *pxk4-4* and *pxk4-5* GABIKat lines tested for homozygosity. The primers used are listed in **Table 3.2.2**. LP=Left Primer, RP=Right Primer, BP= Border Primer, NT=Negative Control and depicted along with EP= Experimental result. **c.** Relative expression analysis of *PXK4* in *pxk4* mutants under LD light conditions harvested at end-of-night. The transcript levels of 14-day-old *pxk4-2*, *pxk4-4*, *pxk4-5* mutants grown under LD light conditions and analyzed with P1 and P2 primer sets were compared. Data were normalized against Col-0 *PXK4* expression levels (Student's t-test * *p-value* ≤ *0.05*).

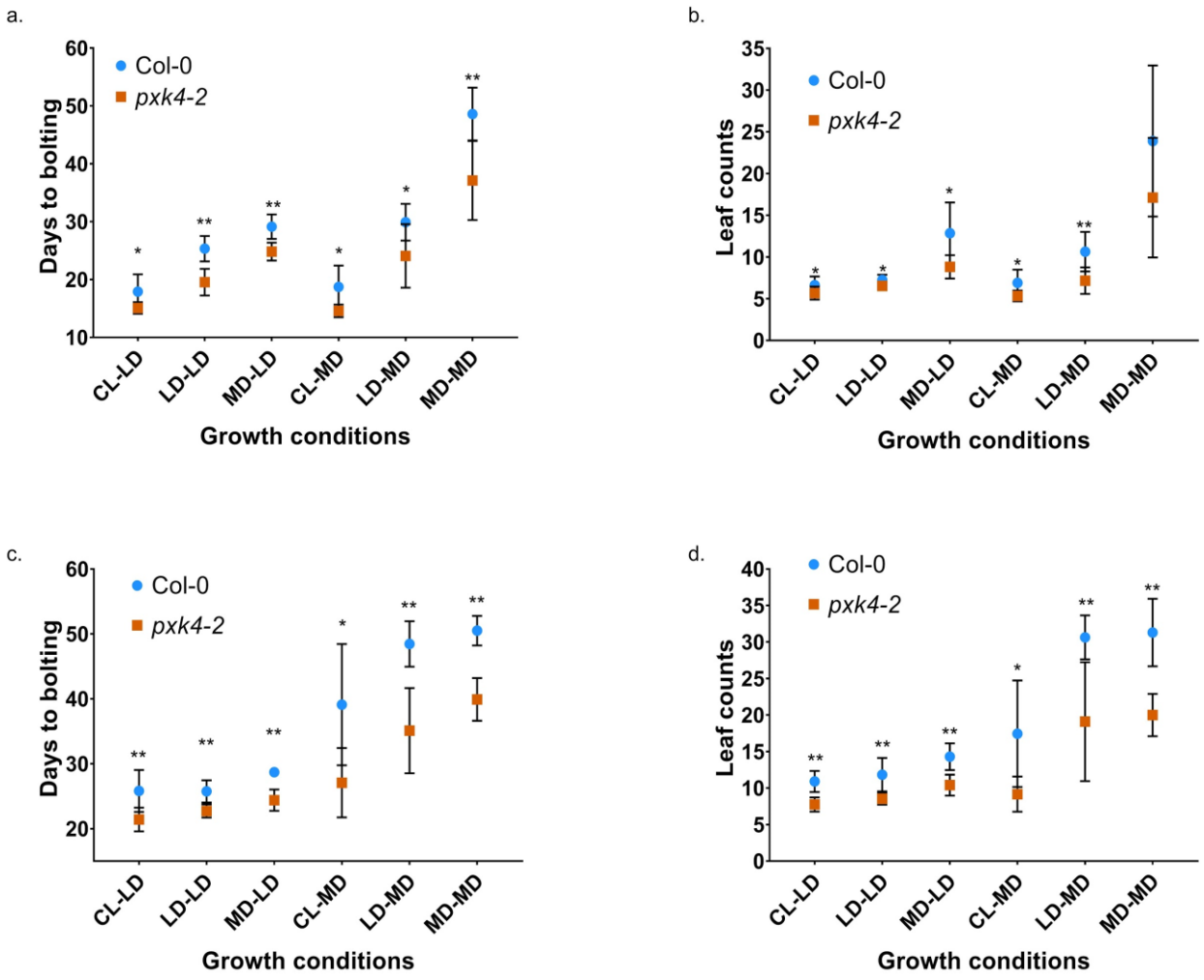

Figure 2.3.2 Comparison of *pxk4-2* versus Col-0 flowering in response to varied photoperiod during germination versus soil growth. **a.** DTB and **b.** LCB for Arabidopsis plants germinated for 14 d under CL, LD and MD. **c.** DTB and d. LCB for Arabidopsis plants germinated for 7d under CL, LD and MD. After germination, 14 d and 7 d seedlings were transplanted into soil and placed in either LD (-LD) or MD (-MD). Student's t-test * *p-value* ≤ *0.05*, ** *p-value* ≤ *0.01* is shown.

Next, *p*xk*4-2* was assessed using a light transition assay, to see if germination under one light condition could augment later growth outcomes under a different light condition. Since we, and many labs, germinate seeds under constant light on MS plates followed by transplanting to soil for growth under a photoperiod, it was important to assess if germination conditions prior to transplant were impacting the observed flowering. Furthermore, this experiment was aimed at dissecting the importance of PXK4 photoperiod regulation of flowering. Here, using 7 DPI (days post-imbibition) plate germinated seedlings, *pxk4-2* demonstrated consistent early flowering relative to Col-0 under all subsequent soil grown conditions. However, late transplantation (14 DPI) of *pxk4-2* to MD chamber from CL and LD led to reduced differences in DTB and LCB between *pxk4-2* and Col-0 (**Figure 2.3.2**). Both Col-0 and *pxk4-2* plants transplanted at 14 DPI were less sensitive to post-transplanting photoperiodic changes (**Figure 2.3.2**). 14 DPI seedlings under CL conditions transferred to LD conditions, took approximately 15 days to flower, which is similar to 14 DPI seedlings under CL treatment then transferred to MD (**Figure 2.3.2a, c**). By contrast, 7 DPI seedlings transplanted to MD from CL exhibited delayed flowering compared with the ones transplanted to LD from CL (**Figure 2.3.2a, c**). These results highlighted the importance of having photoperiod for triggering flowering, rendering our further interests in investigating photoperiod flowering pathways.

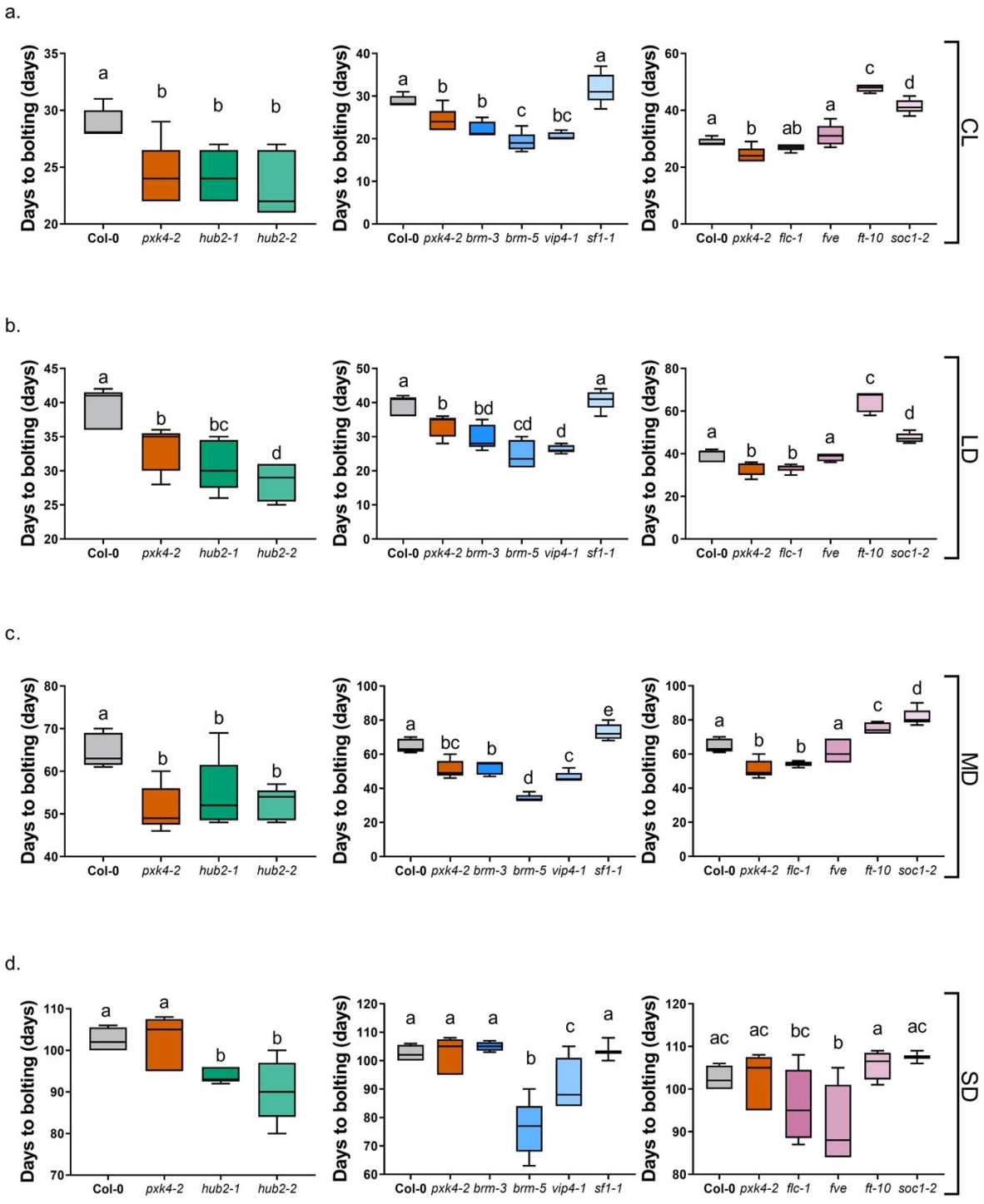

Figure 2.3.3 Flowering time of Arabidopsis flowering mutant lines versus Col-0 under CL, LD, MD and SD. a-d. DTB under CL, LD, MD, SD. Homozygous Arabidopsis PXK4 substrate mutants, *hub2-1*, *hub2-2*, *brm-3*, *brm-5, vip4-1*, *sf1-1*, and flowering mutants *flc-1*, *fve*, *soc1-2*, *ft-10,* along with Col-0 and *pxk4-2,* were grown under CL, LD, MD, and SD light conditions. The DPI (flower initiation) was recorded for each plant (One-way ANOVA *p-value* ≤ *0.05*).

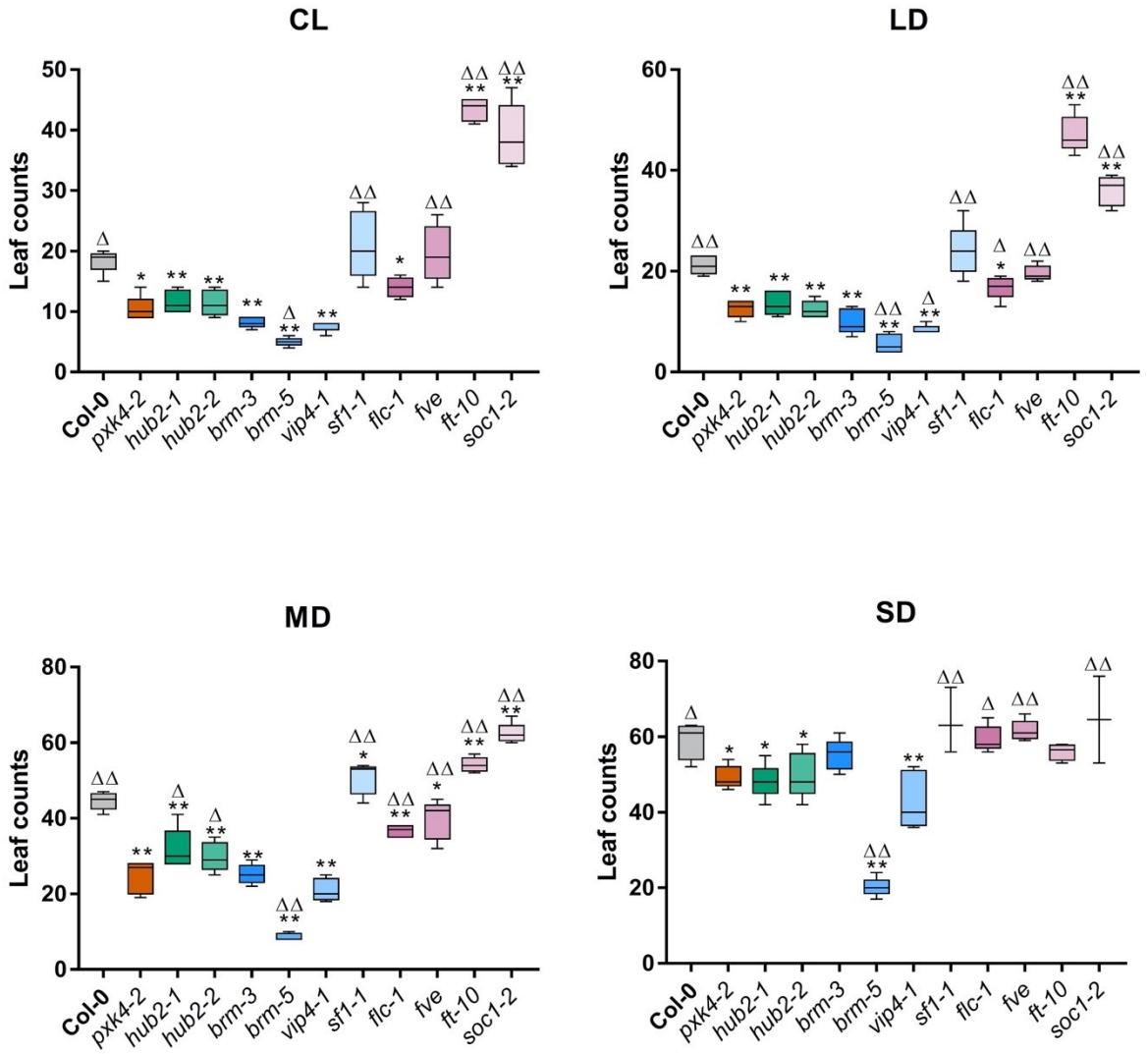

Figure 2.3.4 LCB for Arabidopsis flowering mutant lines under CL, LD, MD and SD. Homozygous Arabidopsis *hub2-1*, *hub2-2*, *brm-3*, *brm-5*, *flc-1*, *vip4-1*, *sf1-1*, *fve*, *soc1-2*, *ft-10* were grown in CL, LD, MD, and SD conditions. LCB was recorded for each plant. Deltas (Δ) and asterisks (*) indicate statistically significant differences were found in relative to *pxk4-2* and Col-0 respectively (Student's t-test Δ/* *p-value* ≤ *0.05*, ΔΔ/** *p-value* ≤ *0.01*).

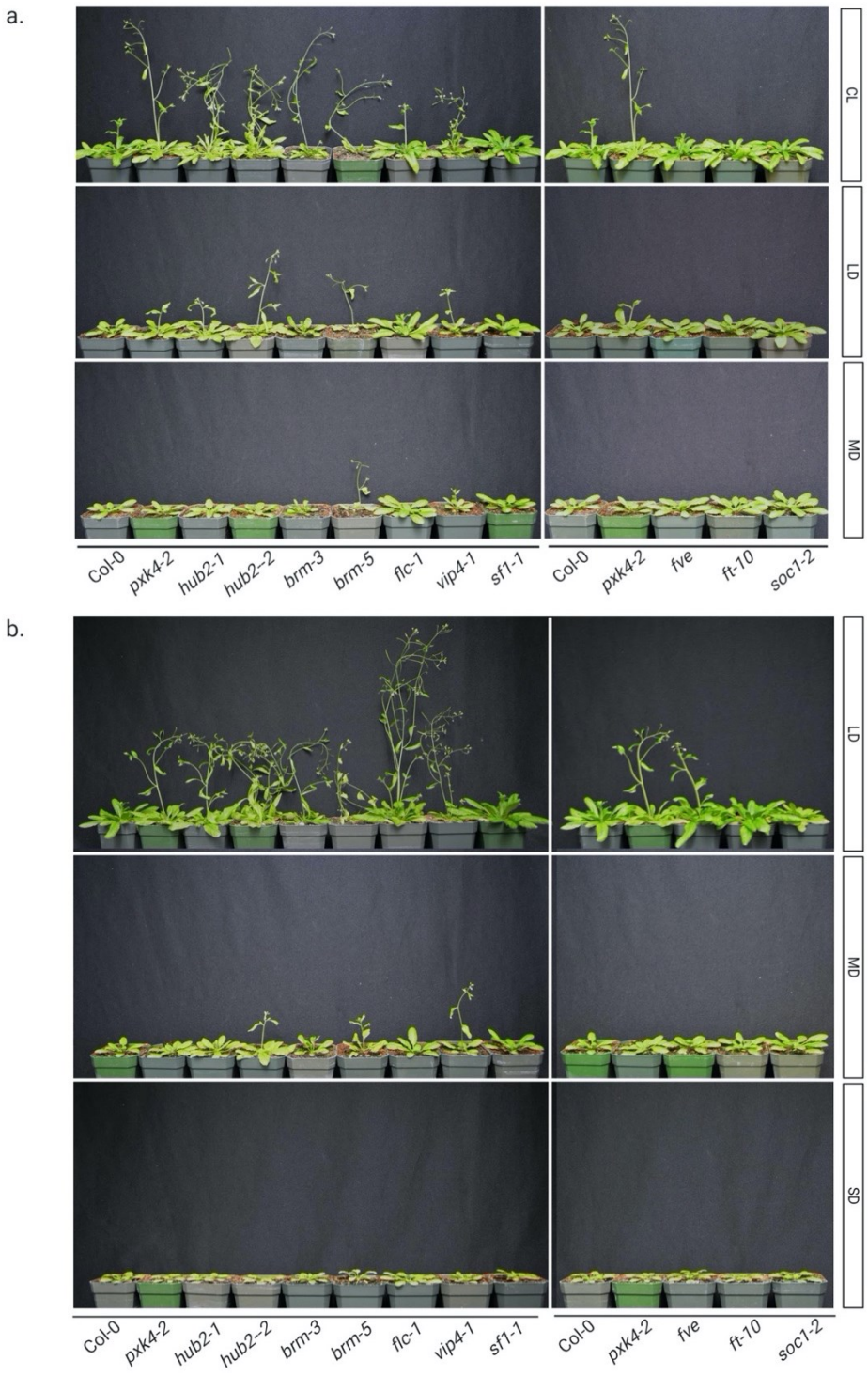

Figure 2.3.5 Developmental analysis of Arabidopsis flowering mutant lines under CL, LD, MD and SD. a. 35-day-old Col-0, *pxk4-2, hub2-1*, *hub2-2*, *brm-3*, *brm-5*, *flc-1*, *vip4-1*, *sf1-1*, *fve, soc1-2, ft-10* under CL and LD. **b.** 49-day-old Col-0, *pxk4-2, hub2-1*, *hub2-2*, *brm-3*, *brm-5*, *flc-1*, *vip4-1*, *sf1-1*, *fve, soc1-2, ft-10* under LD, MD and SD.

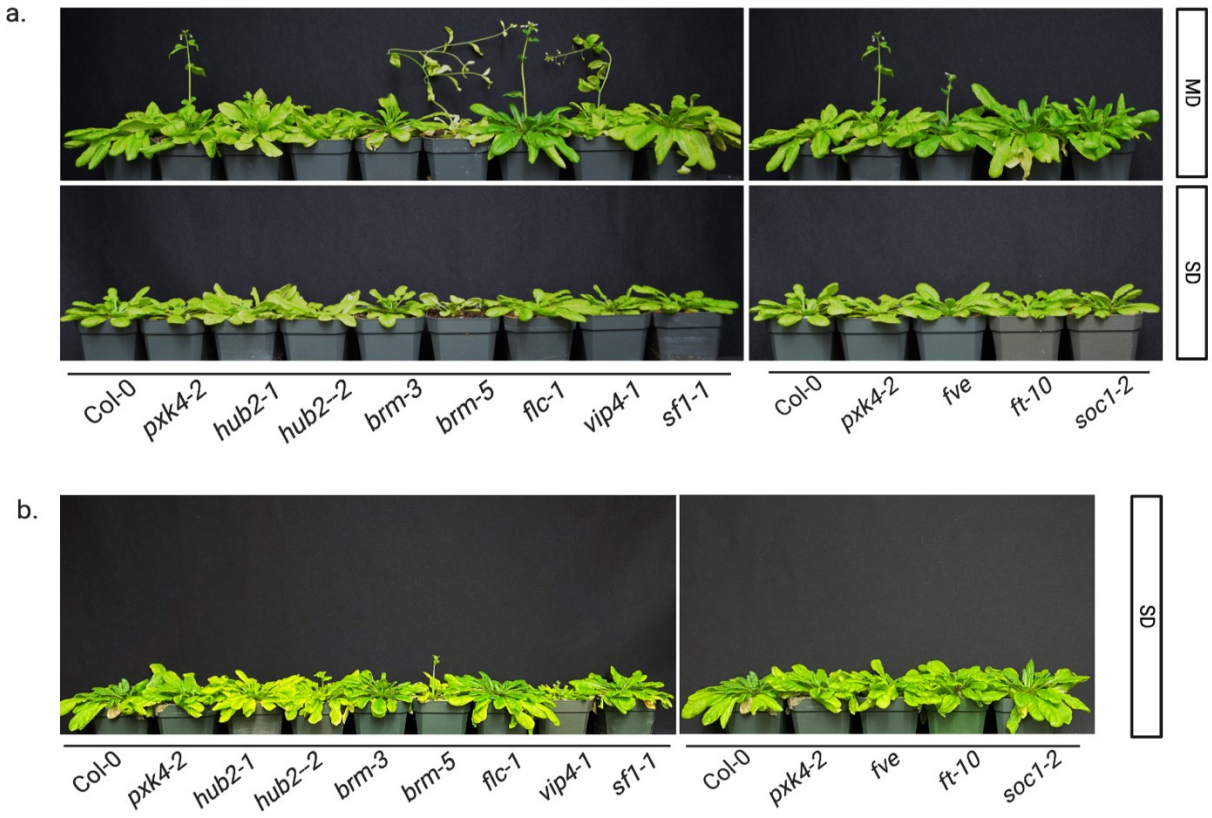

Figure 2.3.6 Side views of 63-day-old and 77-day-old Arabidopsis flowering mutants under MD and SD. a. Comparison of 63-day-old Col-0, *pxk4-2, hub2-1*, *hub2-2*, *brm-3*, *brm-5*, *flc-1*, *vip4-1*, *sf1-1, fve, soc1-2, ft-10* under MD and SD. **b.** 77-day-old Col-0, *pxk4-2, hub2-1*, *hub2-2*, *brm-3*, *brm-5*, *flc-1*, *vip4-1*, *sf1-1*, *fve, soc1-2,* and *ft-10* plants under SD.

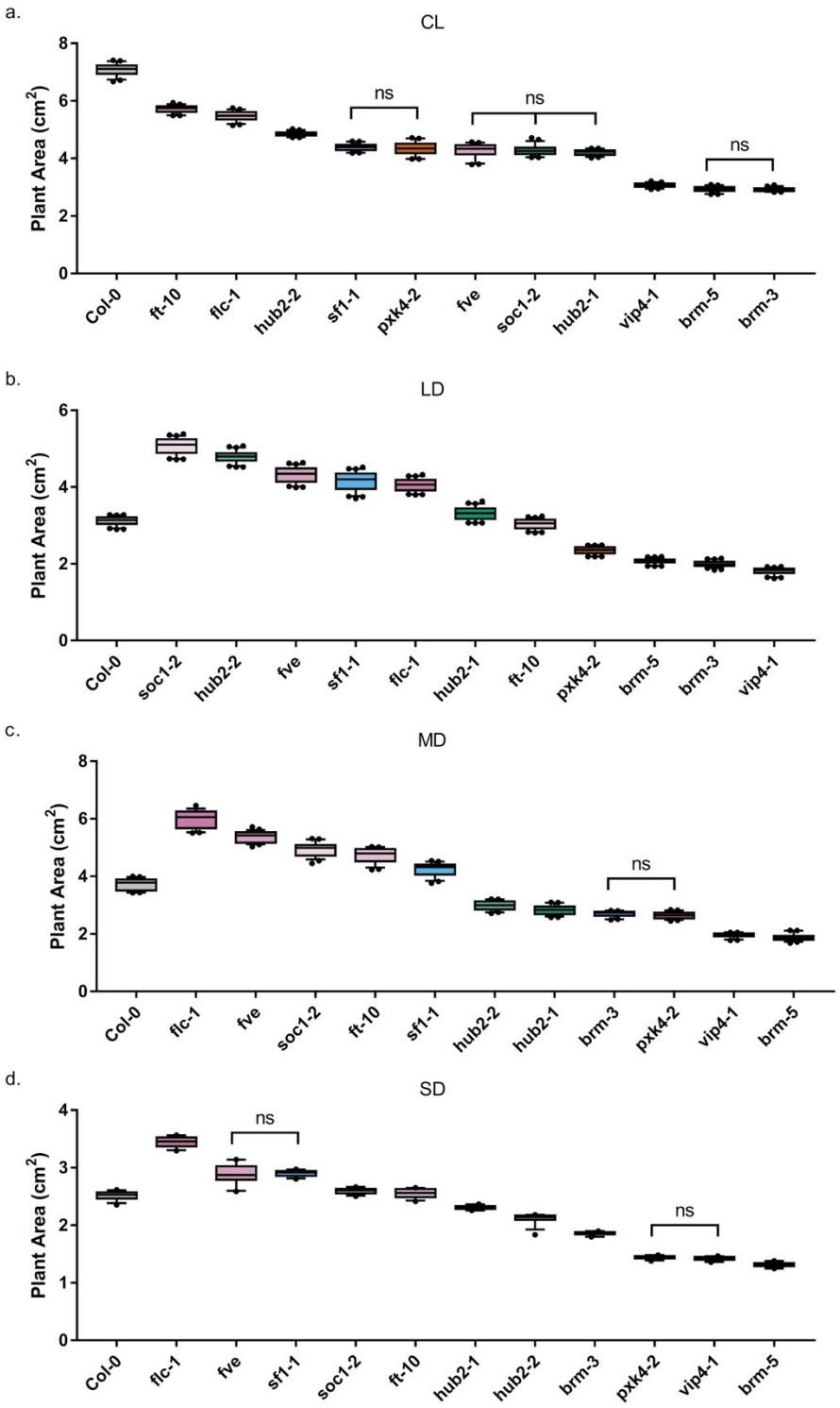

Figure 2.3.7 Leaf area of Arabidopsis flowering mutant lines versus Col-0 under CL, LD, MD and SD. Average leaf area of a. 22 d, b. 25 d, c. 28 d and d. 33 d-old *hub2-1*, *hub2-2*, *brm-3*, *brm-5*, *flc-1*, *vip4-1*, *sf1-1*, *fve*, *soc1-2*, *ft-10* versus Col-0 and *pxk4-2* plants under CL, LD, MD and SD respectively. (One-way ANOVA *p-value* ≤ *0.05*, ns=no significant difference).

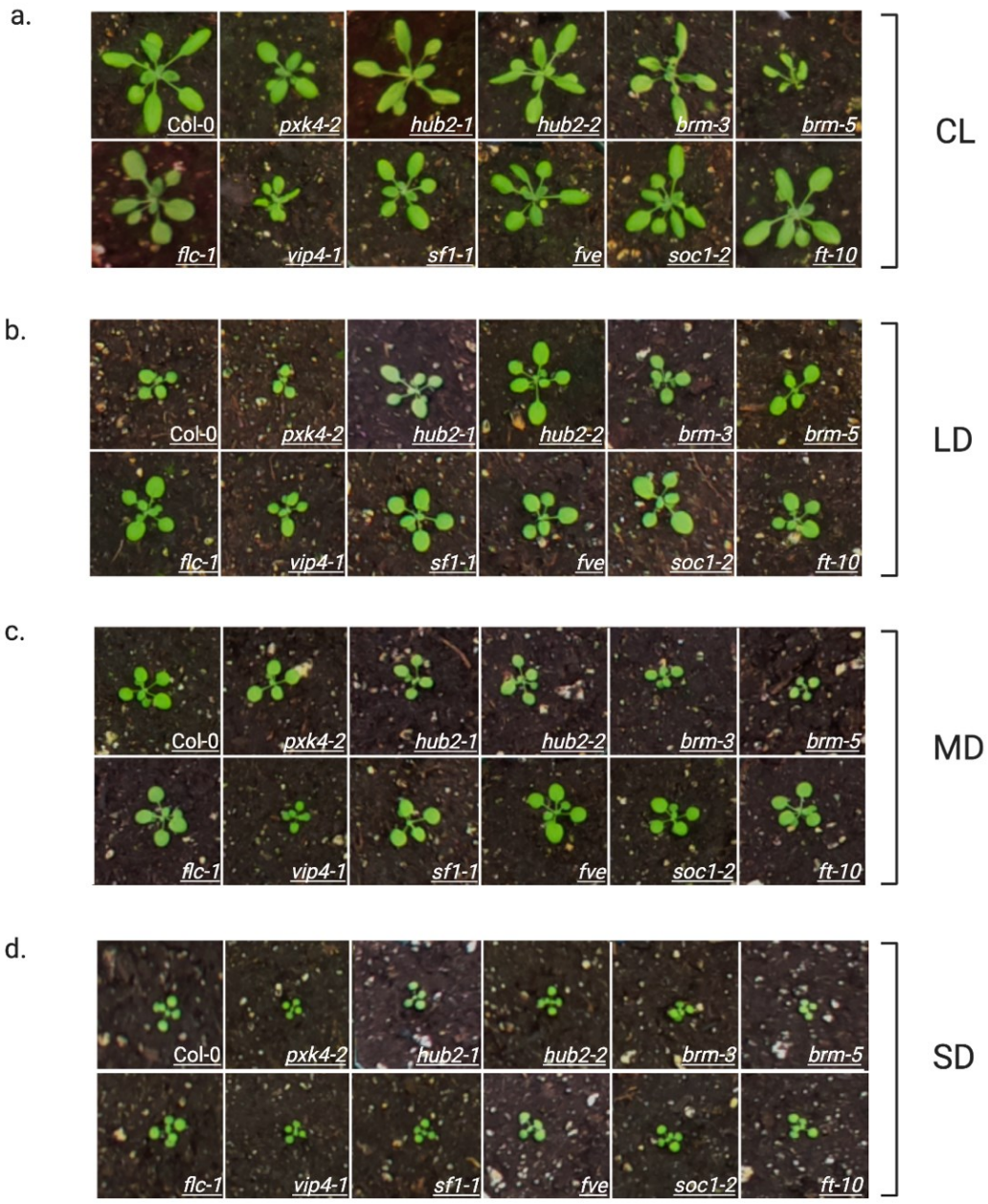

Figure 2.3.8 Rosette growth of 21-day-old Arabidopsis flowering mutant lines versus Col-0 under CL, LD, MD and SD. 21-day-old Arabidopsis *hub2-1*, *hub2-2*, *brm-3*, *brm-5*, *flc-1*, *vip4-1*, *sf1-1*, *fve*, *soc1-2*, *ft-10* versus *pxk4-2* and Col-0 under **a.** CL. **b.** LD. **c.** MD. **d.** SD

To gain insights into the photoperiodic impacts on PXK4-associated flowering, *p*xk*4-2* was compared to established early and delayed flowering mutant lines. This included: *flc* (early flowering), *fve* (delayed flowering), *ft-10* (delayed flowering), and *soc1-2* (delayed flowering); respectively, under the same four growth conditions. Similar to *pxk4-2*, mutation of flower inhibitor *flc* displayed early flowering under LD and MD compared to Col-0, while no significant differences were found in DTB between *pxk4-2* and *flc-1* under CL or SD (**Figure 2.3.3; Figure 2.3.5-2.3.6**). Nevertheless, *pxk4-2* had fewer LCB and a reduced leaf area relative to *flc-1* plants (**Figure 2.3.4**; **Figure 2.3.7-2.2.8).** Mutation of *fve* had early flowering only under SD, and otherwise flowered normally under CL, LD, MD in terms of DTB (**Figure 2.3.3**). The leaf area of *fve*; however, was much greater than Col-0 under LD, MD, and SD (**Figure 2.2.7b-d**). Both mutant flower integrators *ft-10* and *soc1-2* present delayed flowering under CL, LD, and MD as expected (**Figure 2.3.3a-c; Figure 2.3.5; Figure 2.3.6a)**. Consistently, their leaf counts at first bolting were much higher than Col-0 and *pxk4-2* under CL, LD and MD growth conditions (**Figure 2.3.4**).

Next, analysis of published flowering mutant alleles that are putative PXK4 substrates, was performed. This included the examination of mutant alleles for: BRM, SF1, VIP4, and HUB2. The specific alleles examined were *brm-3*, *brm-5*, *sf1-1, vip4-1*, *hub2-1*, and *hub2-2*. Firstly, comparison of *brm* mutants found *brm-3* to exhibit a *pxk4-2* like early flowering pattern, in that they both flowered earlier than Col-0 under CL, LD, MD but not under SD (**Figure 2.3.3-2.3.6**). A stronger early flowering phenotype and smaller rosette size was observed in the point-mutated *brm-5* mutant regardless of light conditions (**Figure 2.3.3-2.3.7**). Likewise, significantly reduced DTB, LCB and rosette

area was observed relative to Col-0, while *vip4-1* bolted early under all light conditions (**Figure 2.3.3-2.3.7**). Conversely, ambient-sensitive splicing factor mutant allele *sf1-1* bolted like Col-0 under CL, LD, SD, with a delay in bolting observed in the MD growth condition (**Figure 2.3.3**). The last putative PXK4 substrate mutant, *hub2-1* and *hub2-2*, both consistently displayed early flowering under all four light conditions (**Figure 2.3.3**). The DTB of *hub2-1* or *hub2-2* did not differ much from *pxk4-2* under CL, LD and MD, neither the leaf number at first bolting under CL, LD, and SD (**Figure 2.3.3-2.3.6; Figure 2.3.9**). Yet, in terms of the vegetative growth, *hub2* mutants had a relatively larger leaf area than *pxk4-2* (**Figure 2.3.7**-**2.3.8**).

The genetic relationship between HUB2 and PXK4 was examined by comparing *hub2-1*/*pxk4-2* and *hub2-2*/*pxk4-2* double mutants to *hub2-1*, *hub2-2*, and *pxk4-2* single mutants (**Figure 2.3.9**). Phenotypic examination of these mutant lines found that *hub2-1*/*pxk4-2* and *hub2-2*/*pxk4-2* double mutants flowered significantly earlier than the corresponding single mutants under CL and LD (**Figure 2.3.9a, c**). Under CL conditions, an approximate 30% and 15% decrease in DTB was observed in *hub2-1*/*pxk4-2* and *hub2-2*/*pxk4-2* double mutants, versus Col-0 and *pxk4-2*, respectively, while under LD, an approximate 20% and 10% decrease of DTB was observed **(Figure 2.3.9b**).

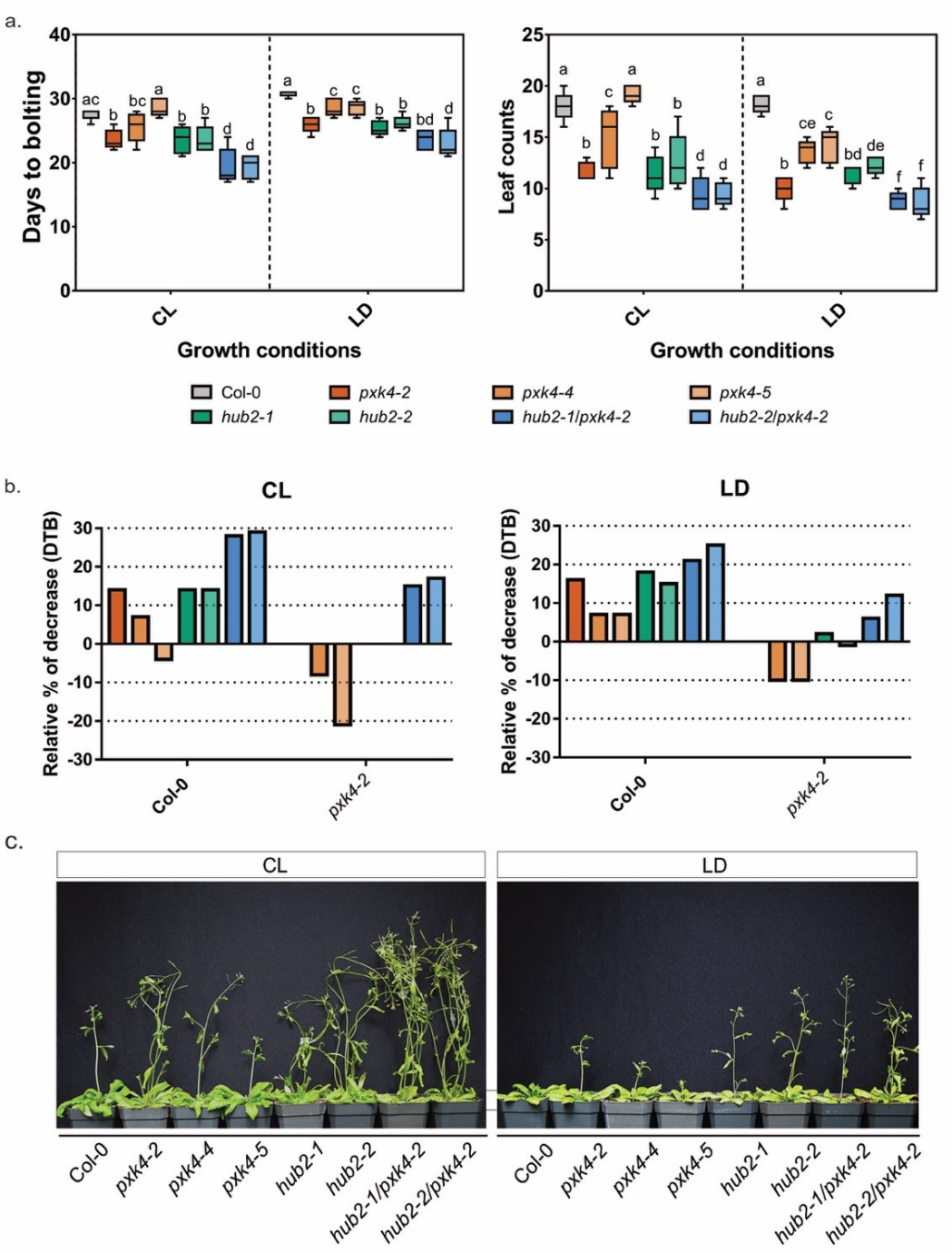

Figure 2.3.9 Flowering time of Arabidopsis *hub2-1*, *hub2-2*, *hub2-1*/*pxk4-2*, *hub2-2*/*pxk4-2* versus *pxk4* mutants and Col-0 under CL and LD light. a. Flowering time of Arabidopsis *hub2-1*, *hub2-2*, *hub2-1*/*pxk4-2*, *hub2-2*/*pxk4-2* versus *pxk4* mutants and Col-0 under CL and LD light (One-way ANOVA *p-value* ≤ *0.05*) **b.** Relative percentage of decrease of flowering time Arabidopsis *pxk4-4*, *pxk4-5*, *hub2-1*, *hub2-2*, *hub2-1*/*pxk4-2*, *hub2-2*/*pxk4-2* to Col-0 and *pxk4-2* under CL and LD LED light. Relative percentage of decrease = (difference of DTB / reference DTB) ×100%. **c.** Plant growth of 35-day-old Arabidopsis Col-0, *pxk4-2*. *pxk4-4, pxk4-5, hub2-1*, *hub2-2*, *hub2-1*/*pxk4-2*, *hub2-2*/*pxk4-2* exposed to CL and LD light.

2.4 Discussion

2.4.1 PXK4 is involved in photoperiod responsive flowering transition

Although PXK4 has been recently been revealed to be involved in osmotic stress response along with other PXKs (Lin, 2020), we have independently deduced that PXK4 is an integral component of flowering transition. This hypothesis was initially supported genetically, where mutation of *PXK4* exhibited an early flowering phenotype and decreased transcript expression in all *pxk4* mutants (**Figure 2.3.1c**; **Figure 2.3.9a, c**). The 5' T-DNA insertional mutants *pxk4-4* and *pxk4-5* only exhibited early flowering under LD conditions, reflecting a sensitivity to photoperiod that is consistent with *PXK4* diurnal oscillations (Diurnal DB; Mockler et al., 2007). This was further supported by *pxk4-2* plants, which exhibit early flowering under both CL and LD (**Figure 2.3.2**). Of the *pxk4* mutant alleles, *pxk4-2* consistently showed the strongest early flowering phenotype in CL and LD (**Figure 2.3.9**). The stronger *pxk4-2* flowering phenotype may be due to the fact that the *pxk4-2* T-DNA insert occurs at a 3' exon that encodes the PK activation loop domain within the PXK4 kinase domain (**Figure 2.3.1**).

The role of the PXK4 kinase domain in flowering was further highlighted by the fluctuation of *PXK4* transcript abundance in *pxk4* mutants at different loci (**Figure 2.3.1a, c**). Unlike *pxk4-2*, which demonstrates a significant decline in relative *PXK4* transcript levels when assessed using 5' (P1) versus 3' (P2) primers, *PXK4* mRNA levels in *pxk4-4* and *pxk4-5* showed either no change or a significant increase, respectively, when assessed by P1 versus P2 primers (**Figure 2.3.1c**). From a transcriptional perspective, this suggests that impairing transcription of the PXK4 kinase domain can have a greater impact on plant function, which is consistent with the stronger early flowering phenotype

observed in *pxk4-2* mutant. It is also possible that the *pxk4-4* and *pxk4-5* mutant alleles affect other aspects of plant development through PB-domain containing proteins, as the 5' T-DNA insertion disrupts the PB1 domain (**Figure 1.3.1**; Finn et al., 2015). Taken together, PXK4 has a photoperiodic impact on flowering transition, likely mediated through its PK activity.

2.4.2 PXK4 phosphorylates substrate protein(s) to regulate flowering in response to photoperiod

The correlation in phenotype between flowering gene single mutants (e.g. *flc-1*), PXK4 substrates (e.g. *hub2-1*) and *pxk4-2* based on photoperiod was assessed. With the finding that AtSF1, VIP4, DSLP, AtBRM, and HUB2 had their phosphorylation status altered in *pxk4-2* (**Table 2.3.1**), we speculated that PXK4 is likely to regulate one or more flowering proteins within the flowering network through reversible protein phosphorylation. Consistent with this hypothesis, the phenotypic data comparing flowering mutants and putative PXK4 substrate mutants indicates a correlation in phenotypic traits between *pxk4-2* and the putative PXK4 substrate mutants across different photoperiodic treatments.

As is expected, mutant alleles of flower integrators, *ft-10* and *soc1-2* caused a significant delay in flowering (Immink, et al., 2012; Yoo et al., 2005), opposing what was observed in *flc-1*, which flowers much earlier than Col-0 under CL, LD, and MD conditions. The DTB of *flc-1* and *pxk4-2* (**Figure 2.3.3**) indicates that there might be a correlation between PXK4 and FLC for the regulation of flowering. Although *flc-1* seems to have bigger leaf area than *pxk4-2* (**Figure 2.3.7-2.3.8**), vegetative development might not be a

determining factor for evaluating *flc-1* flowering due to the fact that FLC can affect leaf development independently from flowering pathways (Willmann & Poethig, 2011).

For the PXK4 substrate mutant *sf1-1*, DTB was much later than *pxk4-2* with only partially delayed flowering relative to Col-0 plants, but still earlier than *ft-10* and *soc1-2*, with slightly fewer LCB (**Figure 2.3.3**). The outcomes were as anticipated, since AtSF1 inhibits flowering by impacting FT derived from the ambient flowering transition pathway (Lee et al., 2017). In addition, a similar phenotype of *sf1-1* was also reported by Jang et al. (2014), who also found that both *sf1-1* and *sf1-3* with T-DNA insertion at 5' showed normal flowering, whereas *sf1-2* with 3' T-DNA insertion flowered ~35% earlier than Col-0 under LD. It also indicates that RRM domain at 3' end (Lee et al., 2017) is a central player for regulating flowering. Given a ~15% decrease of flowering time in *pxk4-2* against Col-0 in LD (**Figure 2.3.9b**), we speculated that flowering might be partially regulated by PXK4 through SF1 by affecting temperature-dependent FLM splicing (Wang et al., 2020).

PXK4 substrate mutant *vip4-1* flowered earlier than Col-0 plants regardless of photoperiodic changes. This is consistent with what was known for VIP4 to regulate *FLC* transcription independent of vernalization (Zhang & Van Nocker, 2002). Likewise, *vip4-1* generally exhibited earlier DTB effects relative to *pxk4-2*; significant DTB and LCB effects were observed under LD and SD (**Figure 2.3.3b, d**; **Figure 2.3.4**), which can be explained by our proposed model where upstream PXK4 phosphorylates VIP4 to regulate flowering (**Figure 3.1.2**). Yet, observation of a minimal leaf area in *vip4-1* suggests that VIP4 might have a role in vegetative growth in addition to an ability to affect flowering (Willmann & Poethig, 2011; Park et al., 2010).

Likewise, similar interactions might also occur between AtBRM and PXK4 by affecting *FLC* expression despite earlier DTB in *brm-5* versus *pxk4-2*. This was supported by transcriptional and genetic studies, where Farrona et al (2011) found increased *FLC* transcript levels in Arabidopsis plants that carries a *brm* mutation. However, the early flowering phenotype of *brm-3* was mitigated by SD growth conditions, suggesting an even more dynamic role for AtBRM in flowering (**Figure 2.3.6b**). Earlier transcriptional studies of *brm* mutants also showed that mutation of *brm* tends to have reduced photoperiod sensitivity, but still promotes *CO*, *FT* and *SOC1* transcript expression (Farrona et al., 2011; Farrona et al., 2004) . Further studies of BRM also confirmed its essential role in flowering working as a SWI2/SNF2 Chromatin Remodeler that regulates gene expression (eg. SVP) by histone modification (Li et al., 2015; Farrona et al., 2011). Thus, it is also possible that PXK4 associates with AtBRM to affect expression of many other flowering genes such as *SVP* and *CO* for regulating flowering (Li et al., 2015; Farrona et al., 2011; **Figure 3.1.2**).

While the phosphorylation status of HUB2 in *pxk4-2* exhibited the greatest change amongst all the putative PXK4 substrate candidates (**Table 2.3.1**), flowering time in *hub2* mutants indicates potential connection between PXK4 and HUB2 as both *hub2-1* and *hub2-2* flower similar to, or earlier than, *pxk4-2*. Mutation of the genes that encode HUB2-interacting proteins may also show a flowering phenotype due to the systemic impacts HUB2 has on the flowering regulatory network. For example, null alleles of HUB2 interactors, *spen3*, *khd1*, *ubc1* and *ubc2* flower later than *hub2*, whereas *hub1* shows an earlier flowering phenotype than *hub2* under the same light conditions (Woloszynska et al., 2019; Gu et al., 2009; Cao et al., 2008). However, double mutation of *hub1*/*spen3*, *hub1*/*khd1*, *hub1*/*hub2* all flowered similar to *hub1* single mutant (Woloszynska et al.,

2019; Cao et al., 2008), suggesting that *hub1* is epistatic to *spen3*, *khd1*, *hub2* in inducing flowering. Likewise, the early flowering phenotype of *hub2-1/pxk4-2* and *hub2-2/pxk4-2* mutants is also concordant with our hypothesis for a relationship between HUB2 and PXK4, given the observed 20-25% decrease of DTB (less addition effects) in *hub2-1*/*pxk4-2* and *hub2-2*/*pxk4-2* and 15% in their single mutants, against Col-0 under LD conditions (**Figure 2.3.9b**; José et al., 2009).

The above results indicate a highly integrated role for PXK4 and its corresponding substrates within the flowering landscape. Additional characterization of all the putative PXK4 substrates was beyond the scope of this thesis; however, given the genetic and molecular intersections between HUB2 and PXK4, further characterizations of how these two proteins work together to regulate flower was undertaken.

Chapter 3: How PXK4 and HUB2 work together to modulate flowering

3.1 Introduction

In Arabidopsis plants, *PXK4* is abundant in the nucleus with the highest expression found in cauline leaf, rosettes, and flowers (ePlant, AT2G35050). It exhibited a diurnal expression pattern (Mockler et al., 2007), where its mRNA peaks near the end of night (ZT20), and is least abundant in the middle of the day (ZT8) in MD. This suggests that PXK4 activities are potentially circadian clock dependent (**Chapter 2**; Johansson & Staiger, 2015). Given that HUB2, in complex with HUB1, SPEN3, KHD1, can alter *CCA1* mRNA splicing (Woloszynska et al., 2019), in addition to altering *FLC* chromatin modification (Cao et al., 2008), it is possible that PXK4 phosphorylation of HUB2 regulates flowering both photoperiodically and autonomously (**Figure 3.1.2)**. Furthermore, *CCA1* peaks four hours later than *PXK4* at the night–to-day transition (ZT24/ZT0), with mRNA levels being least abundant at ZT14 in MD (**Figure 3.1.1**; Mockler et al., 2007). Although the diurnal patterns of *HUB2* and *PXK4* mRNA expression do not seem to coincide (**Figure 3.1.1**; Mockler et al., 2007), it is known that peak transcript and protein abundancies are often temporally disconnected (Uhrig et al., 2019; Barenfaller et al., 2012). The lack of HUB2 phosphorylation in *pxk4-2* mutant represents a possible mechanism by which PXK4 influences flowering, as HUB2 is confirmed to play a role in both *CCA1* mRNA splicing (Woloszynska et al., 2019) and *FLC* chromatin modification (**Figure 3.1.2;** Xu et al., 2009).

The genetic analyses of Chapter 2 have provided indications of PXK4 involvement in flowering through the regulation of HUB2, therefore, molecular studies were undertaken to better understand how PXK4 may intersect with HUB2 within the larger flowering network. In this chapter, I will examine the molecular properties of PXK4 floral regulation by assessing changes in the relative transcriptional abundance of HUB2- and other flowering-related genes both in *pxk4-2* and Col-0 plants at different time-points and under different growth conditions using quantitative Polymerase Chain Reaction (qPCR).

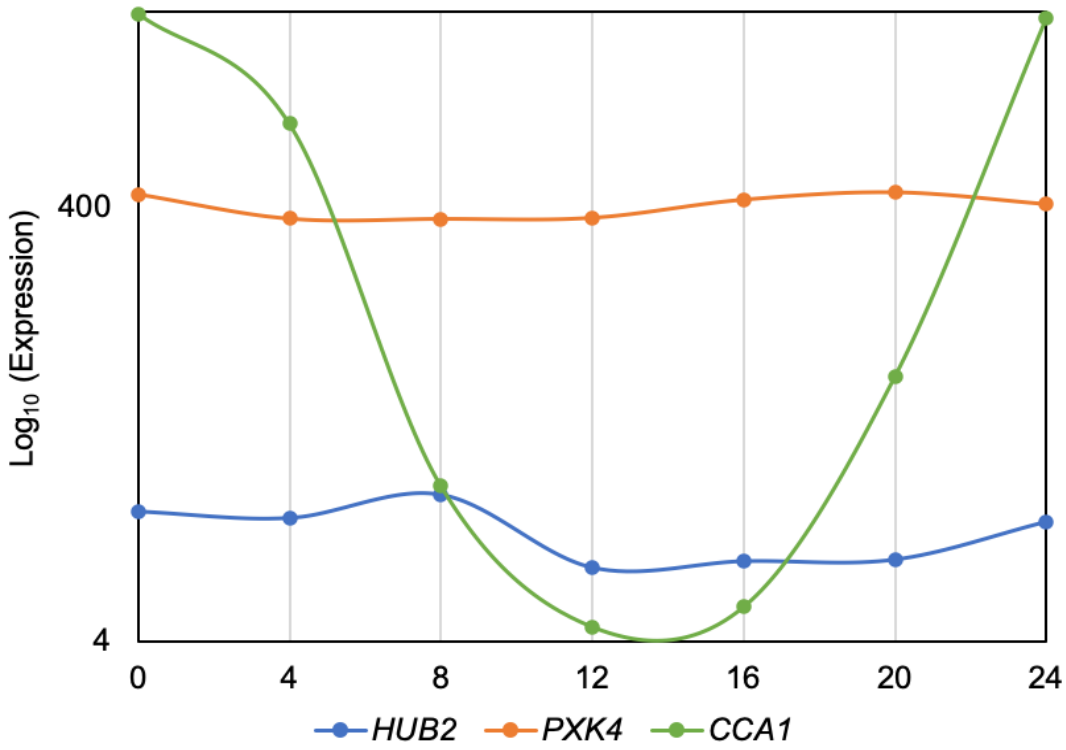

Figure 3.1.1 Diurnal expression patterns of *HUB2*, *PXK4*, and *CCA1* in MD. The data were generated from Diurnal database (Mockler et al., 2007; http://diurnal.mocklerlab.org/), and normalized with $\log_{10}$ change. The expression patterns of *HUB2*, *PXK4*, and *CCA1*, were represented by blue, orange, green scatters with smooth lines respectively. The expression pattern of *PXK4* proportionally antagonizes *HUB2*. *CCA1* has a high amplitude that peaks at ZT0/ZT24.

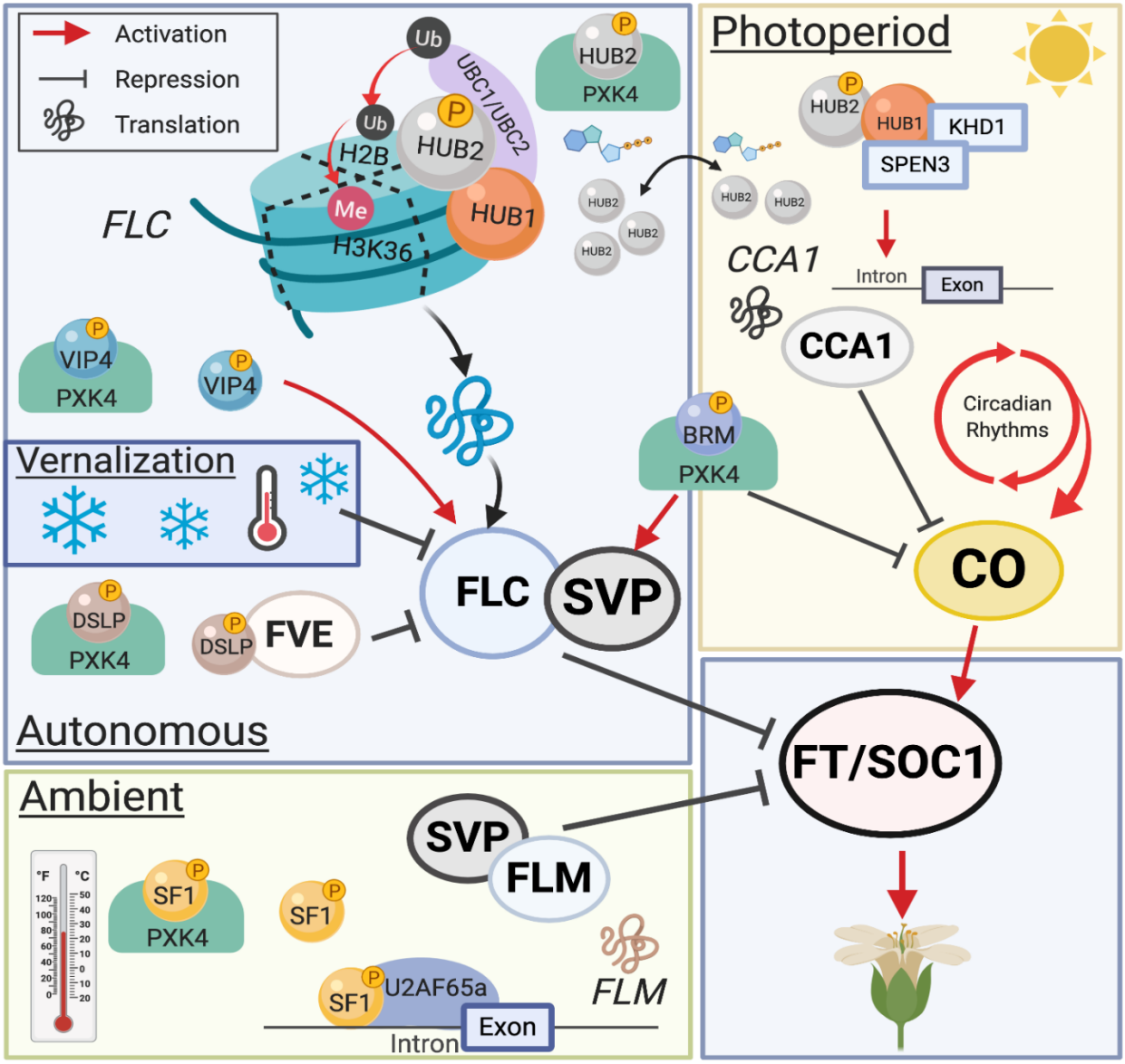

Figure 3.1.2 Putative schematic of PXK4-involvement in flowering pathways. PXK4 substrates, VIP4, AtBRM, HUB2, AtSF1, DSLP regulate flowering time through multiple different signalling pathways. HUB2 is a central player for *CCA1* mRNA splicing and FLC chromatin modification (Woloszynska et al., 2019; Xu et al., 2009). AtBRM functions to delay flowering by activating SVP (Li et al., 2015) and/or reducing CO abundance (Farrona et al., 2011). VIP4 directly activates FLC independent of vernalization signals (Zhang & Van Nocker, 2002), while DSLP autonomously coordinates with FVE to promote flowering by inhibiting FLC (Kenzior & Folk, 2015). Lastly, AtSF1 is involved in alternative splicing of *FLM*, a homolog of FLC that represses flowering in response to ambient temperature (Lee et al., 2017).

3.2 Materials and Methods

3.2.1 Plant Growth Conditions

Sterilized and stratified (4°C, 24h) Col-0 and *pxk4-2* seeds were germinated on 0.5x MS media under different photoperiod conditions (**Table 3.2.1**). All seedlings were then harvested by immediate snap freezing in liquid nitrogen at different time points of day after 14-d of growth on the plates (**Table 3.2.1**) and stored at -80 °C until extracted.

3.2.2 cDNA synthesis

RNA was extracted from plant samples were using TRI Reagent® (Sigma-Aldrich, cat.no. T9424) and 100% Chloroform. RNA was then quantified using ND-1000 Spectrophotometer (NanoDrop®). RNA from each sample was then treated with Amplification Grade DNAse I (Invitrogen™). RevertAid RT Reverse Transcription Kit (ThermoFisher™) was used for cDNA synthesis.

3.2.3 Quantitative PCR

Quantitative PCR (qPCR) was run using an Applied Biosystems 7500™ with a master mix of SYBR green reagent (MBSU, Department of Biological Sciences, University of Alberta, AB, Canada). The gene specific primers were listed in **Table 3.2.2**. UBC21 was selected as reference gene (Oh & Montgomery, 2013).

Table 3.2.1 Growth conditions of three sets of comparative Col-0 *vs pxk4-2* seedling samples.

	Sample 1	**Sample 2**	**Sample 3**	**Sample 4**
Age	14	14	14	14
Light conditions	CL	CL	MD	MD
Time of harvesting	ZT20-21	ZT11-12	ZT22-23	ZT11-12

* ZT = Zeitgeber Time

Table 3.2.2 Gene-specific primers used for qPCR.

Gene	Forward primers (5' → 3')	Reverse primers (5' → 3')	Reference
PXK4-P1	GGAGGGGTACAGATGTTGCTATCAAG	CTTCATGCCAGAACTCCGAGGT	*
PXK4-P2	CATTGAGACCAACCGTGCCAAAC	GGGAACGCAGGTCGAACAAATG	*
FLC	GCTACTTGAACTTGTGGATAGCAA	GGAGAGGGCAGTCTCAAGGT	Hyun et al., 2019
FT	TTGTTTCGACAGCTTGGCAG	GCGAGTGTTGAAGTTCTGGC	*
SOC1	GCTCAAGCAAAAGGAGAAAGC	AGATCCCCACTTTTCAGAGAGC	*
CO	ACGAGCTACGGGGGAGATAG	CTGGTGGCCCCTTGATTCTT	*
CCA1	CAGCTCCAATATAACCGATCCAT	CAATTCGACCCTCGTCAGACA	Mockler et al., 2004
HUB1	GGCAGTGCATATGCCAGTTT	TGTGCAGAACCTCAACTGATCT	*
HUB2	TGCCGGGGCTAATCAAGAG	GCATGGTGGAACTCGCTTTTTA	*
UBC1	GAAAGCAAGCGCGAGTACAA	CAGCAGTCCAGCTTTGCTCA	*
UBC2	GCACGAATGTTCAGTGAAAGCA	GCTTTGTTCGACAACCTCGC	*
SPEN3	CCCTGCATCAAGTCCCATGT	ACCGATCAAGCATTCCGAGG	Woloszynska et al., 2019
KHD1	CCCCATTTGGACCGAGACAA	CCAGGACCATGACAATGCCT	Woloszynska et al., 2019
UBC21	CAAATGGACCGCTCTTATCAAAG	CTGAAAAACACCGCCTTCGT	Oh & Montgomery, 2013

* Designed by Primer-BLAST

3.3 Results

To further explore the molecular underpinnings of the relationship between HUB2 and PXK4 with regards to flowering transition, I next compared the relative mRNA expression patterns of known *HUB2*-related genes, *HUB1*, *UBC1*, *UBC2*, *CCA1*, *SPEN3*, *KHD1*, in addition to *PXK4* and known flowering-related genes, *CO*, *FLC*, *FT*, *SOC1*, in both Col-0 and *pxk4-2* mutants.

3.3.1 Diurnal regulation of HUB2- and flowering-related gene expression in Col-0

To understand how different photoperiod influences transcript levels of each gene, we collected seedling samples from CL and MD at two time points, ZT11 and ZT22; 2-3 hours after *PXK4* is expected to drop and peak, respectively (**Figure 3.1.1**). By comparing *PXK4* expression in Col-0 alone, we found that the average *PXK4* abundance was similar between ZT11 and ZT22 under CL, while *PXK4* transcript levels were higher at ZT22 than ZT11 under MD (**Figure 3.3.1-3.3.4**), which is consistent with what was found on Diurnal DB (Mockler et al., 2007).

Genes regulated by the autonomous pathway, in particular *FLC*, were stably expressed under CL, but substantially increased at ZT22 under MD (**Figure 3.2.1-3.3.4**). Alternatively, *FT* transcript levels accumulated from 0.2 at ZT11 to 1 at ZT22 under CL, while both remained lowly expressed under MD at either time-point. Unlike *FT*, the transcript levels of its downstream partner SOC1 experienced a drop at ZT22 under both CL and MD (**Figure 3.3.1-3.3.4**).

From a photoperiodic output standpoint, *CO*, had higher expression at ZT22 versus ZT11 under MD conditions as expected (Mockler et al., 2007), while CL also

increased *CO* abundance at ZT22 versus ZT11 (**Figure 3.3.1-3.3.4**). The upstream circadian component *CCA1*, increased in relative abundance at ZT22 versus ZT11 as expected, whereas under CL, *CCA1* transcript levels at ZT22 were much lower versus ZT11 (**Figure 3.3.1-3.3.4**). There are still some diurnal fluctuations in *CCA1* expression.

The putative PXK4 substrate *HUB2* did not differ between ZT22 and ZT11 under CL; however, the HUB2-associated genes *HUB1*, *UBC1*/*UBC2*, *SPEN3*, *KHD1* tended to increase at ZT22. Furthermore, the presence of a photoperiod resulted in a slight increase of *HUB1*, *HUB2*, *SPEN3* and *KHD1*, accompanied by a large decrease in *UBC1* and *UBC2*, which may indicate how HUB2 likely intersects with PXK4 to regulate flowering in response to photoperiod.

3.3.2 Transcriptional changes as a result of *pxk4* mutation

To further elucidate a possible PXK4-HUB2 association in the regulation of flowering, I next evaluated the gene expression patterns in *pxk4-2* versus Col-0. In the scenario where *PXK4* expression was eliminated in *pxk4-2* ($p<0.001$), *FLC* also had significantly lower expression ($p<0.001$) regardless of photoperiod (**Figure 3.3.1-3.3.4**). Conversely, in both CL and MD conditions, *FT* tended to accumulate in *pxk4-2* mutant at ZT11, but only saw a statistical increase ($p<0.05$) at ZT22 (**Figure 3.3.1-3.3.4**).

Significant changes ($p<0.05$) in transcript levels were also observed at ZT11 in both CL and MD for multiple HUB2-related genes. Under CL, *HUB2* abundance experienced a drop associated with *pxk4-2* (**Figure 3.3.1**); Under MD, however, *HUB1* and *UBC1* changed their expression in an opposite manner, where *HUB1* accumulates in parallel with a decline in *UBC1* (**Figure 3.3.3**). No other statistical differences were found in *HUB2*, *HUB1* or *UBC1* expression between *pxk4-2* and Col-0, and none of the

other flowering-related or HUB2-related genes, *SOC1*, *CO*, *CCA1*, *SPEN3*, *KHD1* showed statistical changes in expression in *pxk4-2* versus Col-0.

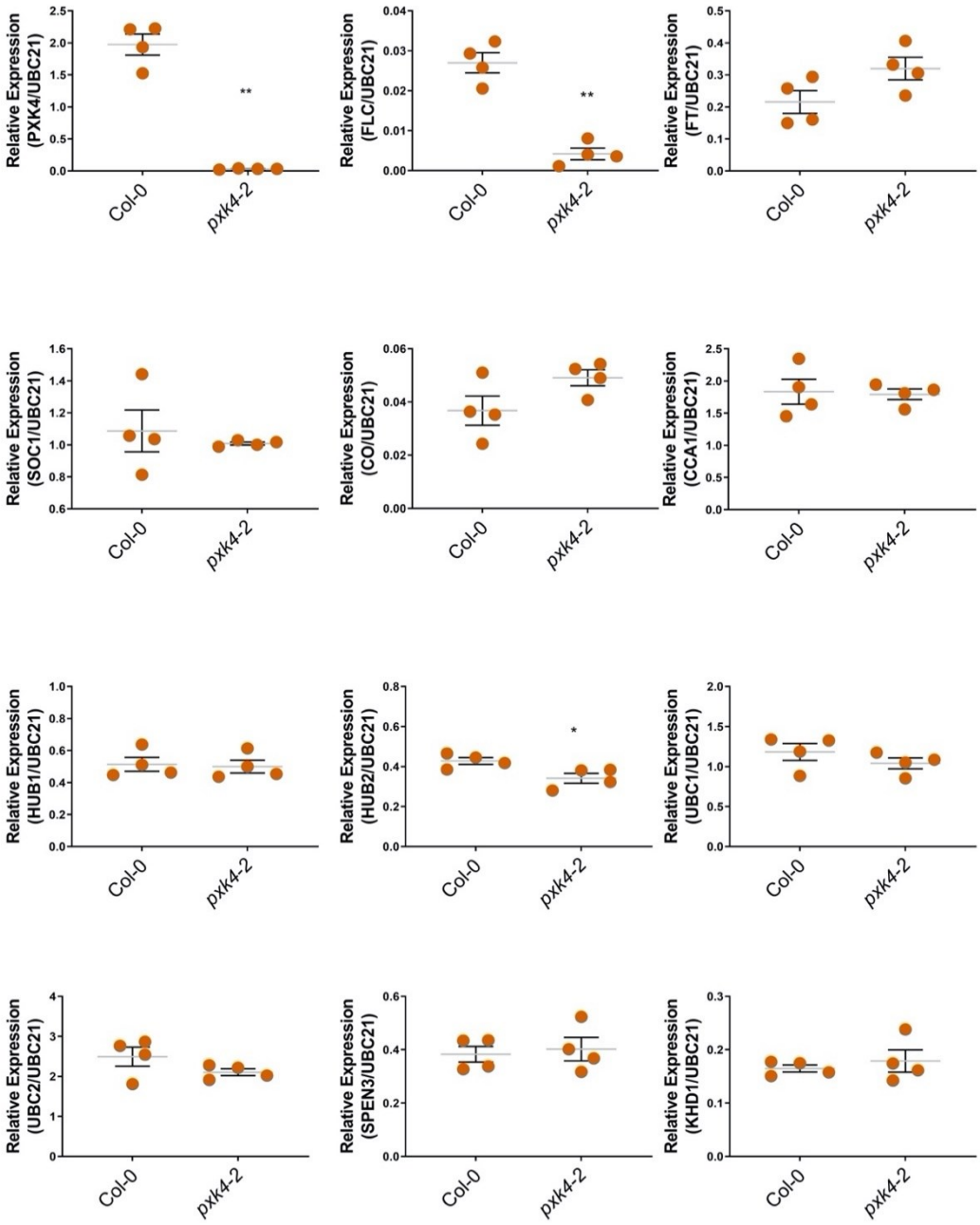

Figure 3.3.1 Relative expression of *PXK4*, flowering genes, HUB2-related genes in 14-DPI Arabidopsis *pxk4-2* mutant seedlings versus Col-0 at ZT11 under CL. *UBC21* was selected as the reference gene. The scatters indicate biological replications (Student's t-test * *p-value* ≤ *0.05*, ** *p-value* ≤ *0.01*).

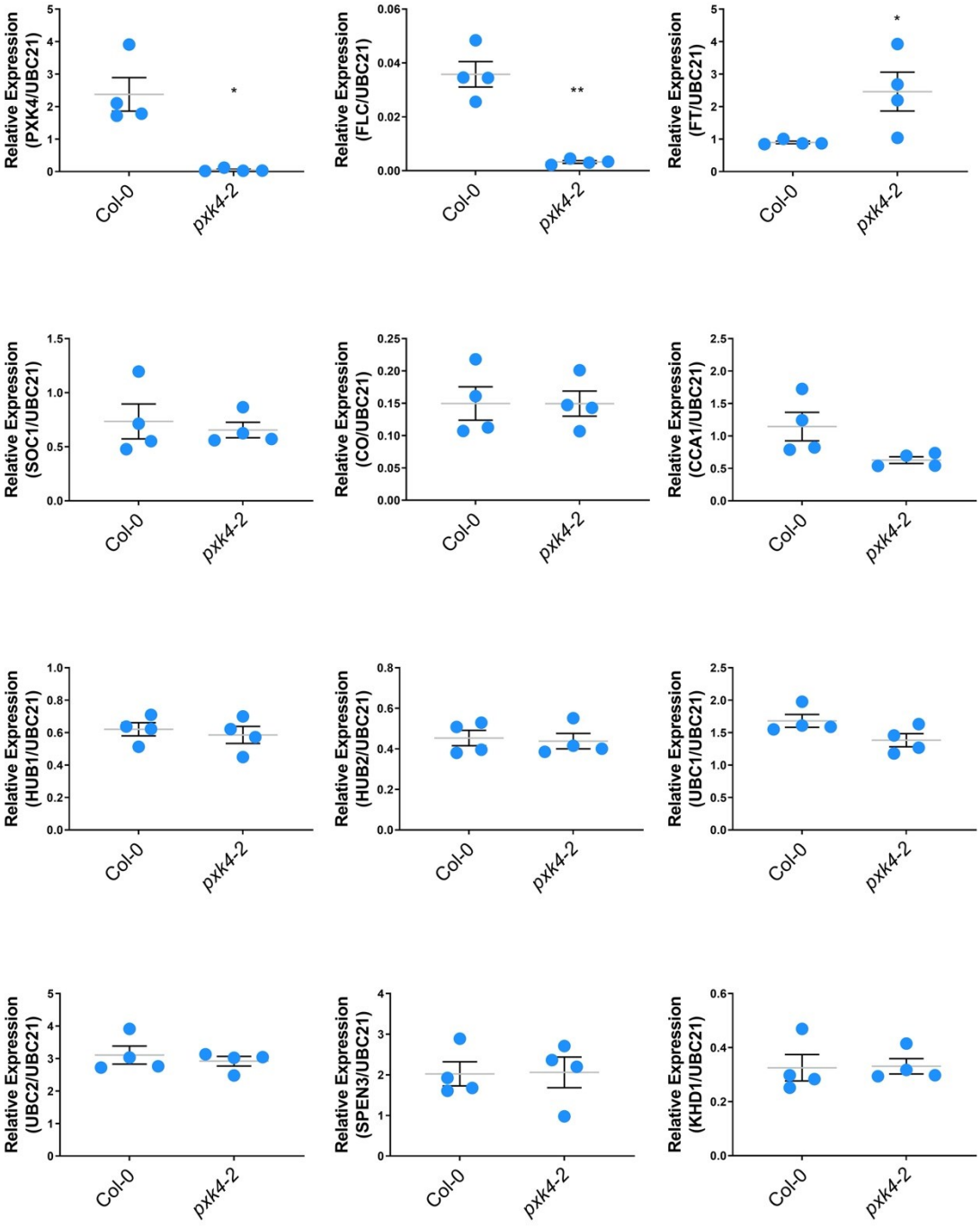

Figure 3.3.2 Relative expression of *PXK4*, flowering genes, HUB2-related genes in 14-DPI Arabidopsis *pxk4-2* mutant seedlings versus Col-0 at ZT22 under CL. UBC21 was selected as the reference gene. The scatters indicate biological replications (Student's t-test * *p-value* ≤ *0.05*, ** *p-value* ≤ *0.01*).

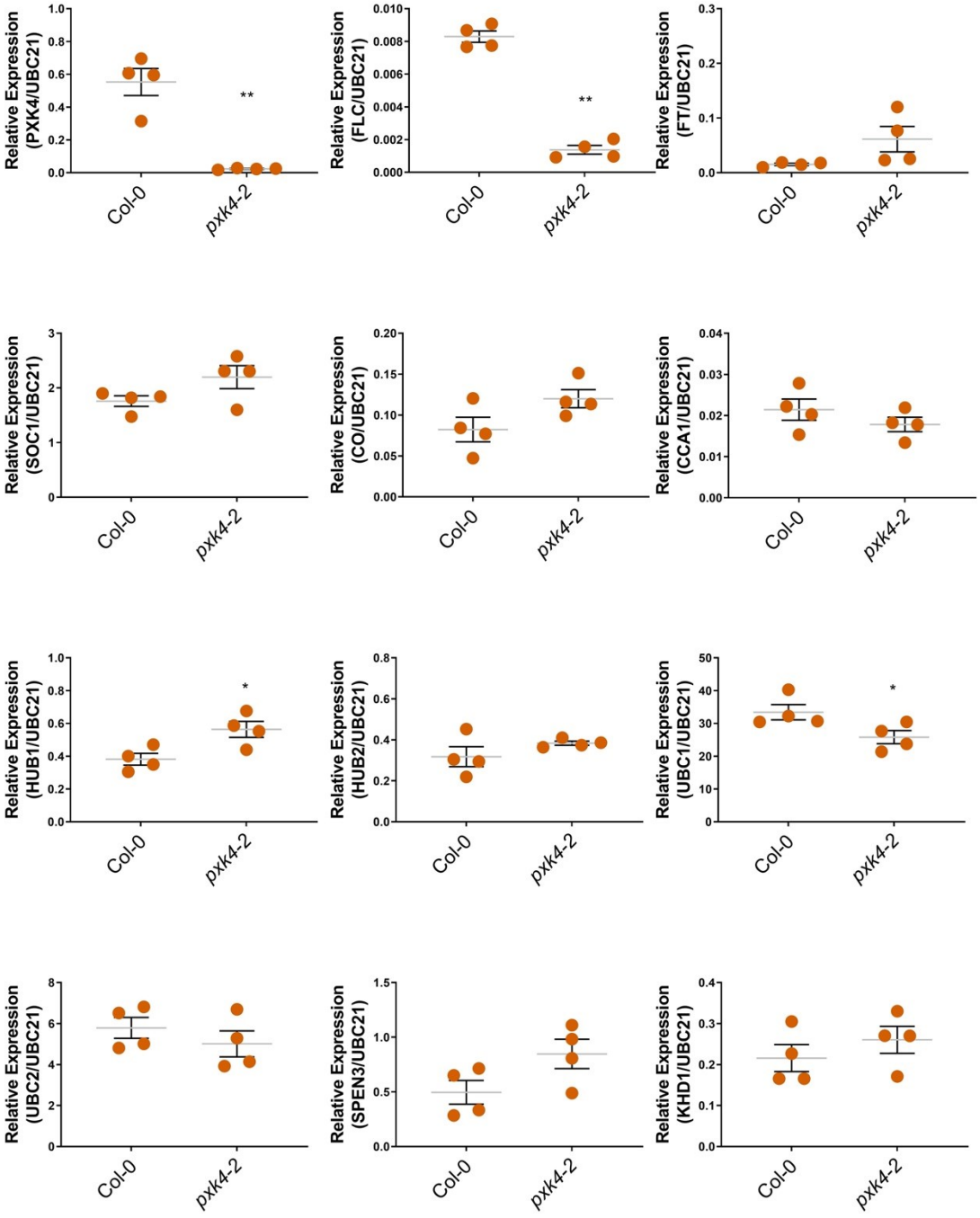

Figure 3.3.3 Relative expression of *PXK4*, flowering genes, HUB2-related genes in 14-DPI Arabidopsis *pxk4-2* mutant seedlings versus Col-0 at ZT11 under MD. *UBC21* was selected as the reference gene. The scatters indicate biological replications (Student's t-test * *p-value* ≤ *0.05*, ** *p-value* ≤ *0.01*).

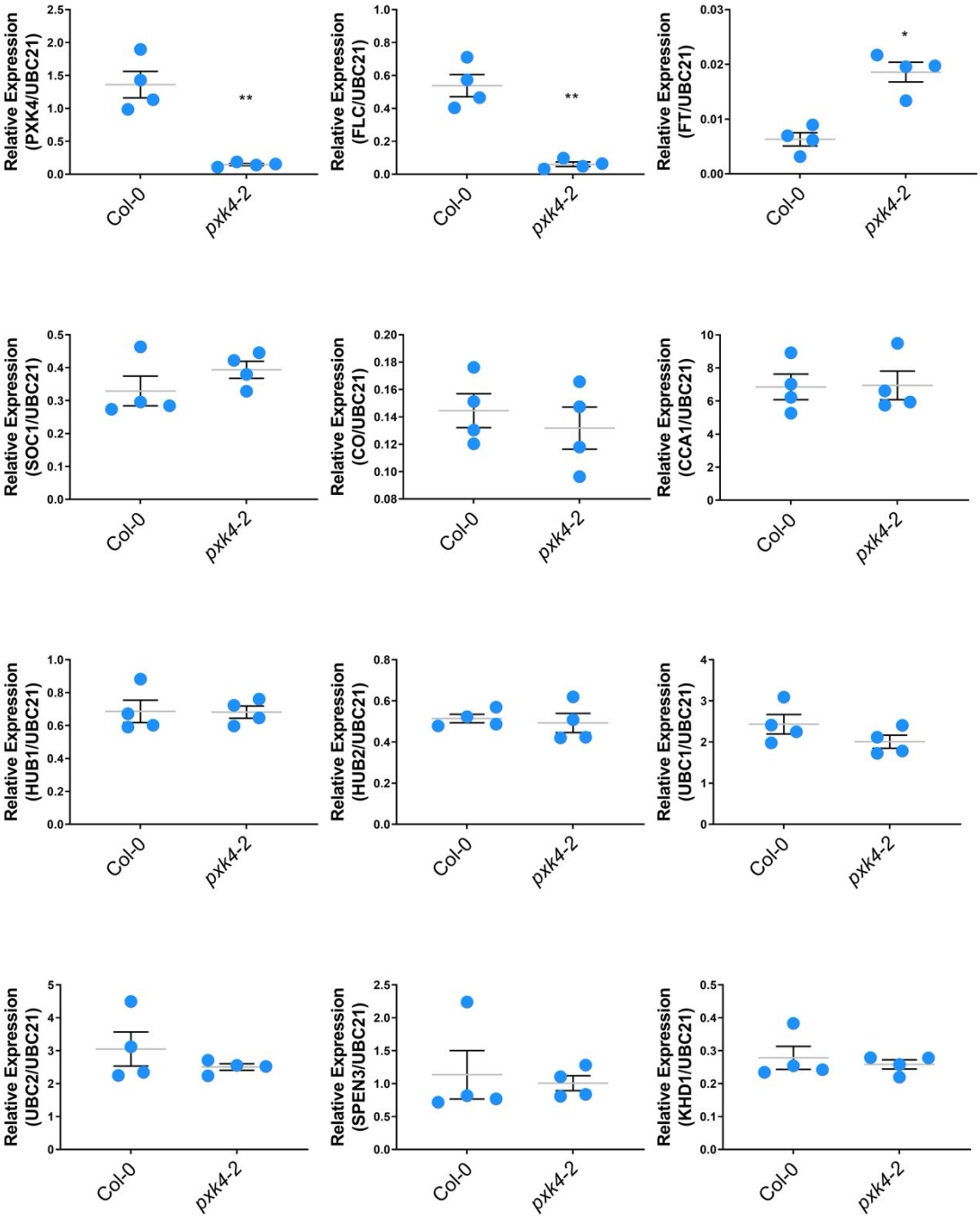

Figure 3.3.4 Relative expression of *PXK4*, flowering genes, HUB2-related genes in 14-DPI Arabidopsis *pxk4-2* mutant seedlings versus Col-0 at ZT22 under MD. *UBC21* was selected as the reference gene. The scatters indicate biological replications (Student's t-test * *p-value* ≤ *0.05*, ** *p-value* ≤ *0.01*).

3.4 Discussion

3.4.1 PXK4-related flowering genes are photoperiod sensitive

Diurnal regulation of *PKX4* is supported by the increased amount of PXK4 transcripts in Col-0 from ZT11 to ZT22 under MD conditions (Mockler et al., 2007; **Figure 3.1.1**), which corresponds to our hypothesis that *PXK4* is maximal at ZT20, and minimal at ZT8 under MD. Interestingly, we also observe that *FLC* is photoperiod sensitive, which is contrary to what has previously been seen for *FLC* expression, which is that *FLC* is not diurnally changing (Cheng et al., 2017; Whittaker & Dean, 2017;Mockler et al., 2007). This novel finding suggests that *FLC* is not completely exempt from photoperiod pathway influence (Blümel et al., 2015). Indirect regulation of *FLC* from regulatory photoperiod components such as HOS1 (Jung et al., 2014) and SPEN3 (Woloszunska et al., 2019) might explain the observed photoperiod changes in *FLC* abundance. Since *PXK4* and *FLC* are likely to be co-expressed in both CL and MD, it is also possible that *PXK4* indirectly affects *FLC* by intersecting with various other flowering transition substrates (**Figure 3.1.2**). These observed correlative changes in *PXK4* and *FLC* expression is also consistent with the early flowering phenotypes found in both *flc-1* and *pxk4-2* single mutants. The variation in *CO*, *FT* and *SOC1* were as expected since they represent the final integration point for the majority of flowering signals (Pin & Nelson, 2012;Turk et al., 2008; Niwa et al., 2007; Mizoguchi et al., 2002).

Accumulation of *HUB1*, *UBC1*, *UBC2* transcripts at ZT22 under CL in Col-0 plants, coupled with a lack of change in *HUB2* abundance under CL, but an increase at ZT 22 under MD, might correspond to *PXK4* and *FLC* co-expression as described previously

(Woloszynska et al., 2019; Cao et al., 2008). Under MD conditions, increase of *PXK4* transcripts from ZT11 to ZT22 may help activate *FLC* transcription by inducing *HUB2*, *HUB1*, *UBC1*, *UBC2* expression (**Figure 3.1.2**)**;** whereas under CL, *PXK4* and *HUB2* remain unchanged, and *HUB1*, *UBC1*, *UBC2* could express independently from PXK4 and thus continue to accumulate (Xu et al., 2009; Cao et al., 2008). From the results above, we can predict that *PXK4*, *HUB2*, *FLC* are interrelated in their regulation of flowering transition in response to photoperiod.

3.4.2 PXK4 associates with HUB2 to regulate flowering through *FLC*

To further examine potential associations between PXK4 and HUB2, we compared their transcript levels in *pxk4-2* with Col-0. As we suspected from the genetic analysis of **Chapter 2**, mutation of *PXK4* impeded both *PXK4* and *FLC* expression levels regardless of photoperiod. This provides some molecular evidence for a connection between these two genes. The idea was supported by Cao et al. (2008) who reported that constant light did not change *FLC* abundance in neither *hub2-1*/*hub2-2* or *hub2-2*; but with the presence of a photoperiod, *FLC* levels began to rise in *hub2-2* mutants (Xu et al., 2009). This suggests that potentially PXK4 and HUB2 act together in regulating *FLC* by indirectly impacting the downstream target, *FT*.

Since mutating *PXK4* gives rise to transcriptional changes in *HUB2* and the expression of known HUB2 protein complex related genes (**Figure 3.3.1; Figure 3.3.3**), we can deduce that PXK4 likely intersects with HUB2 in response to photoperiod changes. Under CL, if PXK4 was involved in autonomous pathway H2B monoubiquitylation, we would have seen a reduction of *HUB1*, *UBC1* and/or *UBC2* instead of them remaining unchanged in *pxk4-2*. Additionally, the increase in *HUB1*,

SPEN3, *KHD1*, coupled with the mild decrease of *CCA1* and *UBC1* under MD at ZT11, fit our hypothesis that loss of PXK4 prevents alternative splicing of *CCA1*.

Together, data presented in the chapter suggests that *PXK4* can affect *HUB2* in a photoperiod-dependent manner, and not aligned with the proposed autonomous pathway, resulting in reduced *FLC* expression. A possible explanation for *pxk4-2* early flowering may relate to SPEN3 reducing *CCA1* expression/splicing and inhibiting *FLC* expression through the induction of *COOLAIR* (the *FLC* anti-sense transcript), without impacting *FLC* H2B monoubiquitylation (Woloszynska et al., 2019). Yet, it is also possible that *PXK4* also affects various flowering-related genes through HUB2 to regulate *FLC* expression (Himanen et al., 2012).

Chapter 4: Multifaceted interplay between HUB2 and PXK4

4.1 Introduction

The initial study of HUB2 protein interaction partners has revealed that the non-redundant H2B monoubiquitylation E3 ligases, HUB2 or HUB1, can heterodimerize, and physically interact with the redundant E2 ligases, UBC1 and UBC2 through RING finger domains to regulate flowering by transcriptionally activating *FLC* (**Figure 3.1.2**; Cao et al., 2008). RING finger domains are highly conserved in many ubiquitin ligases such as yeast Bre1, an ortholog of HUB1 and HUB2 that is known to be functionally essential for H2B monoubiquitylation (Hwang et al., 2003). Removal of the RING finger domain in HUB proteins results in dissociation of HUB-UBC complex (Cao et al., 2008). After a decade, two pre-mRNA splicing factors, SPEN3 and KHD1, were identified by Woloszynska et al. (2019) to associate with the HUB1-HUB2 heterodimer to form a tetrameric complex. This complex seems to assemble in a similar way as the HUB-UBC complex, as HUB2, SPEN3 and KHD1 proteins were no longer detected by tandem-affinity purifications (TAPs) when point mutations were introduced to HUB1 at RING domains (Woloszynska et al., 2019). With SPEN3 suggested to play a role in regulating *FLC* expression, HUB2 seems to have a multifaceted impact on flowering (Himanen et al., 2012; Gu et al., 2009; Xu et al., 2009). Given this dynamic regulatory system, understanding how HUB2 is regulated by upstream signals will give a broader view of its role in flowering transition, in addition to characterizing the outcomes of these signals.

Inferred from the previous phosphoproteomic findings (**Chapter 2**), together with genetic and transcriptional results (**Chapter 3**), I hypothesize that PXK4 might regulate HUB2 through reversible protein phosphorylation to repress flowering through either the photoperiod and / or autonomous pathway by ultimately affecting *FLC* and *FT* expression levels. To characterize this possibility, TAP-tagged HUB2 genomic DNA constructs were expressed in either Col-0 and *pxk4-2* plants to see if the protein interactome of HUB2 is altered by the lack of PXK4.

4.2 Materials and Methods

4.2.1 Overexpression of HUB2 Genomic Clone in Arabidopsis

The 35S::pKNGSrhino-HUB2G (n-terminal TAP-HUB2; **Figure 4.1.1**) plasmid constructs were obtained from VIB-UGent Center for Plant Systems Biology, Ghent University, Ghent, Belgium (Woloszynska et al., 2019), and transformed into GV3101 *Agrobacterium* GV3101 by electroporation (2.5V). A single colony of each construct was picked to grow in 2ml liquid culture consisting of LB + 50 µg/µl Spectinomycin, 25 µg/ul Rifampicillin and 40 µg/µl Gentamicin. Agrobacterium were grown at 28 °C 150 rpm for 48 hours followed by additional 24-hour sub-culturing with 1:20 dilution. The following day, the pink pullet was spun down at 4 °C 3000 x g. Agrobacterium pellets were then re-suspended in 40 ml 5% (w/v) sucrose, 10 ml LB and 3% (v/v) Silwet L-77 immediately prior to Arabidopsis transfection.

Floral dipping consisted of soaking Col-0 and *pxk4-2* flowers in the corresponding suspension for 30 seconds. The dipped plants were laid down on trays cushioned with pre-moistened paper towels and were placed in the dark with a non-ventilated dome for

two days before being exposed to the light. A second dip was performed for a better transfection efficiency using the same methods mentioned above. Eventually, the plants were grown to seed in a 16:8 (22 °C, 60 % RH, level 1, Conviron) growth chamber to seed. The transgenic seeds were firstly selected on 50 μg/μl Kanamycin + 0.5x MS plates, and then grown to be screened under compound microscope (Olympus BX51 Fluorescence Microscope®). Protein expression was confirmed by immunoblotting (**Figure 4.3.1c**).

4.2.2 Tandem Affinity Purification (TAP) and Liquid Chromatography-Mass Spectrometry (LC-MS)

Plant growth of 35S::pKNGSrhino-HUB2G/Col-0 (35S::nTAP-HUB2G/Col-0 or TAP-HUB2G/Col-0) and 35S:: pKNGSrhino-HUB2G/*pxk4*-2 (35S::nTAP-HUB2G/*pxk4-2* or TAP-HUB2G/*pxk4-2*) followed the same protocol as shown in **Chapter 3.1.2** with LD treatment applied. 14 d-old TAP-HUB2G/Col-0 and TAP-HUB2G/*pxk4-2* seedlings were collected at ZT14 and ZT22 respectively. Proteins were extracted using a solution comprised of 50mM HEPES-KOH (pH7.5), 100mM NaCl, 0.1% (v/v) NP-40, 50mM NaPPi, 1mM NaOV, 2mM PMSF, 1x Roche cOmplete™, EDTA-free protease tablet and 1x Roche PhosSTOP™ phosphatase inhibitor cocktail tablet. Protein concentrations were measured by Bradford Assay (Bradford, 1976). Custom made magnetic IgG-Sepharose beads (Cytiva) were used to perform a one-step tandem affinity purification of TAP-tagged HUB2G. HUB2 TAP pull-downs were then digested with trypsin and subjected to LC-MS/MS analysis in order identify and quantify protein interactors. The raw data were analyzed by Dr. R. Glen Uhrig and Dr. Devang Mehta using Spectronaut™.

4.2.3 qPCR analysis of *COOLAIR*

COOLAIR abundance was examined for sample 3 and sample 4 (**Table 3.2.1)** by qPCR following the same protocol as indicated in **Chapter 3.2**. The COOLAIR specific primers are: GCCGTAGGCTTCTTCACTGT, TGTATGTGTTCTTCACTTCTGTCAA.

4.2.4 Phenotyping

The transgenic T_2 TAP-HUB2G/Col-0 and TAP-HUB2G/*pxk4-2*, *hub2-1*, *hub2-2*, *hub2-1*/*pxk4-2*, *hub2-2*/*pxk4-2* seeds were germinated in-parallel with Col-0 and *pxk4-2* seeds under LD conditions for 7 days after 48-hour pre-stratification. The transplanted seedlings were placed in LD growth chamber (22 °C, 60 %RH, level 1, Conviron). The DTB and number of LCB were recorded.

4.3 Results

To confirm 35S::nTAP-HUB2 expression in Arabidopsis Col-0 and *pxk4-2* mutant, I examined T_1 seedlings under microscopy due to the kanamycin antibiotic resistance still present in *pxk4-2* and the kanamycin selectivity of the transfected 35S::nTAP-HUB2 constructs. Driven by an independent promoter, but part of the same T-DNA cassette transfected into Col-0 and *pxk4-2*, GFP florescence was detected indicating a potential positive with successful T-DNA insertion (**Figure 4.3.1b**). The transgenic nature selected seedlings were further confirmed by immunoblotting by showing protein expression of a 125kD TAP-HUB2 in rosette leaves (**Figure 4.3.1b, c**) with Histone H3 protein used as a control group.

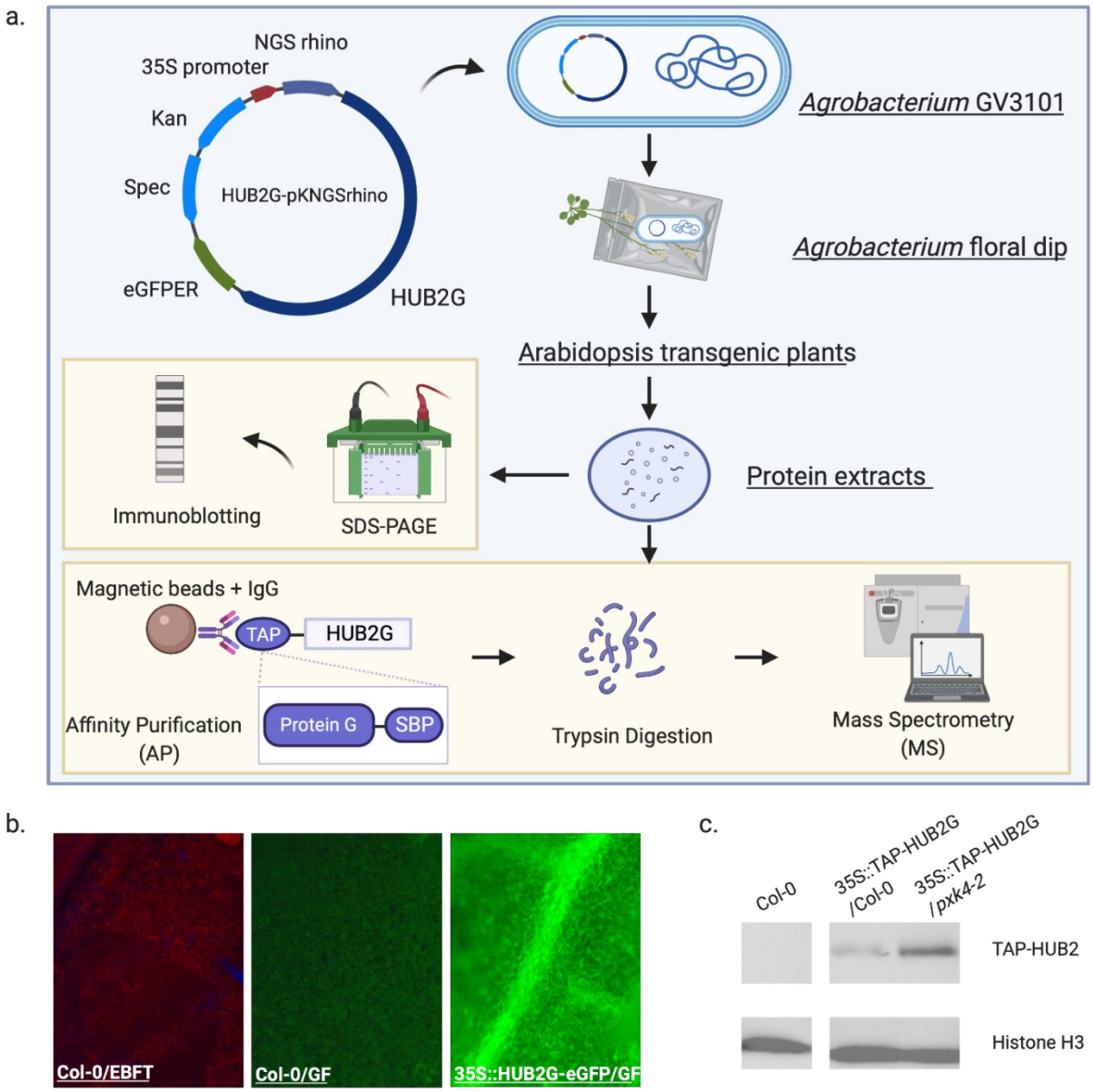

Figure 4.3.1 Workflow from cloning to affinity purification (AP) mass spectrometry (MS) analysis. a. The procedure of generation of 35S::TAP-HUB2G /Col-0 and 35S::TAP-HUB2G /*pxk4*-2 transgenic plants and the corresponding AP-MS analysis. b. Positive transgenic plant screening by microscopy for GFP expression. c. Protein expression levels of 35S::TAP-HUB2G/Col-0 and 35S::TAP-HUB2G/*pxk4*-2 plants.

To better understand the underlying flowering physiology associated with HUB2 and PXK4, respective two lines of 35S::nTAP-HUB2/Col-0 (#1, #4) and 35S::nTAP/*pxk4-2* (#1, #5) were compared with Col-0, *pxk4-2*, *hub2-1*, *hub2-2*, *hub2-1*/*pxk4-2*, and *hub2-*

2/*pxk4-2*. The results suggested that all the *pxk4* and *hub2* single mutants (*pxk4-2*, *hub2-1*, *hub2-2*), double mutants (*hub2-1*/*pxk4-2*, and *hub2-2*/*pxk4-2*), and HUB2-overexpressed lines exhibited early flowering phenotype under LD conditions (**Figure 4.3.2a, c**), with significant fewer LCB at time of bolting relative to Col-0 (**Figure 4.3.2b**).

Table 4.2.1 Flowering-related HUB2 interactome. Putative nucleus-localized proteins found differences between *pxk4-2* versus Col-0 (logFC) in LD at ZT14 or ZT22 (Student's t-test, *p-value ≤ 0.05*).

Gene ID	ProtID	Descriptions	logFC (ZT14)	p-value (ZT14)	logFC (ZT22)	p-value (ZT22)
AT5G09740.1; AT5G09740.2; AT5G64610.1	HAM1,2	histone acetyltransferase of the MYST family	-0.137	0.33	-0.668	0.015
AT1G20960.1; AT1G20960.2	BRR2A	U5 small nuclear ribonucleoprotein helicase	-1.136	0.02	-0.721	0.022
AT2G22540.1; AT2G22540.2; AT2G22540.3	SVP	K-box region and MADS-box transcription factor family protein	-0.347	0.08	-1.316	0.002
AT2G23080.1; AT2G23080.2; AT3G50000.1; AT5G67380.1; AT5G67380.2	CKIIA (CKA1,2,3)	casein kinase II, alpha chain 1,2,3	0.465	0.29	-1.400	0.003

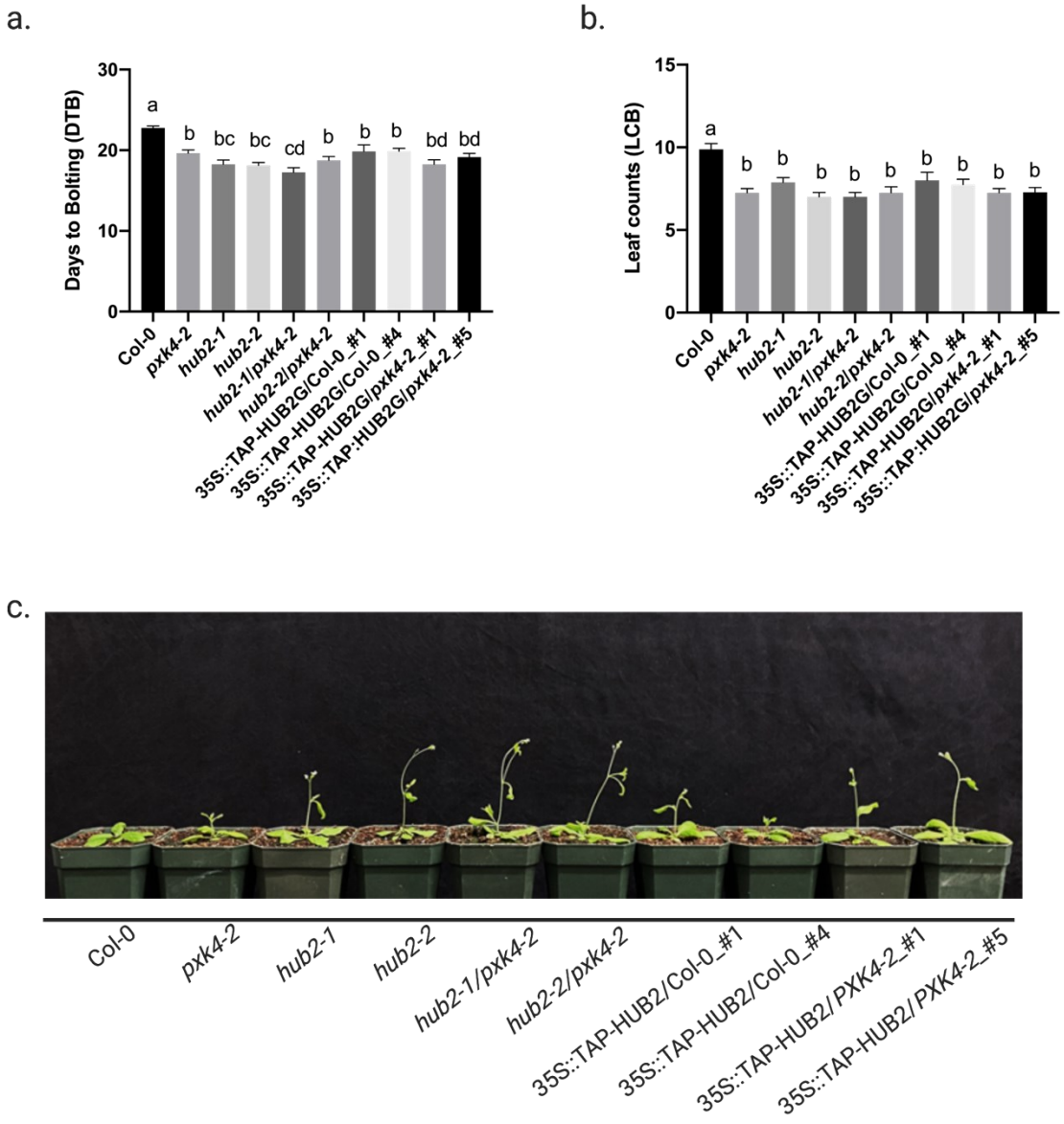

Figure 4.3.2 Flowering time of 35S::TAP-HUB2G /Col-0, 35S::TAP-HUB2G /*pxk4*-2, *pxk4-2* and *hub2* mutants under LD. a. DTB **b.** LCB. (One-way ANOVA *p-value* ≤ *0.05*). **c.** Flowering of 25-day-old plants.

Subsequent proteomic analysis comparing the proteins associated with 35S::nTAP-HUB2/Col-0 found that HUB2 and HUB1 had lower overall abundance at ZT22 versus ZT14 (**Figure 4.3.3a,b**). Overexpression HUB2 in *pxk4-2* found all HUB2

associated proteins (HUB1, SPEN3 and KHD1) were consistently detected. No significant changes were found between the HUB2-complex isolated at ZT14 from either 35S::TAP-HUB2/Col-0 and 35S::TAP-HUB2/*pxk4-2*; however, at ZT22 a significant decrease in the amount of SPEN3 and KHD1 that co-immunoprecipitated with HUB2 was found, despite equal amounts of HUB2 and HUB1 being present (**Figure 4.3.3a,b**). Since SPEN3 activates *COOLAIR* antisense expression to affect *FLC* expression, I then examined *COOLAIR* abundance under MD. Here, *COOLAIR* was found to exhibit lower expression at ZT11 versus ZT22, which was even lower in *pxk4-2* (**Figure 4.3.3b**).

HUB2 interactome analysis provided us with further indications on the potential interplay between HUB2 and PXK4. Among all the nucleus-localized proteins specific to HUB2, additional flowering related genes were found (**Table 4.2.1**), including histone acetyltransferases HAM1 (AT5G09740) and HAM2 (AT5G64610), which are involved in chromatin regulation of *FLC* (Xiao et al., 2013), BRR2A (or EMBRYONIC LETHAL 1507, EMB1507; AT1G20960), an essential protein responsible for *FLC* splicing (Mahrez et al., 2016), SVP (AT2G22540), α-subunits of Casein Kinase II (CKIIA; CKA1,2,3; AT2G23080, AT3G50000, AT5G67380), which are important in the phosphorylation of CCA1 (Lu et al., 2011). The data showed that both time point at ZT14 and ZT22, in *pxk4-2* we saw significant decreases of logFC by 1.136 and 0.721 respectively in BRR2A proteins. For other proteins including HAM1, HAM2, SVP, and CKIIA, even if without statistical changes at ZT11, a significant decrease at ZT22 was found with a logFC of -0.668, -1.316, -1.4; respectively (**Table 4.2.1**).

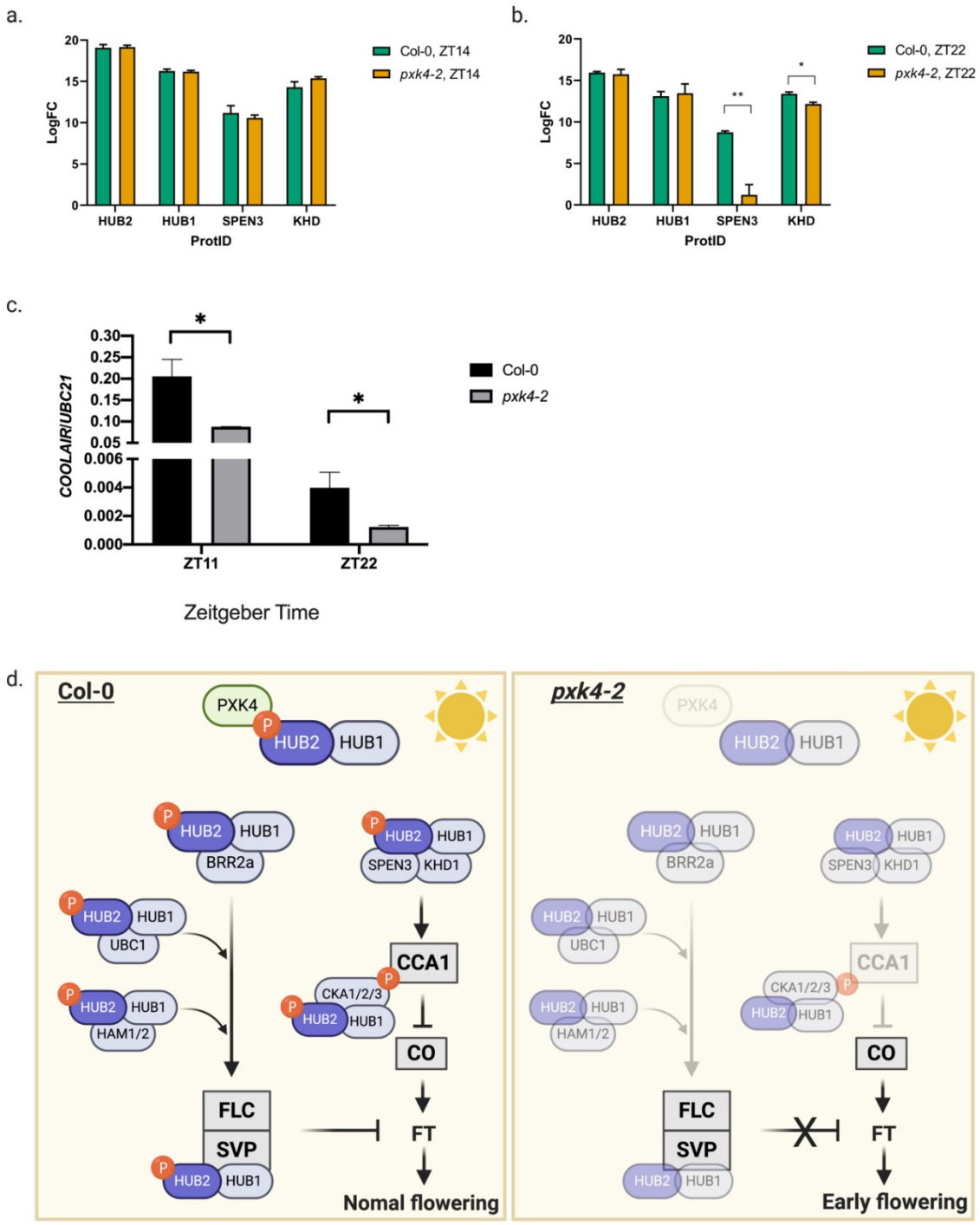

Figure 4.3.3 Putative interplay between PXK4 and HUB2. a. AP-MS analysis of TAP-HUB2G/Col-0 and TAP-HUB2G/*pxk4*-2 transgenic plants at ZT14. **b.** AP-MS of TAP-HUB2G/Col-0 and TAP-HUB2G/*pxk4*-2 transgenic plants at ZT22. **c.** Relative expression of *COOLAIR* at ZT11 and ZT22 in MD. **d.** Proposed model for PXK4 and HUB2 association in regulating flowering under LD.

4.4 Discussion

H2B monoubiquitylation mediated by HUB1 and HUB2 plays an important role in activating flowering inhibitors by interacting with UBC1/UBC2 (Gu et al., 2008). Consistent with previous flowering phenotype findings, *pxk4-2*, *hub2-1*, *hub2-2* and their double mutants flowered earlier than Col-0 under LD (**Figure 2.3.9**). Interestingly, constitutive overexpression of HUB2 in Col-0 (Woloszynska et al., 2019) and *pxk4-2* also results in an early flowering phenotype (**Figure 4.3.2**), whereas *hub2-2* mutants were successfully recovered from early flowering by overexpressing HUB2 driven by a native promoter (Cao et al., 2008). This suggests that an optimal amount of HUB2 is required for flowering regulation (Lee et al., 2017). Up to this point, how PXK4 intersects with HUB2 is still unclear because HUB2 can regulate flowering by multiple means, including: *CCA1* splicing (Woloszynska et al., 2019), and transcriptional activation of *FLC* (Cao et al., 2008; Gu et al., 2008).

Therefore, we explored the HUB2 interactome by comparing TAP-HUB2G/Col-0 and TAP-HUB2G/*pxk4*-2 at ZT14 and ZT22; respectively. As we expected, HUB1, SPEN3, and KHD1 were associated with HUB2, confirming the interactions between HUB2 and HUB1, SPEN3, KHD1. In the previous molecular analysis, we confirmed that both *PXK4* and *FLC* higher expressed at ZT22 versus ZT11 under MD (**Figure 3.3.3-3.3.4**). Here, we found a parallel decrease in the relative protein abundance of HUB2 and HUB1 at ZT22 versus ZT14 in both TAP-HUB2G/Col-0 and TAP-HUB2G/*pxk4*-2, opposing our hypothesis that PXK4 phosphorylates HUB2 to transcriptionally activate H2B ubiquitination of *FLC*. Yet, we can not rule out this possibility since we did see significant changes in *HUB2*, *HUB1*, *UBC1*, *FLC* transcripts (**Chapter 3**). Although SPEN3 and

KHD1 also had a slight increase in relative abundance at ZT22 versus ZT14, significant decreases were found in TAP-HUB2G/*pxk4*-2, suggesting that PXK4 impacts the formation of the HUB2-HUB1-SPEN3-KHD1 complex.

It is also possible that PXK4 associates with HUB2 to regulate flowering through the photoperiod pathway by affecting *CCA1* splicing (Woloszynska et al., 2019). Another possibility is that HUB2-HUB1-SPEN3-KHD1 are involved in the alternative splicing of *FLC* antisense transcript *COOLAIR.* This hypothesis is supported by our discovery of PRP8 spliceosomal protein present in both TAP-HUB2G pull-downs (**S.4**; Marquardt et al., 2014) and decreased transcript abundance at both ZT11 and ZT22 (**Figure 4.3.3**).

However, given that *COOLAIR* opposes *FLC* in response to vernalization (Qi et al., 2019) and that *coolair* and *spen3* mutant plants give rise to an increase in *FLC* levels and delayed flowering (Tian et al., 2019; Woloszynska et al., 2019), it is possible that PXK4-HUB2 interaction results in the formation of multiple protein complexes that affect flowering. This hypothesis is supported by the four additional flowering related proteins (BRR2A, HAM1/HAM2, SVP and CKIIa) uncovered by TAP-HUB2G pull-downs, among which, BRR2A had significant decreases in abundance regardless of time of day (**Table 4.2.1**).

As a U5 small nuclear ribonucleoprotein helicase, BRR2A is an essential component of spliceosome to promote *FLC* splicing efficiency (Mahrez et al., 2016). With a point mutation at Thr^{895}, *FLC* is significantly diminished resulting in an early flowering phenotype (Mahrez et al., 2016). Additional evidence supporting the potential interactions between BRR2A and PXK4-associated HUB2 is that Mahrez et al. (2016) found that PPR8-dependent *COOLAIR* levels were significantly reduced along with *FLC* in *brra2-2*.

Likewise, MYST histone acetyltransferases HAM1 and HAM2 also represent logical intersections with HUB2 to delay flowering as HAM1 and 2 abundance decreased in transgenic plants with a *pxk4-2* background (**Table 4.2.1**). Consistent with what we observed in TAP-HUB2G/*pxk4-2*, mutation in *ham1* and *ham2* alleles was reported to show early flowering with a reduction in *FLC* transcripts, further supporting proposed potential PXK4-HUB2-HUB1 regulatory model for regulating flowering (**Figure 4.3.3**).

HUB2 protein interactors SVP and CKIIA might work in a same way, in that they form a complex with PXK4-assocciated HUB2 to impact flowering transition (**Figure 4.3.3c**). Since it is well known that SVP binds FLC to delay flowering by activating *FT* (Gregis et al., 2013; Hartmann et al., 2000), a relative reduction in SVP abundance in the TAP-HUB2G/*pxk4-2* suggests that PXK4-regulated HUB2-HUB1 complex could also form a complex with SVP (**Figure 4.3.3c**). Lastly, since constitutive expression of CCA1 was confirmed to show delayed flowering (Seo et al., 2012; Wang & Tobin, 1998), CKIIA proteins might also associate with HUB2 for repressing flowering by phosphorylating CCA1 (**Figure 4.3.3c**; Lu et al., 2011).

Despite not yet knowing precisely how PXK4 intersects with the HUB2-HUB1 complex (Direct or Indirect) to influence their binding of other flowering-related proteins and inhibit flowering, this AP-MS analysis has provided us with strong indications that HUB2 is at the center of a larger regulatory network, and that the presence or absence of PXK4 impacts this regulatory network. Collectively, the AP-MS data suggests a model in which HUB2 is phosphorylated by PXK4 at Ser^{314}. Phosphorylated HUB2, in a heterodimeric complex with HUB1, can then bind BBR2A, SPEN3, KHD1, HAM1/2, SVP,

α-subunits of CK2 and/or UBC1/2 to deliver an integrated repressive flowering signal to down-regulate *FT* expression and delay flowering.

Chapter 5: Conclusions and Future Directions

5.1 Conclusions

Through a combination of molecular genetics and proteomics, my thesis provides multiple lines of evidence for PXK4 having a key role in the regulation of flowering transition, in particular, my thesis reveals that PXK4 impacts multiple facets of the flowering pathway, among which, HUB2 represents a primary PXK4 substrate.

In **Chapter 2**, I present five putative PXK4 substrates including: HUB2, AtBRM, VIP4, SF1, and DSLP based on the mining of PXK4-mutant phosphoproteomic data, leading to the hypothesis that PXK4 is likely negatively regulating flowering through the phosphorylation of a variety of substrates in response to autonomous pathway signals or environmental stimuli such as photoperiod.

Next, the genetic analysis of *pxk4* plant growth relative to putative substrate mutants, established a general view of the PXK4 flowering network (**Figure 3.2.1**). Here, we found that the *pxk4-2* accession carrying a T-DNA insertion at kinase domain (3'), showed the earliest flowering phenotype. This is especially apparent in other *pxk4* accessions with 5' insertions under CL versus LD, implying the essential role of kinase domain in regulating flowering in response to photoperiodic impacts. Subsequent phenotypic comparisons suggested that, between *pxk4-2* and substrate mutants *hub2-1*, *hub2-2*, *brm-3*, *brm-5*, *vip4-1*, and *sf1-1*, mutation at HUB2 alleles (*hub2-1*, *hub2-2*) exhibited a closer flowering phenotype to *pxk4-2* in response to photoperiodic changes, rendering our further investigations of *hub2*/*pxk4-2* double mutants. Consistent with our

hypothesis that PXK4 and HUB2 are genetically connected, mutation at both HUB2 and PXK4 alleles showed additive early flowering phenotype.

In **Chapter 3**, I tested the relative expression levels of established flowering genes and corresponding HUB2-related genes in *pxk4-2* and Col-0 at ZT11 and ZT22 time-points under CL and MD. The results not only confirmed diurnal expression pattern of PXK4 but provided us with strong indications of PXK4-regulated flowering, as we saw a significant decrease in *FLC* expression, coupled with a slight increase of *FT* expression in *pxk4-2* regardless of photoperiodic change. This was highlighted by HUB2-related genes *HUB1* and *UBC1*, which experienced significant changes in expression associated with *pxk4-2*.

In **Chapter 4**, myself and others performed TAP-HUB2G pull-down assays combined with mass spectrometry analysis to elucidate the PXK4-mediated HUB2 interactome. This found HUB1, SPEN3 and KHD1 associated with TAP-HUB2G in both Col-0 and *pxk4-2*. SPEN3 and KHD1 experienced a significant decrease in abundance in the TAP-HUB2G pull-downs from *pxk4-2*. Although HUB1, SPEN3, KHD1 can form a functional complex with HUB2, loss of PXK4 resulted in decreased SPEN3 and KHD1 abundance without a corresponding changing in HUB2 or HUB1, suggesting that PXK4 impacts the ability of HUB2 to form this protein complex. This hypothesis was ultimately confirmed by finding significant decreases in other flowering genes that seem to be associated with HUB2, including; BBR2a, SPEN3, KHD1, HAM1/2, SVP, α-subunits of CKII in TAP-HUB2G/*pxk4-2*. Together, these proteins help us to depict a potential PXK4-dependent HUB2 interactome for the regulation of flowering (**Figure 4.3.3c**).

5.2 Future directions

5.2.1 Protein phosphomimetic studies

Phosphomimetic mutation of identified phosphorylation sites is a useful approach for studying the impacts of protein phosphorylation on protein structure-function. It is facilitated by substituting known phosphorylated Ser/Tyr/Thr sites with either aspartate or glutamate, which mimics phosphorylation of a protein substrate due to the negative charge of these amino acids (Baliova & Jursky, 2020; Shao et al., 2019; Tariq et al., 2018). This method is also applicable to PXK4 substrates since currently no reciprocal direct evidence has been obtained to support the hypothesis that PXK4 regulates flowering through the phosphorylation of Ser^{314} on HUB2. Therefore, to confirm that phosphorylation of HUB2 at Ser^{314} likely by PXK4 functions to repress flowering, I created HA-tagged HUB2 phosphomimetic constructs with a substitution at Ser^{314} to either aspartate (35S::HA-HUB2-D; phosphorylated) or alanine (35S::HA-HUB2-A; null-phosphorylated). By constitutively expressing 35S::HA-HUB2-D and 35S::HA-HUB2-A in Col-0 and *pxk4-2* plants, we expect to observe: (i) some recovery of the early flowering phenotype of *pxk4-2* in 35S::HA-HUB2-D/*pxk4-2*, (ii) further delayed flowering in 35S::HA-HUB2-D/Col-0 and (iii) continued early flowering in 35S::HA-HUB2-A/*pxk4-2* and 35S::HA-HUB2-A/Col-0.

5.2.2 Multiple facets of the flowering transition network are impacted by PXK4

Based on the genetic evidence in **Chapter 1**, PXK4 likely contributes to different aspects of multiple the flowering pathways through the phosphorylation of other flowering-

related substrates, including: VIP4, AtSF1, AtBRM, and DSLP. Environmental stimuli other than photoperiod, such as ambient/prolonged temperature, plant hormones (especially GA), can also be studied to extend the spectrum of flowering network in relation to PXK4. Since I have generated *vip4-1*/*pxk4-2*, *sf1-1*/*pxk4-2*, *brm-3*/*pxk4-2*, *fve*/*pxk4-2*, *flc-1*/*pxk4-2*, *ft-10*/*pxk4-2*, along with *hub2*/*pxk4* double mutant lines, genetic links between PXK4 and those four additional substrates can be further examined in-parallel with through qPCR. In addition to genetic and transcriptional studies, those putative PXK4 substrates can also be confirmed by phosphomimetics following the procedures outlined in **5.2.1**.

5.2.3 Complementation of *pxk4-2* mutant and subcellular localization

Since two companies were unable to synthesize the codon optimized coding sequence for PXK4, in addition to other independent groups being unable to express a PXK4-CDS for enzyme assays (Lin et al., 2020), three alternative methods can be explored to complement *pxk4* mutant alleles and study subcellular localization (Lin et al., 2020; Soma et al., 2020). These include: 1) utilizing the PXK4 kinase domain (KD) alone to try and complement the early flowering phenotype using a 35S::YFP:PXK4KD construct. 2) Utilizing a 35S driven PXK4 genomic clone (35S::YFP-PXK4G) to complement plants and perform subcellular localization and 3) Create a PXK4promoter::PXK4g:cYFP construct to also drive PXK4 complementation, but under natural levels of PXK4 expression and with natural opportunities for gene splicing. Each approach will serve to provide evidence that validates our hypothesis that PXK4 is a nucleus-localized PK with a functional kinase domain that plays an essential role in regulating flowering. Furthermore, additional YFP pull-downs and LC-MS analysis will

provide additional insight into the PXK4 interactome to better understand how PXK4 is directly impacting other proteins to regulate flowering.

5.2.4 TurboID proximity labeling and Bimolecular Fluorescence Complementation (BiFC)

Enzyme-catalyzed proximity labeling (PL) has become a popular approach for protein compartmentalization and interaction studies due to its high labeling efficiency among which TurboID has the most outstanding performance; it only takes 10 min to have the equal amounts of labeling that BioID/BioID2/BASU would have after 18 hours (Branon et al., 2018). The advantage of PL is that it is applicable for transient interactions (Trinkle-Mulcahy, 2019), which might complement to our unresolved phosphomemic analysis by demonstrating that PXK4 is closely localized to HUB2 and specific HUB-related protein complexes.

Both PXK4 genomic clone and HUB2 CDS clone, will be fused to a TurboID tag to be expressed in plant tissues. HUB2 interacting proteins will become biotinylated and then bound by streptavidin (Trinkle-Mulcahy, 2019) for subsequent LC-MS/MS analysis. Through this approach it is expected that PXK4 substrates, such as HUB2, will be found to be directly associated with PXK4, with phosphorylation changes also being detected.

Alternatively, we can also confirm HUB2 protein interactions using BiFC. We could do this using the HUB2 CDS which as either S->D and S->A phosphomimetic and ablative mutations (HUB2-D and HUB2-A) expressed N-terminal eYFP (35S::NYFP) fusion constructs and BRR2a, SPEN3, KHD1, HAM1/HAM2, SVP, CKA1/2/3 expressed as C-terminal eYFP (35S::CYFP) constructs to see if the interactions are truly phosphorylation dependent.

References

Abbasi, A., & Fahlgren, N. (2017). Naïve Bayes pixel-level plant segmentation. *2016 IEEE Western New York Image and Signal Processing Workshop, WNYISPW 2016*. https://doi.org/10.1109/WNYIPW.2016.7904790

Alexandre, C. M., & Hennig, L. (2008). FLC or not FLC: The other side of vernalization. In *Journal of Experimental Botany* (Vol. 59). https://doi.org/10.1093/jxb/ern070

Ausín, I., Alonso-Blanco, C., Jarillo, J. A., Ruiz-García, L., & Martínez-Zapater, J. M. (2004). Regulation of flowering time by FVE, a retinoblastoma-associated protein. *Nature Genetics*. https://doi.org/10.1038/ng1295

Baerenfaller, K., Massonnet, C., Walsh, S., Baginsky, S., Bühlmann, P., Hennig, L., Hirsch-Hoffmann, M., Howell, K. A., Kahlau, S., Radziejwoski, A., Russenberger, D., Rutishauser, D., Small, I., Stekhoven, D., Sulpice, R., Svozil, J., Wuyts, N., Stitt, M., Hilson, P., Gruissem, W. (2012). Systems-based analysis of Arabidopsis leaf growth reveals adaptation to water deficit. *Molecular Systems Biology*, *8*(1), 606. https://doi.org/10.1038/msb.2012.39

Berry, J. C., Fahlgren, N., Pokorny, A. A., Bart, R. S., & Veley, K. M. (2018). An automated, high-Throughput method for standardizing image color profiles to improve image-based plant phenotyping. *PeerJ*. https://doi.org/10.7717/peerj.5727

Blümel, M., Dally, N., & Jung, C. (2015). Flowering time regulation in crops-what did we learn from Arabidopsis? *Current Opinion in Biotechnology*, *32*, 121–129. https://doi.org/10.1016/j.copbio.2014.11.023

Boss, P. K., Bastow, R. M., Mylne, J. S., & Dean, C. (2004). Multiple pathways in the decision to flower: Enabling, promoting, and resetting. In *Plant Cell* (Vol. 16). https://doi.org/10.1105/tpc.015958

Bourbousse, C., Ahmed, I., Roudier, F., Zabulon, G., Blondet, E., Balzergue, S., Colot, V., Bowler, C., & Barneche, F. (2012). Histone H2B monoubiquitination facilitates the rapid modulation of gene expression during arabidopsis photomorphogenesis. *PLoS Genetics*. https://doi.org/10.1371/journal.pgen.1002825

Bürkle, A. (2001). Posttranslational Modification. *Encyclopedia of Genetics*, 1533. https://doi.org/10.1006/rwgn.2001.1022

Cao, Y., Dai, Y., Cui, S., & Ma, L. (2008). Histone H2B monoubiquitination in the chromatin of Flowering Locus C regulates flowering time in Arabidopsis. *Plant Cell*. https://doi.org/10.1105/tpc.108.062760

Capovilla, G., Schmid, M., & Posé, D. (2015). Control of flowering by ambient temperature. *Journal of Experimental Botany*, *66*(1), 59–69. https://doi.org/10.1093/jxb/eru416

Chen, Y., Song, S., Gan, Y., Jiang, L., Yu, H., & Shen, L. (2020). SHAGGY-like kinase 12 regulates flowering through mediating CONSTANS stability in Arabidopsis. In *Sci. Adv* (Vol. 6, pp. 413–425). http://advances.sciencemag.org/

Cheng, J. Z., Zhou, Y. P., Lv, T. X., Xie, C. P., & Tian, C. E. (2017). Research progress on the autonomous flowering time pathway in Arabidopsis. In *Physiology and Molecular Biology of Plants* (Vol. 23). Springer India. https://doi.org/10.1007/s12298-017-0458-3

Chow, B. Y., Helfer, A., Nusinow, D. A., & Kay, S. A. (2012). ELF3 recruitment to the PRR9 promoter requires other Evening Complex members in the Arabidopsis

circadian clock. *Plant Signaling & Behavior*, *7*(2), 170–173. https://doi.org/10.4161/psb.18766

Cohen, P. (2002). The origins of protein phosphorylation. *Nature Cell Biology*, *4*(5). https://doi.org/10.1038/ncb0502-e127

De Lucia, F., Crevillen, P., Jones, A. M. E., Greb, T., & Dean, C. (2008). *A PHD-Polycomb Repressive Complex 2 triggers the epigenetic silencing of FLC during vernalization*. www.pnas.org/cgi/content/full/

Ebner, P., Versteeg, G. A., & Ikeda, F. (2017). *Critical Reviews in Biochemistry and Molecular Biology Ubiquitin enzymes in the regulation of immune responses*. https://doi.org/10.1080/10409238.2017.1325829

Eckert, D., Andrée, N., Razanau, A., Zock-Emmenthal, S., Lützelberger, M., Plath, S., Schmidt, H., Guerra-Moreno, A., Cozzuto, L., Ayté, J., & Käufer, N. F. (2016). Prp4 Kinase Grants the License to Splice: Control of Weak Splice Sites during Spliceosome Activation. *PLoS Genetics*. https://doi.org/10.1371/journal.pgen.1005768

Fahlgren, N., Feldman, M., Gehan, M. A., Wilson, M. S., Shyu, C., Bryant, D. W., Hill, S. T., McEntee, C. J., Warnasooriya, S. N., Kumar, I., Ficor, T., Turnipseed, S., Gilbert, K. B., Brutnell, T. P., Carrington, J. C., Mockler, T. C., & Baxter, I. (2015). A versatile phenotyping system and analytics platform reveals diverse temporal responses to water availability in Setaria. *Molecular Plant*. https://doi.org/10.1016/j.molp.2015.06.005

Farrona, S., Hurtado, L., Bowman, J. L., & Reyes, J. C. (2004). The Arabidopsis thaliana SNF2 homolog AtBRM controls shoot development and flowering. *Development*, *131*(20), 4965–4975. https://doi.org/10.1242/dev.01363

Farrona, S., Hurtado, L., March-Díaz, R., Schmitz, R. J., Florencio, F. J., Turck, F., Amasino, R. M., & Reyes, J. C. (2011). Brahma is required for proper expression of the floral repressor FLC in Arabidopsis. *PLoS ONE*, *6*(3). https://doi.org/10.1371/journal.pone.0017997

Finn, R. D., Coggill, P., Eberhardt, R. Y., Eddy, S. R., Mistry, J., Mitchell, A. L., Potter, S. C., Punta, M., Qureshi, M., Sangrador-Vegas, A., Salazar, G. A., Tate, J., & Bateman, A. (2015). The Pfam protein families database: Towards a more sustainable future. *Nucleic Acids Research*, *44*(D1), D279–D285. https://doi.org/10.1093/nar/gkv1344

Fornara, F., Panigrahi, K. C. S., Gissot, L., Sauerbrunn, N., Rühl, M., Jarillo, J. A., & Coupland, G. (2009). Arabidopsis DOF Transcription Factors Act Redundantly to Reduce CONSTANS Expression and Are Essential for a Photoperiodic Flowering Response. *Developmental Cell*, *17*(1), 75–86. https://doi.org/10.1016/j.devcel.2009.06.015

Gehan, M. A., Fahlgren, N., Abbasi, A., Berry, J. C., Callen, S. T., Chavez, L., Doust, A. N., Feldman, M. J., Gilbert, K. B., Hodge, J. G., Hoyer, J. S., Lin, A., Liu, S., Lizárraga, C., Lorence, A., Miller, M., Platon, E., Tessman, M., & Sax, T. (2017). PlantCV v2: Image analysis software for high-throughput plant phenotyping. *PeerJ*. https://doi.org/10.7717/peerj.4088

Giakountis, A., & Coupland, G. (2008). Phloem transport of flowering signals. In *Current Opinion in Plant Biology* (Vol. 11). https://doi.org/10.1016/j.pbi.2008.10.003

Glen Uhrig, R., Echevarría-Zomeño, S., Schlapfer, P., Grossmann, J., Koerber, N., Fiorani, F., Gruissem, W., & Author, C. (2020). Diurnal Dynamics of the Arabidopsis Rosette Proteome and Phosphoproteome 1. *BioRxiv*, 2020.09.11.293779. https://doi.org/10.1101/2020.09.11.293779

Gregis, V., Andrés, F., Sessa, A., Guerra, R. F., Simonini, S., Mateos, J. L., Torti, S., Zambelli, F., Prazzoli, G. M., Bjerkan, K. N., Grini, P. E., Pavesi, G., Colombo, L., Coupland, G., & Kater, M. M. (2013). Identification of pathways directly regulated by SHORT VEGETATIVE PHASE during vegetative and reproductive development in Arabidopsis. *Genome Biology*, *14*(6), 1–26. https://doi.org/10.1186/gb-2013-14-6-r56

Gu, X., Jiang, D., Wang, Y., Bachmair, A., & He, Y. (2009). Repression of the floral transition via histone H2B monoubiquitination. *The Plant Journal*, *57*(3), 522–533. https://doi.org/10.1111/j.1365-313X.2008.03709.x

Han, Z. J., Feng, Y. H., Gu, B. H., Li, Y. M., & Chen, H. (2018). The post-Translational modification, SUMOylation, and cancer (Review). In *International Journal of Oncology*. https://doi.org/10.3892/ijo.2018.4280

Hannoun, Z., Greenhough, S., Jaffray, E., Hay, R. T., & Hay, D. C. (2010). Post-translational modification by SUMO. In *Toxicology*. https://doi.org/10.1016/j.tox.2010.07.013

He, Y., Doyle, M. R., & Amasino, R. M. (2004). *PAF1-complex-mediated histone methylation of FLOWERING LOCUS C chromatin is required for the vernalization-*

responsive, winter-annual habit in Arabidopsis. https://doi.org/10.1101/gad.1244504

He, Y., Michaels, S. D., & Amasino, R. M. (2003). Regulation of Flowering Time by Histone Acetylation in Arabidopsis. *Science*. https://doi.org/10.1126/science.1091109

Heidari, B., Nemie-Feyissa, D., Kangasjärvi, S., & Lillo, C. (2013). Antagonistic Regulation of Flowering Time through Distinct Regulatory Subunits of Protein Phosphatase 2A. *PLoS ONE*. https://doi.org/10.1371/journal.pone.0067987

Henderson, I. R., Shindo, C., & Dean, C. (2003). The Need for Winter in the Switch to Flowering. *Annual Review of Genetics*, *37*(1), 371–392. https://doi.org/10.1146/annurev.genet.37.110801.142640

Himanen, K., Woloszynska, M., Boccardi, T. M., De Groeve, S., Nelissen, H., Bruno, L., Vuylsteke, M., & Van Lijsebettens, M. (2012). Histone H2B monoubiquitination is required to reach maximal transcript levels of circadian clock genes in Arabidopsis. *Plant Journal*, *72*(2), 249–260. https://doi.org/10.1111/j.1365-313X.2012.05071.x

Hu, H., & Sun, S.-C. (2016). Ubiquitin signaling in immune responses. *REVIEW Npg Cell Research*, *26*, 457–483. https://doi.org/10.1038/cr.2016.40

Huang, W., Pérez-García, P., Pokhilko, A., Millar, A. J., Antoshechkin, I., Riechmann, J. L., & Mas, P. (2012). Mapping the core of the Arabidopsis circadian clock defines the network structure of the oscillator. *Science*. https://doi.org/10.1126/science.1219075

Huang, Y., Deng, T., & Winston, B. W. (2000). Characterization of hPRP4 kinase activation: Potential role in signaling. *Biochemical and Biophysical Research Communications*. https://doi.org/10.1006/bbrc.2000.2651

Hui Lee, M., Yoo, Y.-J., Heon Kim, D., Hong Hanh, N., Kwon, Y., & Hwang, I. (2020). *The Prenylated Rab GTPase Receptor PRA1.F4 Contributes to Protein Exit from the Golgi Apparatus 1*. https://doi.org/10.1104/pp.17.00466

Humphrey, S. J., James, D. E., & Mann, M. (2015). Protein Phosphorylation: A Major Switch Mechanism for Metabolic Regulation. *Trends in Endocrinology and Metabolism*, *26*(12), 676–687. https://doi.org/10.1016/j.tem.2015.09.013

Hwang, W. W., Venkatasubrahmanyam, S., Ianculescu, A. G., Tong, A., Boone, C., & Madhani, H. D. (2003). A conserved RING finger protein required for histone H2B monoubiquitination and cell size control. *Molecular Cell*, *11*(1), 261–266. https://doi.org/10.1016/S1097-2765(02)00826-2

Hyun, Y., Vincent, C., Tilmes, V., Bergonzi, S., Kiefer, C., Richter, R., Martinez-Gallegos, R., Severing, E., & Coupland, G. (2019). Plant science: A regulatory circuit conferring varied flowering response to cold in annual and perennial plants. *Science*, *363*(6425), 409–412. https://doi.org/10.1126/science.aau8197

Imaizumi, T., Schultz, T. F., Harmon, F. G., Ho, L. A., & Kay, S. A. (2005). Plant science: FKF1 F-box protein mediates cyclic degradation of a repressor of CONSTANS in Arabidopsis. *Science*. https://doi.org/10.1126/science.1110586

Immink, R. G. H., Posé, D., Ferrario, S., Ott, F., Kaufmann, K., Valentim, F. L., de Folter, S., van der Wal, F., van Dijk, A. D. J., Schmid, M., & Angenent, G. C. (2012). Characterization of SOC1's central role in flowering by the identification of its

upstream and downstream regulators. *Plant Physiology*, *160*(1), 433–449. https://doi.org/10.1104/pp.112.202614

Ito, T., Matsui, Y., Ago, T., Ota, K., & Sumimoto, H. (2001). Novel modular domain PB1 recognizes pc motif to mediate functional protein-protein interactions. *EMBO Journal*, *20*(15), 3938–3946. https://doi.org/10.1093/emboj/20.15.3938

Jang, I. C., Henriques, R., Seo, H. S., Nagatani, A., & Chua, N. H. (2010). Arabidopsis PHYTOCHROME INTERACTING FACTOR proteins promote phytochrome B polyubiquitination by COP1 E3 ligase in the nucleus. *Plant Cell*. https://doi.org/10.1105/tpc.109.072520

Jang, Y. H., Park, H.-Y., Lee, K. C., Thu, M. P., Kim, S.-K., Suh, M. C., Kang, H., & Kim, J.-K. (2014). A homolog of splicing factor SF1 is essential for development and is involved in the alternative splicing of pre-mRNA in \textlessi\textgreaterArabidopsis thaliana\textless/i\textgreater. *The Plant Journal*, *78*(4), 591–603. https://doi.org/10.1111/tpj.12491

Jin, J., & Pawson, T. (2012). Modular evolution of phosphorylation-based signalling systems. *Philosophical Transactions of the Royal Society B: Biological Sciences*, *367*(1602), 2540–2555. https://doi.org/10.1098/rstb.2012.0106

Johansson, M., & Staiger, D. (2015). Time to flower: Interplay between photoperiod and the circadian clock. *Journal of Experimental Botany*, *66*(3), 719–730. https://doi.org/10.1093/jxb/eru441

José Ripoll, J., Ferrándiz, C., Martínez-Laborda, A., & Vera, A. (2006). PEPPER, a novel K-homology domain gene, regulates vegetative and gynoecium development in Arabidopsis. *Developmental Biology*. https://doi.org/10.1016/j.ydbio.2005.10.037

Joshi, H. J., Hirsch-Hoffmann, M., Baerenfaller, K., Gruissem, W., Baginsky, S., Schmidt, R., Schulze, W. X., Sun, Q., van Wijk, K. J., Egelhofer, V., Wienkoop, S., Weckwerth, W., Bruley, C., Rolland, N., Toyoda, T., Nakagami, H., Jones, A. M., Briggs, S. P., Castleden, I., … Heazlewood, J. L. (2011). MASCP gator: An aggregation portal for the visualization of arabidopsis proteomics data. *Plant Physiology*, *155*(1), 259–270. https://doi.org/10.1104/pp.110.168195

Jossier, M., Bouly, J. P., Meimoun, P., Arjmand, A., Lessard, P., Hawley, S., Grahame Hardie, D., & Thomas, M. (2009). SnRK1 (SNF1-related kinase 1) has a central role in sugar and ABA signalling in Arabidopsis thaliana. *Plant Journal*. https://doi.org/10.1111/j.1365-313X.2009.03871.x

Jung, J. H., Lee, H. J., Park, M. J., & Park, C. M. (2014). Beyond ubiquitination: Proteolytic and nonproteolytic roles of HOS1. In *Trends in Plant Science* (Vol. 19). https://doi.org/10.1016/j.tplants.2014.03.012

Jung, J.-H., Seo, J., & Park, C.-M. (2012). *The E3 Ubiquitin Ligase HOS1 Regulates Arabidopsis Flowering by Mediating CONSTANS Degradation Under Cold Stress* * □ *S*. https://doi.org/10.1074/jbc.M112.394338

Kanno, T., Venhuizen, P., Wen, T. N., Lin, W. D., Chiou, P., Kalyna, M., Matzke, A. J. M., & Matzke, M. (2018). PRP4KA, a putative spliceosomal protein kinase, is important for alternative splicing and development in arabidopsis Thaliana. *Genetics*, *210*(4), 1267–1285. https://doi.org/10.1534/genetics.118.301515

Kenzior, A., & Folk, W. R. (2015). Arabidopsis thaliana MSI4/FVE associates with members of a novel family of plant specific PWWP/RRM domain proteins. *Plant Molecular Biology*. https://doi.org/10.1007/s11103-014-0280-z

Kerk, D., Templeton, G., & Moorhead, G. B. G. (2008). Evolutionary radiation pattern of novel protein phosphatases revealed by analysis of protein data from the completely sequenced genomes of humans, green algae, and higher plants. *Plant Physiology*, *146*(2), 351–367. https://doi.org/10.1104/pp.107.111393

Kobayashi, Y., & Weigel, D. (2007). Move on up, it's time for change—Mobile signals controlling photoperiod-dependent flowering. In *Genes and Development* (Vol. 21). https://doi.org/10.1101/gad.1589007

Korasick, D. A., Chatterjee, S., Tonelli, M., Dashti, H., Lee, S. G., Westfall, C. S., Fulton, D. B., Andreotti, A. H., Amarasinghe, G. K., Strader, L. C., & Jez, J. M. (2015). Defining a two-pronged structural model for PB1 (Phox/Bem1p) domain interaction in plant auxin responses. *Journal of Biological Chemistry*, *290*(20), 12868–12878. https://doi.org/10.1074/jbc.M115.648253

Krogan, N. J., Dover, J., Wood, A., Schneider, J., Heidt, J., Boateng, M. A., Dean, K., Ryan, O. W., Golshani, A., Johnston, M., Greenblatt, J. F., & Shilatifard, A. (2003). The Paf1 complex is required for histone H3 methylation by COMPASS and Dot1p: Linking transcriptional elongation to histone methylation. *Molecular Cell*. https://doi.org/10.1016/S1097-2765(03)00091-1

Kwak, Jun S., Son, G. H., Kim, S. I., Song, J. T., & Seo, H. S. (2016a). Arabidopsis HIGH PLOIDY2 Sumoylates and stabilizes flowering locus C through Its E3 ligase activity. *Frontiers in Plant Science*, *7*(APR2016), 1–9. https://doi.org/10.3389/fpls.2016.00530

Kwak, Jun Soo, Son, G. H., Song, J. T., & Seo, H. S. (2016b). *Post-translational modifications of FLOWERING LOCUS C modulate its activity*. https://doi.org/10.1093/jxb/erw431

Laubinger, S., Fittinghoff, K., & Hoecker, U. (2004). The SPA quartet: A family of WD-repeat proteins with a central role in suppression of photomorphogenesis in Arabidopsis. *Plant Cell*, *16*(9), 2293–2306. https://doi.org/10.1105/tpc.104.024216

Lazaro, A., Mouriz, A., Piñeiro, M., & Jarillo, J. A. (2015). Red light-mediated degradation of constans by the e3 ubiquitin ligase hos1 regulates photoperiodic flowering in arabidopsis. *Plant Cell*. https://doi.org/10.1105/tpc.15.00529

Lee, H., Suh, S. S., Park, E., Cho, E., Ahn, J. H., Kim, S. G., Lee, J. S., Kwon, Y. M., & Lee, I. (2000). The AGAMOUS-IIKE 20 MADS domain protein integrates floral inductive pathways in Arabidopsis. *Genes and Development*. https://doi.org/10.1101/gad.813600

Lee, I., Aukerman, M. J., Gore, S. L., Lohman, K. N., Michaels, S. D., Weaver, L. M., John, M. C., Feldmann, K. A., & Amasino, R. M. (1994). Isolation of LUMINIDEPENDENS: A gene involved in the control of flowering time in Arabidopsis. *Plant Cell*. https://doi.org/10.1105/tpc.6.1.75

Lee, J. H., Chung, K. S., Kim, S.-K., & Ahn, J. H. (2014). *Plant Signaling & Behavior Post-translational regulation of SHORT VEGETATIVE PHASE as a major mechanism for thermoregulation of flowering*. https://doi.org/10.4161/psb.28193

Lee, J. H., Ryu, H. S., Chung, K. S., Posé, D., Kim, S., Schmid, M., & Ahn, J. H. (2013). Regulation of temperature-responsive flowering by MADS-box transcription factor repressors. *Science*. https://doi.org/10.1126/science.1241097

Lee, J., & Lee, I. (2010). Regulation and function of SOC1, a flowering pathway integrator. In *Journal of Experimental Botany* (Vol. 61). https://doi.org/10.1093/jxb/erq098

Lee, J., Oh, M., Park, H., & Lee, I. (2008). SOC1 translocated to the nucleus by interaction with AGL24 directly regulates LEAFY. *Plant Journal*. https://doi.org/10.1111/j.1365-313X.2008.03552.x

Lee, K. C., Jang, Y. H., Kim, S. K., Park, H. Y., Thu, M. P., Lee, J. H., & Kim, J. K. (2017). RRM domain of Arabidopsis splicing factor SF1 is important for pre-mRNA splicing of a specific set of genes. *Plant Cell Reports*, *36*(7), 1083–1095. https://doi.org/10.1007/s00299-017-2140-1

Lehti-Shiu, M. D., & Shiu, S. H. (2012). Diversity, classification and function of the plant protein kinase superfamily. *Philosophical Transactions of the Royal Society B: Biological Sciences*, *367*(1602), 2619–2639. https://doi.org/10.1098/rstb.2012.0003

Li, C., Chen, C., Gao, L., Yang, S., Nguyen, V., Shi, X., Siminovitch, K., Kohalmi, S. E., Huang, S., Wu, K., Chen, X., & Cui, Y. (2015). The Arabidopsis SWI2/SNF2 Chromatin Remodeler BRAHMA Regulates Polycomb Function during Vegetative Development and Directly Activates the Flowering Repressor Gene SVP. *PLoS Genetics*, *11*(1), 1–25. https://doi.org/10.1371/journal.pgen.1004944

Li, C., Gu, L., Gao, L., Chen, C., Wei, C.-Q., Qiu, Q., Chien, C.-W., Wang, S., Jiang, L., Ai, L.-F., Chen, C.-Y., Yang, S., Nguyen, V., Qi, Y., Snyder, M. P., Burlingame, A. L., Kohalmi, S. E., Huang, S., Cao, X., … Cui, Y. (2016). Concerted genomic targeting of H3K27 demethylase REF6 and chromatin-remodeling ATPase BRM in Arabidopsis. *Nature Publishing Group*, *48*(6). https://doi.org/10.1038/ng.3555

Li, D., Liu, C., Shen, L., Wu, Y., Chen, H., Robertson, M., Helliwell, C. A., Ito, T., Meyerowitz, E., & Yu, H. (2008). A Repressor Complex Governs the Integration of Flowering Signals in Arabidopsis. *Developmental Cell*, *15*(1), 110–120. https://doi.org/10.1016/j.devcel.2008.05.002

Lim, W. A., & Pawson, T. (2010). Phosphotyrosine Signaling: Evolving a New Cellular Communication System. In *Cell*. https://doi.org/10.1016/j.cell.2010.08.023

Lin, X., Kaul, S., Rounsley, S., Shea, T. P., Benito, M. I., Town, C. D., Fujii, C. Y., Mason, T., Bowman, C. L., Barnstead, M., Feldblyum, T. V., Buell, C. R., Ketchum, K. A., Lee, J., Ronning, C. M., Koo, H. L., Moffat, K. S., Cronin, L. A., Shen, M., … Venter, J. C. (1999). Sequence and analysis of chromosome 2 of the plant Arabidopsis thaliana. *Nature*. https://doi.org/10.1038/45471

Lin, Z., Li, Y., Zhang, Z., Liu, X., Hsu, C. C., Du, Y., Sang, T., Zhu, C., Wang, Y., Satheesh, V., Pratibha, P., Zhao, Y., Song, C. P., Tao, W. A., Zhu, J. K., & Wang, P. (2020). A RAF-SnRK2 kinase cascade mediates early osmotic stress signaling in higher plants. *Nature Communications*, *11*(1). https://doi.org/10.1038/s41467-020-14477-9

Liu, B., Zuo, Z., Liu, H., Liu, X., & Lin, C. (2011). Arabidopsis cryptochrome 1 interacts with SPA1 to suppress COP1 activity in response to blue light. *Genes and Development*, *25*(10), 1029–1034. https://doi.org/10.1101/gad.2025011

Liu, L. J., Zhang, Y. C., Li, Q. H., Sang, Y., Mao, J., Lian, H. L., Wang, L., & Yang, H. Q. (2008). COP1-mediated ubiquitination of CONSTANS is implicated in cryptochrome regulation of flowering in Arabidopsis. *Plant Cell*, *20*(2), 292–306. https://doi.org/10.1105/tpc.107.057281

Lu, S. X., Liu, H., Knowles, S. M., Li, J., Ma, L., Tobin, E. M., & Lin, C. (2011). *A Role for Protein Kinase Casein Kinase2 a-Subunits in the Arabidopsis Circadian Clock 1[W][OA]*. https://doi.org/10.1104/pp.111.179846

Macknight, R., Bancroft, I., Page, T., Lister, C., Schmidt, R., Love, K., Westphal, L., Murphy, G., Sherson, S., Cobbett, C., & Dean, C. (1997). FCA, a gene controlling flowering time in arabidopsis, encodes a protein containing RNA-binding domains. *Cell*. https://doi.org/10.1016/S0092-8674(00)80256-1

Mahrez, W., Shin, J., Muñoz-Viana, R., Figueiredo, D. D., Trejo-Arellano, M. S., Exner, V., Siretskiy, A., Gruissem, W., Köhler, C., & Hennig, L. (2016). BRR2a Affects Flowering Time via FLC Splicing. *PLoS Genetics*, *12*(4), 1005924. https://doi.org/10.1371/journal.pgen.1005924

Mann, M., & Jensen, O. N. (2003). Proteomic analysis of post-translational modifications. In *Nature Biotechnology*. https://doi.org/10.1038/nbt0303-255

Manning, G, Whyte, D. B., Martinez, R., & Hunter, T. (2002a). *The Protein Kinase Complement of the Human Genome*. *298*(December).

Manning, Gerard, Plowman, G. D., Hunter, T., Sudarsanam, S., Manning, G., & Plowman, G. D. (2002b). *Evolution of protein kinase signaling from yeast to man*. *27*(10), 514–520.

Matsoukas, I. G. (2015). Florigens and antiflorigens: A molecular genetic understanding. *Essays in Biochemistry*, *58*, 133–149. https://doi.org/10.1042/BSE0580133

Mergner, J., Frejno, M., List, M., Papacek, M., Chen, X., Chaudhary, A., Samaras, P., Richter, S., Shikata, H., Messerer, M., Lang, D., Altmann, S., Cyprys, P., Zolg, D. P., Mathieson, T., Bantscheff, M., Hazarika, R. R., Schmidt, T., Dawid, C., …

Kuster, B. (2020). Mass-spectrometry-based draft of the Arabidopsis proteome. *Nature*, *579*(7799), 409–414. https://doi.org/10.1038/s41586-020-2094-2

Michniewicz, M., Zago, M. K., Abas, L., Weijers, D., Schweighofer, A., Meskiene, I., Heisler, M. G., Ohno, C., Zhang, J., Huang, F., Schwab, R., Weigel, D., Meyerowitz, E. M., Luschnig, C., Offringa, R., & Friml, J. (2007). Antagonistic Regulation of PIN Phosphorylation by PP2A and PINOID Directs Auxin Flux. *Cell*. https://doi.org/10.1016/j.cell.2007.07.033

Mizoguchi, T., Wheatley, K., Hanzawa, Y., Wright, L., Mizoguchi, M., Song, H. R., Carré, I. A., & Coupland, G. (2002). LHY and CCA1 are partially redundant genes required to maintain circadian rhythms in Arabidopsis. *Developmental Cell*, *2*(5), 629–641. https://doi.org/10.1016/S1534-5807(02)00170-3

Mockler, T. C., Michael, T. P., Priest, H. D., Shen, R., Sullivan, C. M., Givan, S. A., Mcentee, C., Kay, S. A., & Chory, J. (2007). The diurnal project: Diurnal and circadian expression profiling, model-based pattern matching, and promoter analysis. *Cold Spring Harbor Symposia on Quantitative Biology*. https://doi.org/10.1101/sqb.2007.72.006

Mockler, Todd C., Yu, X., Shalitin, D., Parikh, D., Michael, T. P., Liou, J., Huang, J., Smith, Z., Alonso, J. M., Ecker, J. R., Chory, J., & Lin, C. (2004). Regulation of flowering time in Arabidopsis by K homology domain proteins. *Proceedings of the National Academy of Sciences of the United States of America*. https://doi.org/10.1073/pnas.0404552101

Moscat, J., Diaz-Meco, M. T., Albert, A., & Campuzano, S. (2006). Cell Signaling and Function Organized by PB1 Domain Interactions. *Molecular Cell*, *23*(5), 631–640. https://doi.org/10.1016/j.molcel.2006.08.002

Mulekar, J. J., Bu, Q., Chen, F., & Huq, E. (2012). Casein kinase II α subunits affect multiple developmental and stress-responsive pathways in Arabidopsis. *Plant Journal*. https://doi.org/10.1111/j.1365-313X.2011.04794.x

Mulekar, J. J., & Huq, E. (2014). Expanding roles of protein kinase CK2 in regulating plant growth and development. In *Journal of Experimental Botany* (Vol. 65). https://doi.org/10.1093/jxb/ert401

Mulekar, J. J., & Huq, E. (2015). Arabidopsis casein kinase 2 α4 subunit regulates various developmental pathways in a functionally overlapping manner. *Plant Science*, *236*, 295–303. https://doi.org/10.1016/j.plantsci.2015.04.013

Mutasa-Göttgens, E., & Hedden, P. (2009). Gibberellin as a factor in floral regulatory networks. In *Journal of Experimental Botany* (Vol. 60). https://doi.org/10.1093/jxb/erp040

Nagel, D. H., & Kay, S. A. (2012). Complexity in the wiring and regulation of plant circadian networks. In *Current Biology*. https://doi.org/10.1016/j.cub.2012.07.025

Nakamichi, N., Kiba, T., Henriques, R., Mizuno, T., Chua, N. H., & Sakakibara, H. (2010). PSEUDO-RESPONSE ReGULATORS 9, 7, and 5 are transcriptional repressors in the Arabidopsis circadian clock. *Plant Cell*, *22*(3), 594–605. https://doi.org/10.1105/tpc.109.072892

Nakamichi, N., Kita, M., Niinuma, K., Ito, S., Yamashino, T., Mizoguchi, T., & Mizuno, T. (2007). Arabidopsis clock-associated pseudo-response regulators PRR9, PRR7

and PRR5 coordinately and positively regulate flowering time through the canonical CONSTANS-dependent photoperiodic pathway. *Plant and Cell Physiology*. https://doi.org/10.1093/pcp/pcm056

Nanao, M. H., Vinos-Poyo, T., Brunoud, G., Thévenon, E., Mazzoleni, M., Mast, D., Lainé, S., Wang, S., Hagen, G., Li, H., Guilfoyle, T. J., Parcy, F., Vernoux, T., & Dumas, R. (2014). Structural basis for oligomerization of auxin transcriptional regulators. *Nature Communications*, *5*, 3617. https://doi.org/10.1038/ncomms4617

Nilsen, T. W., & Graveley, B. R. (2010). Expansion of the eukaryotic proteome by alternative splicing. In *Nature* (Vol. 463). Nature Publishing Group. https://doi.org/10.1038/nature08909

Niwa, Y., Ito, S., Nakamichi, N., Mizoguchi, T., Niinuma, K., Yamashino, T., & Mizuno, T. (2007). Genetic linkages of the circadian clock-associated genes, TOC1, CCA1 and LHY, in the photoperiodic control of flowering time in Arabidopsis thaliana. *Plant and Cell Physiology*, *48*(7), 925–937. https://doi.org/10.1093/pcp/pcm067

Noda, Y., Kohjima, M., Izaki, T., Ota, K., Yoshinaga, S., Inagaki, F., Ito, T., & Sumimoto, H. (2003). Molecular Recognition in Dimerization between PB1 Domains. *Journal of Biological Chemistry*, *278*(44), 43516–43524. https://doi.org/10.1074/jbc.M306330200

Ogiso, E., Takahashi, Y., Sasaki, T., Yano, M., & Izawa, T. (2010). The role of casein kinase II in flowering time regulation has diversified during evolution. *Plant Physiology*. https://doi.org/10.1104/pp.109.148908

Oh, S., & Montgomery, B. L. (2013). Phytochrome-induced SIG2 expression contributes to photoregulation of phytochrome signalling and photomorphogenesis in

Arabidopsis thaliana. *Journal of Experimental Botany*, *64*(18), 5457–5472. https://doi.org/10.1093/jxb/ert308

Oh, S., Zhang, H., Ludwig, P., & Van Nocker, S. (2004). A mechanism related to the yeast transcriptional regulator Paf1c is required for expression of the Arabidopsis FLC/MAF MADS box gene family. *Plant Cell*, *16*(11), 2940–2953. https://doi.org/10.1105/tpc.104.026062

Ó'Maoiléidigh, D. S., Graciet, E., & Wellmer, F. (2014). Gene networks controlling Arabidopsis thaliana flower development. In *New Phytologist*. https://doi.org/10.1111/nph.12444

Park, H. J., Kim, W. Y., Pardo, J. M., & Yun, D. J. (2016). Molecular Interactions Between Flowering Time and Abiotic Stress Pathways. In *International Review of Cell and Molecular Biology* (Vol. 327, pp. 371–412). https://doi.org/10.1016/bs.ircmb.2016.07.001

Park, H.-Y., Lee, H. T., Lee, J. H., & Kim, J.-K. (2019). Arabidopsis U2AF65 Regulates Flowering Time and the Growth of Pollen Tubes. *Frontiers in Plant Science*, *10*, 569. https://doi.org/10.3389/fpls.2019.00569

Park, S., Oh, S., Ek-Ramos, J., & van Nocker, S. (2010). Plant homologous to parafibromin is a component of the paf1 complex and assists in regulating expression of genes within h3k27me3-enriched chromatin. *Plant Physiology*, *153*(2), 821–831. https://doi.org/10.1104/pp.110.155838

Pérez-Pérez, J. M., Candela, H., & Micol, J. L. (2009). Understanding synergy in genetic interactions. In *Trends in Genetics* (Vol. 25). Elsevier Current Trends. https://doi.org/10.1016/j.tig.2009.06.004

PIN, P. A., & NILSSON, O. (2012). The multifaceted roles of FLOWERING LOCUS T in plant development. *Plant, Cell & Environment*, *35*(10), 1742–1755. https://doi.org/10.1111/j.1365-3040.2012.02558.x

Piñeiro, M., & Jarillo, J. A. (2013). Ubiquitination in the control of photoperiodic flowering. In *Plant Science* (Vol. 198). https://doi.org/10.1016/j.plantsci.2012.10.005

Qi, H. D., Lin, Y., Ren, Q. P., Wang, Y. Y., Xiong, F., & Wang, X. L. (2019). RNA Splicing of FLC Modulates the Transition to Flowering. In *Frontiers in Plant Science* (Vol. 10). Frontiers Media S.A. https://doi.org/10.3389/fpls.2019.01625

Richter, R., Kinoshita, A., Vincent, C., Martinez-Gallegos, R., Gao, H., van Driel, A. D., Hyun, Y., Mateos, J. L., & Coupland, G. (2019). Floral regulators FLC and SOC1 directly regulate expression of the B3-type transcription factor TARGET of FLC and SVP 1 at the Arabidopsis shoot apex via antagonistic chromatin modifications. *PLoS Genetics*, *15*(4), e1008065. https://doi.org/10.1371/journal.pgen.1008065

Robaglia, C., Thomas, M., & Meyer, C. (2012). Sensing nutrient and energy status by SnRK1 and TOR kinases. *Current Opinion in Plant Biology*, *15*(3), 301–307. https://doi.org/10.1016/j.pbi.2012.01.012

Rudrabhatla, P., Reddy, M. M., & Rajasekharan, R. (2006). Genome-wide analysis and experimentation of plant serine/threonine/ tyrosine-specific protein kinases. *Plant Molecular Biology*, *60*(2), 293–319. https://doi.org/10.1007/s11103-005-4109-7

Sawa, M., Nusinow, D. A., Kay, S. A., & Imaizumi, T. (2007). FKF1 and GIGANTEA complex formation is required for day-length measurement in Arabidopsis. *Science*. https://doi.org/10.1126/science.1146994

Schmitges, F. W., Prusty, A. B., Faty, M., Stützer, A., Lingaraju, G. M., Aiwazian, J., Sack, R., Hess, D., Li, L., Zhou, S., Bunker, R. D., Wirth, U., Bouwmeester, T., Bauer, A., Ly-Hartig, N., Zhao, K., Chan, H., Gu, J., Gut, H., Thomä, N. H. (2011). Histone Methylation by PRC2 Is Inhibited by Active Chromatin Marks. *Molecular Cell*. https://doi.org/10.1016/j.molcel.2011.03.025

Schomburg, F. M., Patton, D. A., Meinke, D. W., & Amasino, R. M. (2001). FPA, a gene involved in floral induction in Arabidopsis, encodes a protein containing RNA-recognition motifs. *Plant Cell*. https://doi.org/10.1105/tpc.13.6.1427

Searle, I., He, Y., Turck, F., Vincent, C., Fornara, F., Kröber, S., Amasino, R. A., & Coupland, G. (2006). The transcription factor FLC confers a flowering response to vernalization by repressing meristem competence and systemic signaling in Arabidopsis. *Genes and Development*. https://doi.org/10.1101/gad.373506

Seo, P. J., Park, M. J., Lim, M. H., Kim, S. G., Lee, M., Baldwin, I. T., & Park, C. M. (2012). A self-regulatory circuit of CIRCADIAN CLOCK-ASSOCIATED1 underlies the circadian clock regulation of temperature responses in Arabidopsis. *Plant Cell*, *24*(6), 2427–2442. https://doi.org/10.1105/tpc.112.098723

Sharma, K., D'Souza, R. C. J., Tyanova, S., Schaab, C., Wiśniewski, J. R., Cox, J., & Mann, M. (2014). Ultradeep Human Phosphoproteome Reveals a Distinct Regulatory Nature of Tyr and Ser/Thr-Based Signaling. *Cell Reports*, *8*(5), 1583–1594. https://doi.org/10.1016/j.celrep.2014.07.036

Shim, J. S., & Imaizumi, T. (2015). Circadian clock and photoperiodic response in arabidopsis: From seasonal flowering to redox homeostasis. In *Biochemistry* (Vol. 54). American Chemical Society. https://doi.org/10.1021/bi500922q

Simpson, G. G., Dijkwel, P. P., Quesada, V., Henderson, I., & Dean, C. (2003). FY is an RNA 3′ end-processing factor that interacts with FCA to control the Arabidopsis floral transition. *Cell*. https://doi.org/10.1016/S0092-8674(03)00425-2

Singh, V., Ram, M., Kumar, R., Prasad, R., Roy, B. K., & Singh, K. K. (2017). Phosphorylation: Implications in Cancer. *Protein Journal*, *36*(1), 1–6. https://doi.org/10.1007/s10930-017-9696-z

Soma, F., Takahashi, F., Suzuki, T., Shinozaki, K., & Yamaguchi-Shinozaki, K. (2020). Plant Raf-like kinases regulate the mRNA population upstream of ABA-unresponsive SnRK2 kinases under drought stress. *Nature Communications*, *11*(1), 1–12. https://doi.org/10.1038/s41467-020-15239-3

Song, Y. H., Ito, S., & Imaizumi, T. (2013). Flowering time regulation: Photoperiod- and temperature-sensing in leaves. In *Trends in Plant Science* (Vol. 18). https://doi.org/10.1016/j.tplants.2013.05.003

Song, Y. H., Shim, J. S., Kinmonth-Schultz, H. A., & Imaizumi, T. (2015). Photoperiodic Flowering: Time Measurement Mechanisms in Leaves. *Annual Review of Plant Biology*, *66*(1), 441–464. https://doi.org/10.1146/annurev-arplant-043014-115555

Song, Y. H., Smith, R. W., To, B. J., Millar, A. J., & Imaizumi, T. (2012). FKF1 Conveys Timing Information for. *Science*, *1045*, 1045–1050. https://doi.org/10.1126/science.1219644

Srikanth, A., & Schmid, M. (2011). Regulation of flowering time: All roads lead to Rome. In *Cellular and Molecular Life Sciences* (Vol. 68). https://doi.org/10.1007/s00018-011-0673-y

Stecker, K. E., Minkoff, B. B., & Sussman, M. R. (2014). Phosphoproteomic analyses reveal early signaling events in the osmotic stress response. *Plant Physiology*, *165*(3), 1171–1187. https://doi.org/10.1104/pp.114.238816

Sumimoto, H., Kamakura, S., & Ito, T. (2007). Structure and function of the PB1 domain, a protein interaction module conserved in animals, fungi, amoebas, and plants. *Science's STKE*, *2007*(401), re6-re6. https://doi.org/10.1126/stke.4012007re6

Sung, S., & Amasino, R. M. (2004). Vernalization in Arabidopsis thaliana is mediated by the PHD finger protein VIN3. *Nature*, *427*(6970), 159–164. https://doi.org/10.1038/nature02195

Swaney, D. L., & Villén, J. (2016). Proteomic analysis of protein posttranslational modifications by mass spectrometry. *Cold Spring Harbor Protocols*, *2016*(3), 207–209. https://doi.org/10.1101/pdb.top077743

Swarbreck, D., Wilks, C., Lamesch, P., Berardini, T. Z., Garcia-Hernandez, M., Foerster, H., Li, D., Meyer, T., Muller, R., Ploetz, L., Radenbaugh, A., Singh, S., Swing, V., Tissier, C., Zhang, P., & Huala, E. (2008). The Arabidopsis Information Resource (TAIR): Gene structure and function annotation. *Nucleic Acids Research*. https://doi.org/10.1093/nar/gkm965

Swiezewski, S., Liu, F., Magusin, A., & Dean, C. (2009). Cold-induced silencing by long antisense transcripts of an Arabidopsis Polycomb target. *Nature*, *462*. https://doi.org/10.1038/nature08618

Tang, X., Hou, A., Babu, M., Nguyen, V., Hurtado, L., Lu, Q., Reyes, J. C., Wang, A., Keller, W. A., Harada, J. J., Tsang, E. W. T., & Cui, Y. (2008). The Arabidopsis

Brahma chromatin-remodeling ATPase is involved in repression of seed maturation genes in leaves. *Plant Physiology*. https://doi.org/10.1104/pp.108.121996

Terman, J. R., & Kashina, A. (2013). Post-translational modification and regulation of actin. In *Current Opinion in Cell Biology*. https://doi.org/10.1016/j.ceb.2012.10.009

Tian, Y., Zheng, H., Zhang, F., Wang, S., Ji, X., Xu, C., He, Y., & Ding, Y. (2019). PRC2 recruitment and H3K27me3 deposition at FLC require FCA binding of COOLAIR. *Science Advances*, *5*(4), 7246–7270. https://doi.org/10.1126/sciadv.aau7246

Turck, F., Fornara, F., & Coupland, G. (2008). Regulation and Identity of Florigen: FLOWERING LOCUS T Moves Center Stage. *Annual Review of Plant Biology*, *59*(1), 573–594. https://doi.org/10.1146/annurev.arplant.59.032607.092755

Ubersax, J. A., & Jr, J. E. F. (2007). *Mechanisms of specificity in protein phosphorylation*. *8*(July), 530–542. https://doi.org/10.1038/nrm2203

Uhrig, R. G., Schläpfer, P., Roschitzki, B., Hirsch-Hoffmann, M., & Gruissem, W. (2019). Diurnal changes in concerted plant protein phosphorylation and acetylation in Arabidopsis organs and seedlings. *The Plant Journal*, *99*(1), 176–194. https://doi.org/10.1111/tpj.14315

Uhrig, R. G., She, Y.-M., Leach, C. A., & Plaxton, W. C. (2008). *Regulatory Monoubiquitination of Phosphoenolpyruvate Carboxylase in Germinating Castor Oil Seeds * □ S*. https://doi.org/10.1074/jbc.M806102200

Valverde, F. (2011). CONSTANS and the evolutionary origin of photoperiodic timing of flowering. In *Journal of Experimental Botany* (Vol. 62). https://doi.org/10.1093/jxb/erq449

Valverde, F., Mouradov, A., Soppe, W., Ravenscroft, D., Samach, A., & Coupland, G. (2004). Photoreceptor Regulation of CONSTANS Protein in Photoperiodic Flowering. *Science*, *303*(5660), 1003–1006. https://doi.org/10.1126/science.1091761

Verhage, L., Severing, E. I., Bucher, J., Lammers, M., Busscher-Lange, J., Bonnema, G., Rodenburg, N., Proveniers, M. C. G., Angenent, G. C., & Immink, R. G. H. (2017). Splicing-related genes are alternatively spliced upon changes in ambient temperatures in plants. *PLOS ONE*, *12*(3), e0172950. https://doi.org/10.1371/journal.pone.0172950

Vincent, O., Townley, R., Kuchin, S., & Carlson, M. (2001). Subcellular localization of the Snf1 kinase is regulated by specific β subunits and a novel glucose signaling mechanism. *Genes and Development*. https://doi.org/10.1101/gad.879301

Waese, J., Fan, J., Pasha, A., Yu, H., Fucile, G., Shi, R., Cumming, M., Kelley, L. A., Sternberg, M. J., Krishnakumar, V., Ferlanti, E., Miller, J., Town, C., Stuerzlinger, W., & Provart, N. J. (2017). ePlant: Visualizing and exploring multiple levels of data for hypothesis generation in plant biology. *Plant Cell*. https://doi.org/10.1105/tpc.17.00073

Walsh, Christopher. (2006). *Posttranslational modification of proteins: Expanding nature's inventory*. Roberts and Co. Publishers.

Walsh, D. A., & Krebs, E. G. (1973). Protein Kinases. *Enzymes*. https://doi.org/10.1016/S1874-6047(08)60076-1

Wang, Y.-Y., Xiong, F., Ren, Q.-P., & Wang, X.-L. (2020). Regulation of flowering transition by alternative splicing: The role of the U2 auxiliary factor. *Journal of Experimental Botany*, *71*(3), 751–758. https://doi.org/10.1093/jxb/erz416

Wang, Z. Y., & Tobin, E. M. (1998). Constitutive expression of the CIRCADIAN CLOCK ASSOCIATED 1 (CCA1) gene disrupts circadian rhythms and suppresses its own expression. *Cell*. https://doi.org/10.1016/S0092-8674(00)81464-6

Whittaker, C., & Dean, C. (2017). The FLC Locus: A Platform for Discoveries in Epigenetics and Adaptation. *Annual Review of Cell and Developmental Biology*, *12*, 39. https://doi.org/10.1146/annurev-cellbio-100616

Willmann, M. R., & Poethig, R. S. (2011). The effect of the floral repressor FLC on the timing and progression of vegetative phase change in Arabidopsis. *Development*, *138*(4), 677–685. https://doi.org/10.1242/dev.057448

Woloszynska, M., Le Gall, S., Neyt, P., Boccardi, T. M., Grasser, M., Längst, G., Aesaert, S., Coussens, G., Dhondt, S., De Slijke, E. V., Bruno, L., Fung-Uceda, J., Mas, P., Van Montagu, M., Inzé, D., Himanen, K., De Jaeger, G., Grasser, K. D., & Van Lijsebettens, M. (2019). Histone 2B monoubiquitination complex integrates transcript elongation with RNA processing at circadian clock and flowering regulators. *Proceedings of the National Academy of Sciences of the United States of America*, *116*(16), 8060–8069. https://doi.org/10.1073/pnas.1806541116

Wu, Z., Fang, X., Zhu, D., & Dean, C. (2020). Autonomous pathway: Flowering locus c repression through an antisense-mediated chromatin-silencing mechanism. *Plant Physiology*, *182*(1), 27–37. https://doi.org/10.1104/pp.19.01009

Xiao, J., Zhang, H., Xing, L., Xu, S., Liu, H., Chong, K., & Xu, Y. (2013). Requirement of histone acetyltransferases HAM1 and HAM2 for epigenetic modification of FLC in regulating flowering in Arabidopsis. *Journal of Plant Physiology*, *170*(4), 444–451. https://doi.org/10.1016/j.jplph.2012.11.007

Xiong, F., Ren, J. J., Yu, Q., Wang, Y. Y., Lu, C. C., Kong, L. J., Otegui, M. S., & Wang, X. L. (2019). AtU2AF65b functions in abscisic acid mediated flowering via regulating the precursor messenger RNA splicing of ABI5 and FLC in Arabidopsis. *New Phytologist*, *223*(1), 277–292. https://doi.org/10.1111/nph.15756

Xu, L., Ménard, R., Berr, A., Fuchs, J., Cognat, V., Meyer, D., & Shen, W. H. (2009). The E2 ubiquitin-conjugating enzymes, AtUBC1 and AtUBC2, play redundant roles and are involved in activation of FLC expression and repression of flowering in Arabidopsis thaliana. *Plant Journal*, *57*(2), 279–288. https://doi.org/10.1111/j.1365-313X.2008.03684.x

Yang, Z., Wang, C., Xue, Y., Liu, X., Chen, S., Song, C. P., Yang, Y., & Guo, Y. (2019). Calcium-activated 14-3-3 proteins as a molecular switch in salt stress tolerance. *Nature Communications*, *10*(1). https://doi.org/10.1038/s41467-019-09181-2

Yoo, S. K., Chung, K. S., Kim, J., Lee, J. H., Hong, S. M., Yoo, S. J., Yoo, S. Y., Lee, J. S., & Ahn, J. H. (2005). CONSTANS activates SUPPRESSOR OF OVEREXPRESSION OF CONSTANS 1 through FLOWERING LOCUS T to promote flowering in Arabidopsis. *Plant Physiology*. https://doi.org/10.1104/pp.105.066928

Yu, X., & Michaels, S. D. (2010). The arabidopsis paf1c complex component CDC73 participates in the modification of FLOWERING LOCUS C chromatin. *Plant Physiology*, *153*(3), 1074–1084. https://doi.org/10.1104/pp.110.158386

Yun, H., Hyun, Y., Kang, M. J., Noh, Y. S., Noh, B., & Choi, Y. (2011). Identification of regulators required for the reactivation of FLOWERING LOCUS C during Arabidopsis reproduction. *Planta*, *234*(6), 1237–1250. https://doi.org/10.1007/s00425-011-1484-y

Zhang, Hua, & Van Nocker, S. (2002). The Vernalization Independence 4 gene encodes a novel regulator of Flowering Locus C. *Plant Journal*. https://doi.org/10.1046/j.1365-313X.2002.01380.x

Zhang, Huiming, Lang, Z., & Zhu, J. K. (2018). Dynamics and function of DNA methylation in plants. In *Nature Reviews Molecular Cell Biology*. https://doi.org/10.1038/s41580-018-0016-z

Zhou, J. X., Liu, Z. W., Li, Y. Q., Li, L., Wang, B., Chen, S., & He, X. J. (2018). Arabidopsis PWWP domain proteins mediate H3K27 trimethylation on FLC and regulate flowering time. In *Journal of Integrative Plant Biology* (Vol. 60). Blackwell Publishing Ltd. https://doi.org/10.1111/jipb.12630

Zulawski, M., Schulze, G., Braginets, R., Hartmann, S., & Schulze, W. X. (2014). The Arabidopsis Kinome: Phylogeny and evolutionary insights into functional diversification. *BMC Genomics*, *15*(1). https://doi.org/10.1186/1471-2164-15-548

Zuo, Z., Liu, H., Liu, B., Liu, X., & Lin, C. (2011). Blue light-dependent interaction of CRY2 with SPA1 regulates COP1 activity and floral initiation in arabidopsis. *Current Biology*, *21*(10), 841–847. https://doi.org/10.1016/j.cub.2011.03.048

Appendices

S.1 List of important flowering genes. Flowering-related genes that encode proteins with phosphorylation sites were denoted as "*".

Gene	Name	AGI(s)	Pathway
AGL24	AGAMOUS-LIKE 24	AT4G24540	Integrator
AP1	APETALA1	AT1G69120	/
AP2*	APETALA 2	AT4G36920	/
ARP6	ACTIN-RELATED PROTEIN 6	AT3G33520	Ambient
BRM*	BRAMA	AT2G46020	/
CCA1	CIRCADIAN CLOCK ASSOCIATED 1	AT2G46830	Photoperiod
CDF1	CYCLING DOF FACTOR 1	AT5G62430	Photoperiod
CDF2*	CYCLING DOF FACTOR 2	AT5G39660	Photoperiod
CDF3	CYCLING DOF FACTO	AT3G47500	Photoperiod
CDF5*	CYCLING DOF FACTOR 5	AT1G69570	Photoperiod
CHE	CCA1 HIKING EXPEDITION	AT5G08330	Photoperiod
CIB1*	CRYPTOCHROME-INTERACTING BASIC-HELIX-LOOP-HELIX 1	AT4G34530	Photoperiod
CK2	CASEIN KINASE II	AT5G67380; AT3G60250*	/
CO	CONSTANS	AT5G15840	Photoperiod
COP1*	CONSTITUTIVE PHOTOMORPHOGENIC1	AT2G32950	Photoperiod
CRY1*	CRYPTOCHROME 1	AT4G08920	Photoperiod
CRY2*	CRYPTOCHROME 2	AT1G04400	Photoperiod
DNF	DAY NEUTRAL FLOWERING,	AT3G19140	Photoperiod
DSLP*	/	AT3G54760	/
ELF3*	EARLY FLOWERING 3	AT2G25930	Photoperiod

ELF4*	EARLY FLOWERING 4	AT2G40080	Photoperiod
ELF5*	EARLY FLOWERING 5	AT5G62640	Photoperiod
FCA*	FLOWERING TIME CONTROL PROTEIN FCA ALPHA	AT4G16280	Autonomous
FD	FD-1	AT4G35900	Photoperiod
FKF1*	FLAVIN-BINDING, KELCH REPEAT, F BOX 1	AT1G68050	Photoperiod
FLC	FLOWER LOCUS C	AT5G10140	Vernalization; autonomous
FLD	FLOWERING LOCUS D	AT3G10390	Autonomous
FLK*	FLOWERING LOCUS KH DOMAIN	AT3G04610	Autonomous
FLM	FLOWERING LOCUS M	AT1G77080	Ambient
FPA*	/	AT2G43410	Autonomous
FRI	FRIGIDA	AT4G00650	Vernalization
FT*	FLOWERING LOCUS T	AT1G65480	Integrator
FVE*	MULTICOPY SUPPRESSOR OF IRA1 4	AT2G19520	Autonomous
FY*	/	AT5G13480	Autonomous
GA1	GIBBERELLIC ACID INSENSITIVE	AT1G14920	GA
GI	GIGANTEA	AT1G22770	Photoperiod
GID1	GIBBERELLIN INSENSITIVE DWARF1	AT3G05120	GA
GNC	GATA	AT5G56860	GA
GNL	GNC-LIKE	AT4G26150	GA
HOS1*	HIGH EXPRESSION OF OSMOTICALLY RESPONSIVE GENES 1	AT2G39810	Photoperiod
HPY2	HIGH PLOIDY2	AT3G15150	/
HUB1*	HISTONE MONO-UBIQUITINATION 1	AT2G44950	/
HUB2*	HISTONE MONO-UBIQUITINATION 2	AT1G55250	/
LD*	LUMINIDEPENDENS	AT4G02560	Autonomous

LFY	LEAFY	AT5G61850	Integrator
LHP1*	LIKE HETEROCHROMATIN 1	AT5G17690	Vernalization
LHY*	LATE ELONGATED HYPOCOTYL	AT1G01060	Photoperiod
LUX*	LUX ARRHYTHMO	AT3G46640	Photoperiod
NF-Y*	NUCLEAR FACTOR Y	AT5G12840; AT3G05690; AT5G47640; AT1G08970; AT5G63470; AT1G54830	/
PEP	PEPPER	AT4G26000	Autonomous
PHYA	PHYTOCHROME A	AT1G09570	Photoperiod
PHYB*	PHYTOCHROME B	AT2G18790	Photoperiod
PHYC*	PHYTOCHROME C	AT5G35840	Photoperiod
PHYD*	PHYTOCHROME D	AT4G16250	Photoperiod
PHYE*	PHYTOCHROME D	AT4G18130	Photoperiod
PP2A-B’ γ	ATB' GAMMA	AT4G15415	/
PRC2*	POLYCOMB REPRESSIVE COMPLEX 2	AT2G23380; AT5G51230	/
PRR5*	PSEUDO-RESPONSE REGULATOR 5	AT5G24470	Photoperiod
PRR7*	PSEUDO-RESPONSE REGULATOR 7	AT5G02810	Photoperiod
PRR9*	PSEUDO-RESPONSE REGULATOR 9	AT2G46790	Photoperiod
RGA*	REPRESSOR OF GA1-3 1	AT2G01570	GA
RVE8	REVEILLE 8	AT3G09600	/
SF1	SPLICING FACTOR 1	AT5G51300	/
SMZ	SCHLAFMÜTZE	AT3G54990	/
SnRK1*	SNF1-RELATED PROTEIN KINASE 1.1	AT3G01090	/

SNZ	SCHNARCHZAPFEN	AT2G39250	/
SOC1	SUPPRESSOR OF OVEREXPRESSION OF CO 1	AT2G45660	Integrator
SPA*	SUPPRESSOR OF PHYA-105 1	AT2G46340	Photoperiod
SPL*	SQUAMOSA PROMOTER BINDING PROTEIN-LIKE	AT2G47070	/
SPY*	SPINDLY	AT3G11540	GA
SVP	SHORT VEGETATIVE PHASE	AT2G22540	/
TEM1*	TEMPRANILLO 1	AT1G25560	/
TEM2*	TEMPRANILLO 2	AT1G68840	/
TFL1	TERMINAL FLOWER 1	AT5G03840	/
TOC1*	TIMING OF CAB EXPRESSION 1	AT5G61380	Photoperiod
TOE1*	TARGET OF EAT1	AT2G28550	/
TOE2*	TARGET OF EAT2	AT5G60120	/
TOE3*	TARGET OF EAT3	AT5G67180	/
TPL*	TOPLESS	AT1G15750	Photoperiod
TPS1	TREHALOSE-6-PHOSPHATE SYNTHASE 1	AT1G78580	/
TSF	TWIN SISTER OF FT	AT4G20370	integrator
UBC1	UBIQUITIN CARRIER PROTEIN 1	AT4G20370	/
UBC2	UBIQUITIN-CONJUGATING ENZYME 2	AT2G02760	/
VIN3*	VERNALIZATION INSENSITIVE 3	AT5G57380	Vernalization
VIP4*	VERNALIZATION INDEPENDENCE 4	AT5G61150	Vernalization
VRN1*	VERNALIZATION 1	AT3G18990	Vernalization
VRN2*	VERNALIZATION 2	AT4G16845	Vernalization
VRN5	VERNALIZATION 5	AT3G24440	Vernalization
WRKY12*	WRKY DNA-BINDING PROTEIN 12	AT2G44745	GA
WRKY71*	WRKY DNA-BINDING PROTEIN 71	AT1G29860	/
WRKY75*	WRKY DNA-BINDING PROTEIN 75	AT5G13080	GA
ZTL	ZEITLUPE	AT5G57360	Photoperiod

S.2 Phosphorylation site(s) of flowering-related proteins.

Number	Protein	Amino acid	Position	Localization prob	Score
1	AT3G60250	S	58	0.91	85
2	AT3G60250	S	16	1	105
5	AT3G60250	S	50	1	165
1	AT2G32950	S	36	1	66
2	AT2G32950	S	39	1	66
3	AT2G32950	S	5	0.87	133
1	AT5G39660	S	102	0.83	186
2	AT5G39660	S	73	0.93	132
3	AT5G39660	S	202	0.98	59
4	AT5G39660	S	280	1	324
5	AT5G39660	S	429	1	59
4	AT4G08920	T	528	1	54
1	AT1G04400	S	525	0.97	260
2	AT1G04400	S	526	0.98	239
3	AT1G04400	S	598	0.76	254
5	AT1G04400	S	605	0.94	387
1	AT2G25930	S	103	0.99	63
2	AT2G25930	S	421	1	112
3	AT2G25930	S	82	1	131
6	AT2G25930	S	604	0.96	77
7	AT2G25930	S	574	1	108
8	AT2G25930	S	589	0.92	154
1	AT2G40080	S	45	1	191
2	AT2G40080	S	89	0.88	116
1	AT5G62640	S	467	0.93	157
2	AT5G62640	T	469	1	144
2	AT4G16280	S	737	1	218
3	AT4G16280	S	63	0.84	66
4	AT4G16280	S	65	0.99	99
6	AT4G16280	T	86	0.96	210
2	AT1G69570	S	94	0.86	130
1	AT1G68050	S	196	0.81	186
2	AT1G68050	S	198	0.89	234
1	AT3G04610	S	141	1	249
2	AT3G04610	S	137	1	126
1	AT1G65480	S	2	1	77

1	AT2G46020	S	1703	0.76	116
2	AT2G46020	S	581	0.88	177
3	AT2G46020	S	599	1	201
5	AT2G46020	S	569	0.99	170
6	AT2G46020	S	1630	0.99	130
7	AT2G46020	S	1633	0.97	83
8	AT2G46020	S	1634	0.95	78
9	AT2G46020	S	1715	1	151
10	AT2G46020	S	1718	0.78	67
11	AT2G46020	S	1719	0.92	112
12	AT2G46020	S	1724	1	275
13	AT2G46020	S	1726	1	170
14	AT2G46020	S	1734	1	266
16	AT2G46020	S	544	1	212
17	AT2G46020	S	545	0.79	250
18	AT2G46020	S	1885	1	223
19	AT2G46020	S	1888	0.84	174
20	AT2G46020	S	1889	0.84	154
21	AT2G46020	S	2137	1	128
22	AT2G46020	S	2140	1	105
24	AT2G46020	S	350	0.83	106
26	AT2G46020	S	355	0.76	290
27	AT2G46020	S	356	1	295
28	AT2G46020	S	2084	0.81	244
29	AT2G46020	S	2089	1	347
30	AT2G46020	S	1751	1	242
31	AT2G46020	S	1754	1	277
32	AT2G46020	S	1877	0.98	117
33	AT2G46020	S	2055	0.88	226
34	AT2G46020	S	2056	1	310
35	AT2G46020	S	2060	1	159
37	AT2G46020	S	161	0.94	84
38	AT2G46020	S	2019	1	233
40	AT2G46020	S	2023	0.96	94
42	AT2G46020	S	1641	1	320
46	AT2G46020	S	511	1	118
47	AT2G46020	S	1450	0.87	111
48	AT2G46020	S	1453	1	265
49	AT2G46020	S	1761	1	258
50	AT2G46020	S	1763	1	304
53	AT2G46020	S	2122	0.99	196

54	AT2G46020	S	2125	1	220
55	AT2G46020	S	638	1	165
58	AT2G46020	T	1880	0.95	117
63	AT2G46020	T	2083	0.93	321
65	AT2G46020	T	2052	1	158
66	AT2G46020	T	2030	0.92	340
67	AT2G46020	T	2032	0.97	240
68	AT2G46020	T	1658	1	271
1	AT2G19520	S	38	0.99	129
2	AT2G19520	S	42	0.97	191
3	AT2G19520	S	43	0.96	236
4	AT2G19520	S	47	0.77	91
5	AT2G19520	S	377	1	118
6	AT2G19520	S	61	1	188
7	AT2G19520	S	3	1	279
8	AT2G19520	S	10	1	347
9	AT2G19520	S	279	0.99	110
10	AT2G19520	S	429	1	137
11	AT2G19520	S	144	0.87	118
12	AT2G19520	S	152	1	187
13	AT2G19520	T	40	1	183
2	AT5G13480	S	23	0.98	114
1	AT2G39810	S	887	0.96	251
2	AT2G39810	S	246	1	311
5	AT2G39810	S	803	1	170
7	AT2G39810	S	902	1	315
8	AT2G39810	S	688	1	72
9	AT2G39810	S	17	1	201
12	AT2G39810	S	128	1	228
14	AT2G39810	S	818	0.99	218
16	AT2G39810	T	901	0.98	179
1	AT2G44950	S	122	0.83	233
2	AT2G44950	S	123	0.99	271
3	AT2G44950	S	18	1	208
1	AT1G55250	S	288	0.97	247
2	AT1G55250	S	295	0.75	80
3	AT1G55250	S	297	1	412
4	AT1G55250	S	21	1	184
6	AT1G55250	S	760	0.89	77
2	AT4G02560	S	478	0.98	159

2	AT5G17690	S	351	1	161
3	AT5G17690	S	279	1	198
4	AT5G17690	S	286	1	187
5	AT5G17690	S	35	1	327
6	AT5G17690	S	42	1	430
7	AT5G17690	S	53	0.98	203
8	AT5G17690	S	31	1	201
9	AT5G17690	S	189	0.77	114
10	AT5G17690	S	241	0.85	41
1	AT1G01060	S	553	0.99	108
2	AT1G01060	S	644	0.91	126
3	AT1G01060	S	179	1	74
4	AT1G01060	S	475	0.76	68
5	AT1G01060	S	477	0.88	59
6	AT1G01060	T	645	0.89	113
7	AT1G01060	T	473	0.98	68
2	AT5G24470	S	336	0.8	44
1	AT2G46790	S	365	0.96	130
2	AT5G02810	S	270	1	192
3	AT5G02810	S	375	0.83	109
4	AT5G02810	S	376	0.77	175
5	AT5G02810	S	378	0.98	201
6	AT5G02810	S	380	0.89	90
7	AT5G02810	S	290	0.92	95
1	AT3G05690	S	110	1	167
1	AT4G18130	S	576	0.82	124
2	AT4G18130	S	581	1	95
5	AT4G18130	S	904	0.8	125
6	AT4G18130	S	53	1	136
2	AT4G36920	S	24	0.85	236
1	AT4G34530	S	81	0.98	60
2	AT3G09600	S	182	1	187
4	AT3G09600	S	130	0.83	158
6	AT3G09600	S	196	1	82
7	AT3G09600	S	157	1	175
1	AT2G47070	S	17	1	133
4	AT2G47070	S	805	1	228
1	AT3G01090	S	199	0.77	354
2	AT3G01090	S	202	0.79	177
3	AT3G01090	S	384	1	72

4	AT3G01090	S	387	1	204
5	AT3G01090	S	33	1	132
7	AT3G01090	T	376	1	385
8	AT3G01090	T	198	1	446
1	AT5G51300	S	84	1	256
2	AT5G51300	S	187	1	244
3	AT5G51300	S	189	1	244
5	AT5G51300	S	77	1	256
1	AT5G47640	S	8	1	53
3	AT5G47640	S	24	0.98	111
4	AT5G47640	S	4	1	84
5	AT5G47640	T	129	1	65
1	AT1G08970	S	168	1	143
1	AT4G15415	S	510	0.96	97
2	AT4G15415	T	513	1	145
1	AT3G46640	S	70	0.8	65
2	AT3G46640	S	82	0.85	124
3	AT3G46640	S	83	0.97	146
4	AT3G46640	S	84	0.95	152
9	AT3G46640	T	57	0.85	67
1	AT5G12840	S	92	1	109
2	AT5G12840	S	92	1	98
1	AT5G51230	S	523	1	183
2	AT5G51230	S	527	1	236
3	AT5G51230	S	8	1	104
1	AT2G23380	S	381	0.89	151
2	AT2G23380	S	248	0.92	49
4	AT2G23380	S	117	0.99	140
1	AT4G16250	S	26	0.99	85
2	AT4G16250	S	34	0.88	94
3	AT4G16250	S	7	0.82	112
1	AT5G35840	S	21	1	110
1	AT2G18790	S	621	1	130
3	AT2G18790	S	24	0.77	83
4	AT2G18790	S	25	0.94	170
6	AT2G18790	S	1161	0.79	141
7	AT2G18790	S	1163	0.97	129
8	AT2G18790	S	74	1	136
9	AT2G18790	S	77	1	89
10	AT2G18790	S	84	0.97	73

11	AT2G18790	S	86	1	178
13	AT2G18790	S	3	1	60
14	AT2G18790	T	62	1	155
15	AT2G18790	T	27	1	177
2	AT2G28550	S	73	0.85	142
3	AT2G28550	S	78	1	360
1	AT5G61380	S	194	1	69
3	AT5G61380	T	400	0.98	142
1	AT1G68840	S	26	1	100
2	AT1G68840	S	40	1	176
1	AT1G29860	S	87	1	123
1	AT5G13080	S	20	1	89
2	AT2G44745	T	208	0.85	139
1	AT5G61150	S	620	1	263
2	AT5G61150	S	227	1	269
3	AT5G61150	S	527	1	192
4	AT5G61150	S	539	1	192
5	AT5G61150	S	164	1	127
9	AT5G61150	S	598	1	276
10	AT5G61150	S	603	1	276
11	AT5G61150	S	548	1	462
12	AT5G61150	S	566	0.9	121
13	AT5G61150	S	570	1	301
14	AT5G61150	S	138	1	263
15	AT5G61150	S	148	1	214
16	AT5G61150	S	195	1	310
17	AT5G61150	S	203	1	245
18	AT5G61150	S	174	1	167
19	AT5G61150	S	175	1	253
20	AT5G61150	S	126	1	133
21	AT5G61150	S	128	1	117
22	AT5G61150	S	131	1	93
23	AT5G61150	S	456	0.85	148
24	AT5G61150	S	473	1	223
25	AT5G61150	S	520	0.94	63
26	AT5G61150	S	522	0.99	63
27	AT5G61150	S	19	0.91	46
28	AT5G61150	S	151	1	267
29	AT5G61150	S	153	1	338
30	AT5G61150	S	566	0.76	100

31	AT5G61150	S	570	1	180
32	AT5G61150	T	531	1	192
33	AT5G61150	T	146	0.96	174
35	AT5G61150	Y	569	0.85	116
1	AT5G57380	S	304	0.98	49
1	AT1G78580	S	45	0.88	76
2	AT1G78580	S	890	1	141
1	AT1G15750	S	214	1	301
3	AT1G15750	S	684	0.91	368
4	AT1G15750	S	685	0.86	412
6	AT1G15750	S	705	0.98	335
7	AT1G15750	S	739	1	207
8	AT1G15750	S	712	0.92	43
9	AT1G15750	S	717	1	78
10	AT1G15750	S	203	1	102
14	AT1G15750	T	286	1	337
18	AT1G15750	T	736	0.99	107
1	AT5G67180	S	7	0.98	78
2	AT5G67180	S	335	0.99	119
1	AT5G60120	S	421	1	77
1	AT1G25560	S	47	0.85	102
1	AT3G11540	S	903	0.92	192
2	AT3G11540	S	13	1	140
5	AT3G11540	S	35	1	230
9	AT3G11540	T	884	0.92	145
1	AT2G43410	S	407	1	252
2	AT2G43410	S	590	1	308
3	AT2G43410	S	362	0.99	146
4	AT2G43410	S	371	0.97	111
5	AT2G43410	S	386	1	167
8	AT2G43410	S	313	0.96	245
10	AT2G43410	T	364	0.88	67
1	AT2G46340	S	666	1	65
3	AT2G46340	S	97	1	261
4	AT2G46340	S	242	0.8	142
5	AT2G46340	S	377	1	48
6	AT2G46340	S	343	1	268
8	AT2G46340	S	158	1	106
9	AT2G46340	S	253	0.86	220
10	AT2G46340	S	254	0.8	220

1	AT3G54760	S	499	1	129
2	AT3G54760	S	504	1	220
3	AT3G54760	S	506	0.75	121
4	AT3G54760	S	464	1	220
5	AT3G54760	S	467	1	298
6	AT3G54760	S	15	1	93
7	AT3G54760	S	186	1	184
8	AT3G54760	S	449	1	161
9	AT3G54760	S	381	1	209
10	AT3G54760	S	387	1	287
12	AT3G54760	S	210	0.97	164
14	AT3G54760	S	358	1	209
15	AT3G54760	S	95	1	122
16	AT3G54760	S	638	1	105
17	AT3G54760	S	645	0.92	146
18	AT3G54760	S	116	1	255
19	AT3G54760	S	422	1	236
20	AT3G54760	S	335	1	124
21	AT3G54760	S	369	1	329
23	AT3G54760	S	481	1	124
24	AT3G54760	S	487	1	223
25	AT3G54760	T	218	1	221
27	AT3G54760	T	384	0.96	126
31	AT3G54760	T	417	0.96	84
32	AT3G54760	T	606	1	114
1	AT3G18990	S	197	1	182
2	AT3G18990	S	198	0.87	159
3	AT3G18990	T	174	0.91	99
4	AT3G18990	T	176	0.99	88
3	AT4G16845	S	289	1	236

S.3 Nucleus-localized *pxk4-2* mutant phosphoproteomics with statistical differences. "*" and "#" refer to undetectable phosphorylation in *pxk4-2* and Col-0 plants respectively.

Proteins	Description	Phospho (STY) Probabilities	Phospho (STY) Score diffs	Log2FC	TTEST
AT4G05150	Octicosapeptide/Phox/Bem1p family protein	DVPS(1)PYGS(0.959)T(0.021)S(0.017)S(0.003)APVMR	DVPS(46.85)PY(-44)GS(16.61)T(-16.61)S(-17.43)S(-25.31)APVMR	-3.4657	0.0088
AT5G14720	Protein kinase superfamily protein	TQAALIS(0.134)DDDT(0.933)S(0.933)HAEEPDFNQK	T(-55.24)QAALIS(-11.11)DDDT(11.11)S(11.11)HAEEPDFNQK	-2.5713	0.0398
AT5G55230	microtubule-associated proteins 65-1	EEAAS(0.177)S(0.822)PVS(0.001)GAADHQVPAS(1)P	EEAAS(-6.67)S(6.67)PVS(-31.66)GAADHQVPAS(49.45)P	-1.9557	0.0212
AT4G11560	bromo-adjacent homology (BAH) domain-containing protein	GRNS(1)AS(1)PEESLGK	GRNS(81.99)AS(38.37)PEES(-38.37)LGK	-1.8781	0.0496
AT4G11560	bromo-adjacent homology (BAH) domain-containing protein	GRNS(1)AS(1)PEESLGKR	GRNS(60.55)AS(69.01)PEES(-60.55)LGKR	-1.8781	0.0496
AT4G05150	Octicosapeptide/Phox/Bem1p family protein	IS(0.417)T(0.583)PELPPPVFIKPES(0.253)PEPVS(0.904)T(0.844)PK	IS(-1.48)T(1.48)PELPPPVFIKPES(-6.82)PEPVS(8.94)T(6.82)PK	-1.8697	0.0442
AT1G18950	DDT domain superfamily	GS(0.178)S(0.77)S(0.052)DIVPDRS(1)PADDVAPVTDTK	GS(-6.36)S(6.36)S(-11.69)DIVPDRS(39.97)PADDVAPVT(-40.32)DT(-47.88)K	-1.6195	0.0000
AT2G46020	transcription regulatory protein SNF2	LVNEPET(0.011)EPS(0.889)S(0.548)PQRS(0.551)QQR	LVNEPET(-18.46)EPS(6.47)S(0)PQRS(0)QQR	-1.2453	0.0282
AT3G07810	RNA-binding (RRM/RBD/RNP motifs) family protein	S(0.011)S(0.011)S(0.978)PGYVGSYSVNK	S(-19.56)S(-19.56)S(19.56)PGY(-45.36)VGS(-49.22)Y(-63.37)S(-57.71)VNK	-1.1669	0.0022
AT4G05150	Octicosapeptide/Phox/Bem1p family protein	EVSTLS(1)DPGS(1)PR	EVS(-63.68)T(-37.49)LS(52.57)DPGS(37.49)PR	-1.1448	0.0109
AT1G17210	IAP-like protein 1	EVNRS(1)DPFS(1)EGNEQVMAFPGAR	EVNRS(98.63)DPFS(98.63)EGNEQVMAFPGAR	-1.1425	0.0127

AT1G17210	IAP-like protein 1	EVNRS(1)DPFS(1)EGNEQVMAFPGAR	EVNRS(98.63)DPFS(98.63)EGNEQVMAFPGAR	-1.1425	0.0127
AT4G05150	Octicosapeptide/Phox/Bem1p family protein	EVS(0.006)T(0.035)LS(0.959)DPGS(1)PRR	EVS(-22.17)T(-14.38)LS(14.38)DPGS(56.55)PRR	-1.0048	0.0469
AT3G54760	dentin sialophosphoprotein-like protein	KVTDMAEDVVTADIET(0.054)ES(0.946)NEAR	KVT(-51.47)DMAEDVVT(-41.68)ADIET(-12.44)ES(12.44)NEAR	-0.5298	0.0361
AT5G61150	leo1-like family protein	KGIES(1)DEEES(1)PPR	KGIES(102.07)DEEES(102.07)PPR	-0.5223	0.0257
AT5G61150	leo1-like family protein	KGIES(1)DEEES(1)PPR	KGIES(102.07)DEEES(102.07)PPR	-0.5223	0.0257
AT1G27090	glycine-rich protein	AAT(0.996)AS(0.551)S(0.445)EAS(0.008)EGPVMGLINK	AAT(21.47)AS(0.94)S(-0.94)EAS(-18.37)EGPVMGLINK	-0.5124	0.0453
AT1G19350	Brassinosteroid signaling positive regulator (BZR1) family protein	IS(0.003)NS(0.997)APVT(1)PPVS(0.101)S(0.866)PT(0.019)S(0.014)R	IS(-24.61)NS(24.61)APVT(83.35)PPVS(-9.34)S(9.34)PT(-16.54)S(-17.93)R	-0.4031	0.0017
AT5G51300	splicing factor-like protein	T(0.001)LS(0.999)GNDKDQS(1)GGEEETTSR	T(-29.11)LS(29.11)GNDKDQS(57.91)GGEEET(-57.91)T(-63.08)S(-76.5)R	-0.1496	0.0460
AT4G38550	phospholipase-like protein (PEARLI 4) family protein	MEAMSYEPET(0.001)NAPS(0.836)S(0.228)PY(0.433)HPAGNRT(0.502)PERPR	MEAMS(-41.89)Y(-42.66)EPET(-25.77)NAPS(7.09)S(-7.09)PY(-0.66)HPAGNRT(0.66)PERPR	0.1741	0.0167
AT2G20950	phospholipase-like protein (PEARLI 4) family protein	GVS(0.989)GS(0.011)S(0.002)T(0.998)PVHYK	GVS(19.56)GS(-19.56)S(-27.19)T(27.19)PVHY(-75.83)K	0.1825	0.0050
AT1G18210	Calcium-binding EF-hand family protein	AMGT(0.01)S(0.99)YTETELNR	AMGT(-19.97)S(19.97)Y(-35.6)T(-36.68)ET(-46.62)ELNR	0.2733	0.0497
AT1G52380	NUP50 (Nucleoporin 50 kDa) protein	LAPAEAVVEDNQKAS(1)DIEEGDEVDSK	LAPAEAVVEDNQKAS(69.49)DIEEGDEVDS(-69.49)K	0.3201	0.0457
AT5G47430	DWNN domain%2C a CCHC-type zinc finger	ALS(1)PT(0.003)T(0.046)S(0.758)VAS(0.193)KGEK	ALS(49.15)PT(-24.55)T(-12.16)S(5.93)VAS(-5.93)KGEK	0.3487	0.0146
AT2G43680	IQ-domain 14	LDAPRPT(0.441)T(0.559)PKPPS(1)PR	LDAPRPT(-1.04)T(1.04)PKPPS(64.82)PR	0.3899	0.0106

AT4G03080	BRI1 suppressor 1 (BSU1)-like 1	QLS(1)LDQFQNESR	QLS(103.53)LDQFQNES(-103.53)R	0.4513	0.0407
AT1G15340	methyl-CPG-binding domain 10	SLEANQVQQQQGAAAS(0.001)VS(0.999)C	S(-148.39)LEANQVQQQQGAAAS(-30.43)VS(30.43)C	0.5882	0.0320
AT2G33830	Dormancy/auxin associated family protein	TVAAVAGS(1)PGTPT(0.005)T(0.002)PGS(0.992)AR	T(-110.16)VAAVAGS(55.64)PGT(-53.29)PT(-22.58)T(-26.81)PGS(22.58)AR	1.3119	0.0165
AT5G42950	GYF domain-containing protein	S(0.001)PS(0.996)S(0.004)DLLSILQGVTDR	S(-31)PS(24.4)S(-24.4)DLLS(-135.47)ILQGVT(-175.96)DR	1.7281	0.0341
AT2G27210	BRI1 suppressor 1 (BSU1)-like 3	LILFGGAT(0.001)ALEGNS(0.061)GGT(0.068)GT(0.862)PT(0.112)S(0.851)AGS(0.044)AGIR	LILFGGAT(-29.69)ALEGNS(-11.67)GGT(-11.27)GT(11.27)PT(-9.24)S(9.24)AGS(-13.02)AGIR	1.7409	0.0483
AT5G38600	Proline-rich spliceosome-associated (PSP) family protein / zinc knuckle (CCHC-type) family protein	NSLES(0.028)GNGS(0.972)PEANSLVGNDENVK	NS(-64)LES(-15.35)GNGS(15.35)PEANS(-53.84)LVGNDENVK	2.0240	0.0246
AT5G01400	HEAT repeat-containing protein	LLVDVIPS(0.211)MS(0.79)VDKLEEFS(0.999)PK	LLVDVIPS(-5.75)MS(5.75)VDKLEEFS(27.44)PK	2.0286	0.0134
AT5G48800	Phototropic-responsive NPH3 family protein	INSGALS(0.398)AT(0.607)MS(0.995)PK	INS(-46.47)GALS(-1.85)AT(1.85)MS(21.24)PK	2.1546	0.0223
AT1G52200	PLAC8 family protein	VTTPSEEDSNNGLPVQQPGT(1)PNQR	VT(-81.4)T(-79.57)PS(-81.09)EEDS(-81.09)NNGLPVQQPGT(79.57)PNQR	2.5294	0.0326
AT2G33830	Dormancy/auxin associated family protein	TVAAVAGS(0.006)PGT(0.988)PT(0.886)T(0.09)PGS(0.03)AR	T(-50.71)VAAVAGS(-22.59)PGT(22.59)PT(10.16)T(-10.16)PGS(-15.08)AR	4.0386	0.0160
AT4G11740	Ubiquitin-like superfamily protein	AAS(0.751)GS(0.249)LAPPNADRS(1)R	AAS(4.79)GS(-4.79)LAPPNADRS(76.9)R	*	0.0019
AT4G05150	Octicosapeptide/Phox/Bem1p family protein	NVAGEEDNDS(0.909)RAS(0.518)S(0.518)IS(0.041)S(0.013)LLDS(0.001)SVNR	NVAGEEDNDS(7.77)RAS(0)S(0)IS(-12.06)S(-17.27)LLDS(-31.83)S(-36.26)VNR	*	0.0033

AT4G29190	Zinc finger C-x8-C-x5-C-x3-H type family protein	NNPLFGFGS(1)PR	NNPLFGFGS(66.67)PR	#	0.0037
AT3G05900	neurofilament protein-like protein	HVVDEPANEEKPS(0.001)ES(0.002)S(0.002)AALS(0.995)PEK	HVVDEPANEEKPS(-32.06)ES(-26.79)S(-26.79)AALS(26.79)PEK	#	0.0063
AT5G10470	kinesin like protein for actin based chloroplast movement 1	AS(1)PNIQPANVNSR	AS(86.39)PNIQPANVNS(-86.39)R	#	0.0083
AT5G38600	Proline-rich spliceosome-associated (PSP) family protein / zinc knuckle (CCHC-type) family protein	NSLES(0.804)GNGS(0.161)PEANS(0.035)LVGNDENVK	NS(-34.96)LES(6.98)GNGS(-6.98)PEANS(-13.67)LVGNDENVK	*	0.0091
AT4G32285	ENTH/ANTH/VHS superfamily protein	S(0.867)RS(0.133)FGDVNEIGAR	S(8.15)RS(-8.15)FGDVNEIGAR	#	0.0112
AT4G22740	glycine-rich protein	S(0.003)GS(0.996)FGSGLVNR	S(-24.75)GS(24.75)FGS(-37.2)GLVNR	#	0.0117
AT1G48610	AT hook motif-containing protein	TALT(1)PPAS(0.142)GS(0.858)EVPR	T(-36.83)ALT(36.83)PPAS(-7.82)GS(7.82)EVPR	*	0.0131
AT1G67310	Calmodulin-binding transcription activator protein with CG-1 and Ankyrin domain	QDVEST(0.002)EDS(0.998)EDEDILK	QDVES(-40.6)T(-26.46)EDS(26.46)EDEDILK	#	0.0141
AT1G24300	GYF domain-containing protein	AFS(1)DEQINR	AFS(114.76)DEQINR	#	0.0149
AT5G25060	RNA recognition motif (RRM)-containing protein	S(0.065)S(0.077)S(0.836)S(0.032)GS(0.694)DNT(0.069)GGIT(0.229)FK	S(-12.78)S(-12.03)S(12.03)S(-16.22)GS(6.13)DNT(-10.42)GGIT(-6.13)FK	*	0.0152
AT1G55250	histone mono-ubiquitination 2	DAACEGHVT(0.458)S(0.542)PAIANGS(0.94)LS(0.06)PEKPVDK	DAACEGHVT(-0.74)S(0.74)PAIANGS(11.97)LS(-11.97)PEKPVDK	*	0.0171
AT3G49590	Autophagy-related protein 13	FFPS(1)PGRS(1)VEGHSFTGR	FFPS(51.4)PGRS(43.14)VEGHS(-43.14)FT(-46.49)GR	#	0.0239
AT3G49590	Autophagy-related protein 13	FFPS(1)PGRS(1)VEGHSFTGR	FFPS(51.4)PGRS(43.14)VEGHS(-43.14)FT(-46.49)GR	#	0.0239
AT5G57610	kinase superfamily with octicosapeptide/Phox/Bem1p domain-containing protein	YGEVEGT(0.053)WS(0.947)PFYS(1)PR	Y(-108.25)GEVEGT(-12.53)WS(12.53)PFY(-60.32)S(60.32)PR	#	0.0273

AT5G57610	kinase superfamily with octicosapeptide/Phox/Bem1p domain-containing protein	YGEVEGT(0.001)WS(0.998)PFY(0.001)S(1)PR	Y(-67.93)GEVEGT(-32.61)WS(29.77)PFY(-29.77)S(44.84)PR	#	0.0273
AT3G43300	HOPM interactor 7	NPDDIKDNGKVS(1)AQAS(1)PR	NPDDIKDNGKVS(54.12)AQAS(54.12)PR	*	0.0375
AT3G43300	HOPM interactor 7	NPDDIKDNGKVS(1)AQAS(1)PR	NPDDIKDNGKVS(54.12)AQAS(54.12)PR	*	0.0375
AT1G73350	ankyrin repeat protein	ISTPS(0.036)S(0.96)PS(0.017)LS(0.987)PPVR	IS(-78.69)T(-66.25)PS(-14.46)S(14.46)PS(-19.44)LS(19.44)PPVR	#	0.0387
AT3G18380	DNA-BINDING TRANSCRIPTION FACTOR 2	DPSLSATPATLVQPS(0.007)S(0.007)NAAT(0.003)VPAGS(0.984)A	DPS(-47.41)LS(-48.83)AT(-47.11)PAT(-44.24)LVQPS(-21.69)S(-21.69)NAAT(-25.46)VPAGS(21.69)A	#	0.0454
AT5G57610	kinase superfamily with octicosapeptide/Phox/Bem1p domain-containing protein	VGS(1)GQMLAQR	VGS(89.46)GQMLAQR	#	0.0465

S.4 TAP-HUB2 interactome.

Gene ID	Proteins	FC	TTEST_ZT14	FC	TTEST_ZT_23
AT1G55250.3; AT1G55250.5	HUB2	0.0733	0.4393	-0.1941	0.3836
AT2G44950.1	HUB1	-0.0845	0.3890	0.3454	0.3960
AT1G27750.1	SPEN3	-0.5988	0.2781	-3.8512	0.0005
AT1G51580.1	KHD	1.0746	0.0866	-1.2325	0.0035
AT5G09740.1; AT5G09740.2; AT5G64610.1	HAM1/HAM2	-0.1368	0.3298	-0.6677	0.0154
AT1G20960.1; AT1G20960.2	BRR2a	-1.1363	0.0159	-0.7206	0.0217
AT2G22540.1; AT2G22540.2; AT2G22540.3	SVP	-0.3474	0.0766	-1.3160	0.0024
AT2G23080.1; AT2G23080.2; AT3G50000.1; AT5G67380.1; AT5G67380.2	CKA1/2/3	0.4649	0.2947	-1.4002	0.0026
AT1G80070.1	PRP8	-0.2526	0.1623	-0.3580	0.0765